VILNIUS UNIVERSITY
LIFE SCIENCES CENTRE

Alena Koida

Analysis of (micro)plastic biodegradation-associated genes in environmental microorganisms

Master's thesis

Genetics study program

Thesis supervisor
Prof. dr. Eglė Lastauskienė

Consultant
PhD student, Gintarė Jansonaitė

Thesis completed at
Department of Microbiology and Biotechnology
of the LSC Institute of Biosciences,

Vilnius 2025

TABLE OF CONTENT

INTRODUCTION

Since the 1950s, plastic has been actively used all over the world. It is cheap to produce, suitable for a wide range of applications, lightweight and relatively chemically stable. Today, plastic is used to produce a huge number of everyday items, replacing other materials that are more difficult to process (Geyer, 2020); they have become a convenient alternative to natural fabrics due the fact that, unlike wool and cotton, they don't require farmlands (Tang et al., 2022). However, at the time of active commercial introduction of plastic, the long-term environmental consequences were not taken into account. Under the influence of time, natural wear and tear, biotic and abiotic factors, plastic breaks down into microplastics (MP) (< 5 mm in diameter) and nanoplastics (< 1 μm) (Maroof et al., 2021). However, its complete decomposition can take decades and centuries (Mohanah, 2020).

In the environment MP alters the physical and chemical properties of soil, has a detrimental effect on aquatic ecosystems. It has been proven to be harmful to human health, being genotoxic (nanoplastics), affecting microbiota and causing inflammation (Çobanoğlu et al., 2021; Maroof et al., 2021). It is estimated that humans consume about 5 grams of microplastics per week (Aliya et al., 2025).

In the last few decades, there has been an active accumulation of knowledge about microbial enzymes involved in the biodegradation of microplastics. Places highly contaminated with plastic waste are considered promising sources for their search. Bioremediation methods are acknowledged as the most sustainable solution to global pollution due to environmental friendliness (Muthukumar & Veerappapillai, 2015). Despite efforts in this field, biodegradation pathways are known for only a few plastics, and for those for which they are known, implementation is still very limited. Finding new enzyme variants with higher efficiency or with fundamentally new mechanisms of action (for plastics with identified biodegradation pathways) and finding biodegradation pathways for more recplastics is a vital task today to mitigate the problem. Screening of metagenomes of different environmental sites is an effective tool to assess the potential of the environment for biodegradation of microplastics.

The aim of this work: to explore different both natural and artificial sources for microorganismal genes that encode enzymes that are associated with degrading various types of (micro)plastics

The objectives of this work:

1. To isolate metagenomic DNA from environmental samples.
2. To amplify genes potentially involved in (micro)plastic biodegradation.
3. To determine the identity and putative microorganismal origin by sequencing amplicons.
4. To assess the potential of tested environments to biodegrade micro(plastic).

1. LITERATURE REVIEW

1.1. The problem of microplastics: general

The issue of microplastics is a growing concern in both scientific and social spheres, as the production of plastic continues to increase. In 2020 production tended to be about 350 to 400 million tons a year and as plastics are very economically beneficial materials, a threefold increase is expected in the nearest 30 years (Purohit et al., 2020). Although plastic recycling efforts have gradually increased as well, most of the plastic waste still ends up in the environment (Wojnowska-Baryła et al., 2022).

In recent years, environmental research has focused on microplastics (MPs), which are defined as plastic particles smaller than 5 mm in their longest dimension and are of different shapes such as beads, fragments, fibres, and films. Today they are found virtually everywhere – from the Everest top (Napper et al., 2020), Arctic sites, in the Alps (Bergmann et al., 2020) to human blood and other tissues (Leslie et al., 2022).

There are two types of MPs according to the origin: primary and secondary. Primary MPs are produced and released into the environment in small sizes without undergoing significant degradation or fragmentation, for instance, small plastic granules of raw material, microbeads and microparticles in personal care products (An et al., 2020, Tang et al., 2022).

Secondary MPs are derived from bigger plastic fragments that were not properly disposed of due to natural stressors such as UV radiation, sunlight, pressure, grinding, biological degradation or due to normal wear and tear during the use of goods (An et al., 2020) such as disposable plastic tableware, plastic packaging, bottles, tires (while rubbing on asphalt), synthetic clothes microfibers (during laundering) (Sommer et al., 2018; Nizzetto et al., 2016). Also, soil invertebrates such as earthworms can shred micropalstice by passing it through the gut. (Huerta Lwanga et al., 2017).

Initially, microplastic pollution was observed in marine environments in the 1970s (Carpenteret al., 1972; Thompson et al., 2004), leading most studies to focus on the origin, prevalence, and fate of marine microplastics. However, for today it is reported that microplastic concentrations in soil are much higher than in water and marine sediment (Zhang and Liu., 2018).

In addition to all, “microplastic can adsorb and transport hydrophobic organic pollutants (such as polychlorinated biphenyls, polycyclic organochlorine pesticides, aromatic hydrocarbons), heavy metals (such as nickel, zinc, cadmium, plumbum), and antibiotics” (Zhang et al., 2020; Menéndez-Pedriza et al., 2020).

1.2. Plastics: overview

Petroleum-derived plastics are widely used throughout the global economy. Their production methods are well-established and highly efficient. They are cheap, lightweight, physically and chemically stable (Hahladakis, 2020). There are many different types of plastics, some examples are presented in (Fig. 1.1). The properties of a plastic depend on its chemical structure, which is determined by the type and arrangement of the monomers used to make it. Different types of plastics have different environmental impacts, with some being more recyclable or biodegradable than others (Zhang Y. et al., 2021).

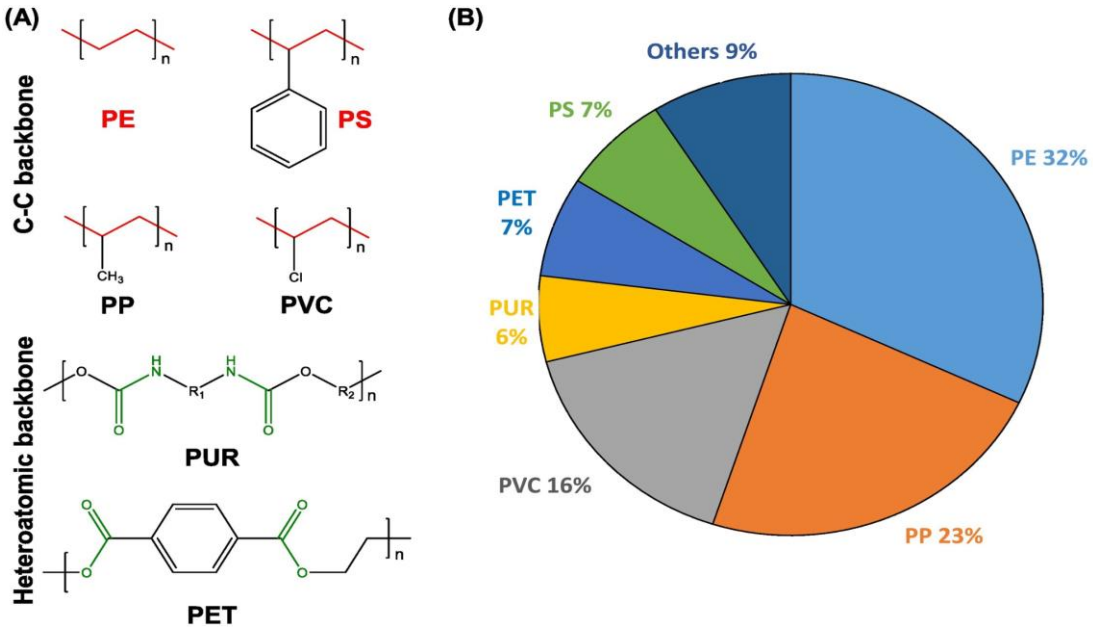

Fig.1.1 (A) Groups of plastics by the C-C backbone structures: PE – polyethylene, PP – polypropylene, PVC – polyvinyl chloride, PS – polystyrene; and heteroatomic backbones: PUR – polyurethane, PET – polyethylene terephthalate. The highly stable C-C backbones are highlighted in red, hydrolysable bonds are green. (**B**) The distribution of plastic demand in 2018. (Zhang Y. et al., 2020).

1.3. Impact of microplastics on environment and human health

Microplastics accumulate in ecosystems and cause physical and chemical changes of it. Unfortunately, it persists there for hundreds of years (Table 1.1), leading to long-term pollution and ecological damage (Mohanah, 2020).

Table 1.1 Approximate life span of major synthetic thermoplastic polymers (Mohanah, 2020)

Polymer	PET	LDPE	HDPE	PS	PP	PVC
Life span (years)	450	10-600	>600	50–80	10–600	50–150

LDPE –low density PE, HDPE – high density

1.3.1. Impact of microplastics on environment

Microplastics affect the quality of soil, water and air. The detrimental effect on soil is that MPs influence its physical properties, such as its texture and water-holding capacity, accumulating in pores

and reducing their size, leading to increased soil compaction and reduced water infiltration. This can make it difficult for plant roots to grow and access nutrients, affecting plant growth as well as alter microbial communities (Machado et al., 2018; Huang et al., 2019). MPs can also affect chemical properties of soil by adsorbing, transferring and releasing toxic substances such as heavy metals and pesticides to different areas (Menéndez-Pedriza, 2020). Microplastics affect water quality primarily by causing physical harm to aquatic organisms. MPs can be ingested by fish, shellfish, and other aquatic animals, leading to injury, starvation, and death (Kumar et al., 2020), it could affect the behaviour and growth of fish (Lehner et al., 2019). They also may affect the chemical properties of water, including pH, salinity, and nutrient levels (Zhu et al., 2021). As in the soil, in aquatic environment MP can adsorb and transfer various substances. It also serves as a surface for the growth of bacteria including pathogens, increasing the risk of waterborne illnesses (Junaid et al., 2022).

Microplastic particles are very light, therefore they can be carried by wind currents, transported through the air and deposited in terrestrial and aquatic environments (Chen et al., 2020). Interestingly, it occurs in both indoor and outdoor air, with higher levels indoors (Wang et al., 2021).

1.3.2. Impact of microplastics on human health

The impact of microplastic on human health is still being studied, but some potential health risks have been identified. There is currently limited scientific evidence to confirm whether it causes cancer, but it is proven, that microplastics causes cellular and DNA damage, inflammation, which are linked to cancer development. Moreover, microplastics may potentially transfer cancerogenic chemicals, such as polycyclic aromatic hydrocarbons (PAHs) and phthalates (Fackelmann & Sommer, 2021).

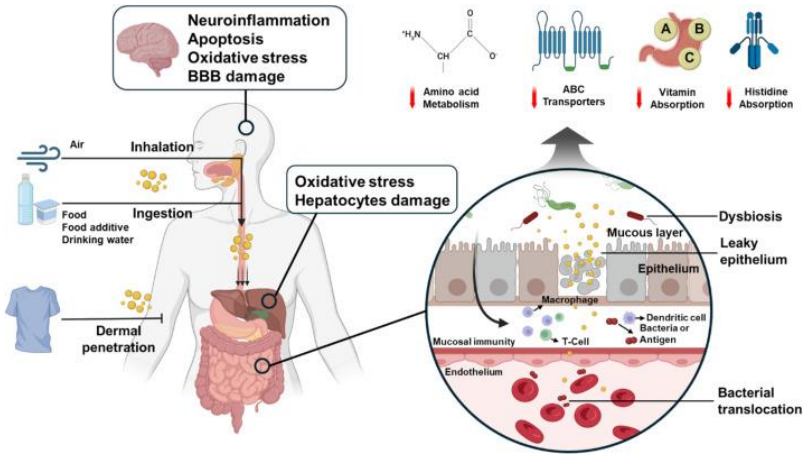

Fig. 1.2 Various ways microplastics may interact with the human body.

There are 3 main ways for MP to enter the human body: ingestion, inhalation and dermal contact (Fig.1.2). Ingestion of microplastics has been linked to various health effects, including

gastrointestinal issues such as intestine inflammation caused by pathogens and substances transported by pieces of plastics and mechanical disruptions caused by pieces themselves (Yan, Z et al, 2022). Furthermore, it influences gut microbiota that has been shown to be linked to cancer development and the effectiveness of anti-cancer drugs (Fackelmann & Sommer, 2021).

Inhalation of microplastics may also pose a health risk. For today there is a lot of evidence that these small pieces cause respiratory and other health problems when inhaled (Wang et al., 2021). The likelihood that airborne MPs enter our respiratory system depends upon its size (Gasperi et al., 2018).

Dermal contact with microplastics contained in cosmetic products, textiles or in the dust is another route of exposure. Even though it is considered as less significant route of exposure, it has been discussed that nanoplastics (<100 nm in the longest dimension) could cross the dermal barrier (Revel et al. 2018). Some studies have suggested that microplastics can cause skin irritation and inflammation, although more research is needed to fully understand the extent of the risk (Rahman et al., 2020).

Another negative effect of plastic is that the plasticisers and additives used to extend shelf life leach out of the plastic over time, whereas more than half of the used plastic additives are categorysed as harmful such as phthalates, bisphenol A (BPA) and other chemicals that can disrupt the endocrine system causing hormonal imbalance. Due to the fact that BPA mimics estrogen, it has been linked to the development of breast cancer (Rochman et al., 2013).

It has also been reported that daily consumption of sea salt increases the risk of MP accumulation in the body. More sources of MP in human body are tap water (Yuan et al., 2022) common kitchen utensils (Luo et al., 2022), sugar (<300 μm), vegetables, honey, beer tea brewed from plastic (nylon) tea bags and many others (Aliya et al., 2025).

1.4. Microbial and Enzymatic Degradation of Synthetic Plastics as the solution for elimination of MPs

Biological methods are considered to be the most sustainable strategy for the removal of microplastics due to environmental friendliness and cost-effectiveness. Unlike incineration, which releases harmful gases, or mechanical removal, which can be costly and time-consuming, biological methods produce no harmful byproducts (Ru et al., 2020).

Microorganisms can be very effective and targeted agents in destroying of petro-polymers due to the production of the specter of extracellular enzymes that can cut the long chains into oligomers and monomers that can be taken up by the cells for further metabolisation resulting in CO_2 and water during aerobic process, CO_2 and CH_4 during anaerobic process (Mohanah et al., 2020; Muthukumar & Veerappapillai, 2015).

The degradation of synthetic plastics involves multiple steps, and different enzymes are needed to catalyse each step. The cooperation of complex microbial communities can optimise the process through syntrophy between species and the development of new functional capabilities (Meyer et al., 2020).

There are several steps in plastic biodegradation process based on Lucas et al., 2008 study:

1) The first step is biodeterioration. During this step, biofilms are formed on the substrate, superficial degradation occurs, and as a result, hydrophilicity of the polymer increases. This can be done enzymatically or mechanically (e.g. by earthworms, abrasion) hence, abiotic factors significantly influence this stage. At this step the mechanical, physical and chemical changes happen, but no significant depolymerisation takes place (Fotopoulou et al, 2019).

2) The second step is depolymerisation. At this step, the reduction of molecular weight with releasing of oligomers and monomers happens due to secretion of microbial extracellular enzymes. Once the fragments are small enough, they can be uptaken by bacteria if they have corresponding transporters. Inside the cells the molecules are being introduced into metabolism (Lucas et al., 2008).

3) The third step is assimilation (sometimes combined with the depolymerisation step) takes place in the cytoplasm converting intermediates into energy, biomass energy, biomass, and primary/secondary metabolites (Asiandu et al. 2021).

4) The last step is mineralisation. At this stage, the intermediates are changed into simpler compounds, may undergo complete oxidation and be released as CO_2, N_2, CH_4, H_2O, etc. (This process ends when all carbon atoms are converted into CO_2 or CH_4 (Lucas et al., 2008; Alshehrei, 2017).

Microorganisms from a wide variety of taxa are involved in the biodegradation of plastic (Fig. 1.3), but interestingly, such activity has not yet been confirmed for any representative of archaea. This may be explained by the fact that archaea are generally difficult to cultivate laboratory conditions (Gambarini et al., 2021).

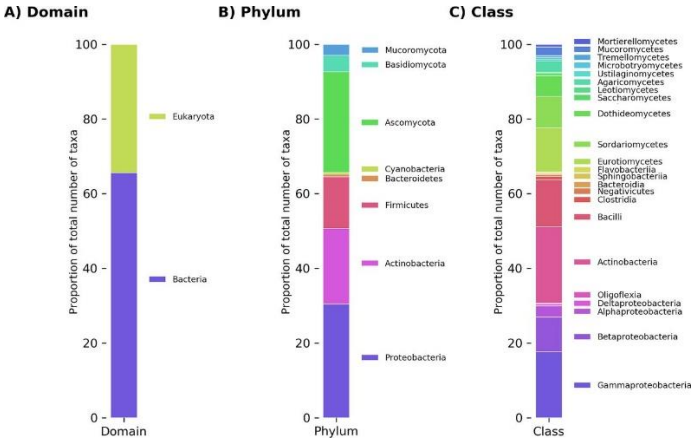

Fig. 1.3 Relative abundance of plastic-degrading taxa (adapted from Gambarini et al., 2021).

1.4.1. Enzymatic degradation of different types of plastics

Microbial biodegradation of plastics is a complex process that is influenced by a lot of factors, among them: the chemical structure of the plastic – the more functional groups, the higher susceptibility (Brydson, 2017), environmental factors such as temperature, moisture, and pH, exposure to UV radiation, the composition and activity of the microbial community (Meyer et al., 2020), the availability of oxygen (Muthukumar & Veerappapillai., 2015), the presence of other xenobiotics in the environment (shifting of pH, toxicity of contaminants) (Liu et al., 2022) and the availability of nutrients (Mohanah et al., 2020). Among important factors are the size and shape of the material as well as the age and degradation status (Liu et al., 2022). Microorganisms such as fungi and bacteria attach to the surface of the polymer, release enzymes and propagate on it, utilisig plastic as a carbon source

Hydrolases are one of the key enzymes in the biodegradation of plastics. Hydrolytic breakdown of ester bonds occurs when water and enzyme penetrate into the least crystallised areas of plastic. Among the hydrolases, esterases, lipases, proteases, ureases and exhibit catalytic activity on plastic substrates (Suresh et al., 2025).

In addition to hydrolases, oxidoreductases (hydroxylases-monooxygenases), which introduce oxygen into the substrate, introducing new functional groups into the polymers, represent another class of key enzymes involved in this process. Among them: oxidoreductases such as peroxidases, for example manganese peroxidases (MnP, utilise H_2O_2 as an oxidant) and laccases, for example, multicopper oxidases (utilise molecular oxygen) (Suresh et al., 2025).

Hydrolysis and oxidation are the two main types of reactions that in plastic biodegradation (Heris , 2024).

1.4.1.1. Biodegradation of polystyrene

Polystyrene (PS) is one of the most abundant plastics produced worldwide (Fig. 1.1). Like other plastics, it has good mechanical properties and is widely applied for food packaging, construction materials, disposable tableware, etc. (Mohanah et al., 2020). The aromatic carbon-carbon backbone in polystyrene exhibits significant resistance to oxidation-reduction enzymatic cleavage (Goldman, 2010). PS is extremely hydrophobic, which makes this polymer highly resistant to biodegradation (Ho et al., 2018).

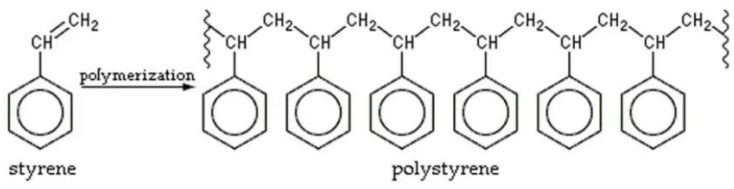

Fig. 1.4 Chemical structure of styrene and polystyrene (from open resources)

The presence of large styrene groups (Fig. 1.4.) prevents the enzymatic breaking of C-C bonds due to steric incompatibilities with the active center of the enzyme, thus depolymerisation is bottleneck of PS biodegradation (Hou & Majumder, 2021).

PS depolymerisation product is its monomer styrene. Styrene is digested by many microorganisms, among them *Pseudomonas, Rhodococcus, Xanthobacter, Nocardia* and *Variovorax,* entering the tricarboxylic acid cycle in several stages (Hou & Majumder, 2021).

According to Oelschlägel genes encoding enzymes that oxidise styrene are often located on one operon, called *styABC*. The genes *styA* and *styB* encode a monooxygenase complex that introduces oxygen into aromatic ring. Styrene monooxygenase is a two-component flavoprotein that catalyses the NADH and FAD-dependent epoxidation of styrene to styrene oxide. StyA is a monooxygenase and StyB is a FAD reductase to supply StyA with the necessary electrons (Oelschlägel et al., 2018).

Several enzymes putatively can be involved in the PS/styrene degradation process (shown in Table 1.2), among them are: alkane hydroxylases, styrene monooxygenases, styrene oxideisomerases, phenylacetaldehyde dehydrogenases and some more (Purohit et al., 2020). The C-C backbone is more susceptible to the cleavage then the side chain (aromatic ring) due to the weaker bonds (Hou & Majumder, 2021).

Table 1.2 Enzymes associated with the biodegradation of polystyrene (PS)

Group of enzymes	**Description**	**References**
Alkane monooxygenases	Introduce oxygen atom into C-C bonds of PS under acidic or alkaline conditions	Purohit et al., 2020; Hou & Majumder, 2021
Styrene monooxygenase (SMO) and styrene oxideisomerase (SOI)	Convert styrene into the oxide and styrene oxide into styrene epoxide (phenylacetaldehyde)	Zhang et al., 2022
Styrene dioxygenase (SDO)	Hydroxylates styrene to generate styrene cis-glycol (both in polymer and monomer state)	
Phenylacetaldehyde dehydrogenase	Oxidises the styrene epoxide (phenylacetaldehyde) into phenylacetic acid that can be included in TCA via β-oxidation	
Hydroquinone peroxidase (*Azotobacter beijerinckii* HM121)	Isolated from lignin decolorising bacteria, possesses the ability to depolymerase the polymer resulting in the formation of styrene oligomers and monomers	Nakamiya et al., 1997, Wei, R.; Zimmermann, W. 2017
P450 monooxygenases (CPY152A1 [*Bacillus subtilis*], CPY153s *[Alcanivorax borkumensis* and *Sphingomonas sp.]*, CYP116B5 [*Acinetobacter radioresistens S13]*	Initiate degradation through an oxygenase-induced free radical mechanism, attack C-C backbone; in the presence of hydrogen peroxide epoxidation of styrene	Xu et al., 2019; Hou & Majumder, 2021

Monooxygenases (4-hydroxybenzoate 3-monooxygenase and 3-hydroxybenzoate 6-monooxygenase)	Performs oxidation of ring aromatic compounds generated from the decomposition of PS main chain	Hou & Majumder, 2021

Putative pathway

According to Zhang, degradation of polystyrene can start either from the main chain or from the aromatic rings. If degradation starts from depolymerisation, i.e. from the C-C backbone, styrene monomer is formed, which, as mentioned above, is efficiently utilised by bacteria. In the cytoplasm, styrene is converted into styrene epoxide by the enzyme styrene monooxygenase, followed by styrene oxide isomerisation and, after a few steps, enters into the tricarboxylic acid cycle. Alternatively, to styrene monooxygenase, the PS monomer can be attacked by styrene dioxygenase, after which it also enters the tricarboxylic acid cycle after several reactions. (Zhang Y. et al., 2022).

1.4.1.2. Biodegradation of polyethylene

Polyethylene (PE) is the most common plastic with a linear C-C backbone. C-C backbone plastics (PS, PE, PVC, PP) do not contain hydrolysable groups/bonds (Fig.1.6) thus very resistant to biodegradation. The high molecular weight and crystalline structure are also inhibiting factors for microbial biodegradation (Mohanan et al., 2020).

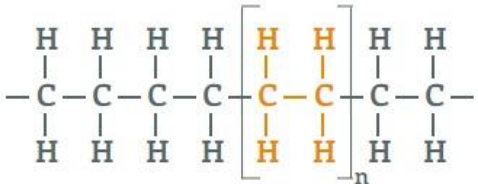

Fig. 1.6 Chemical structure of PE (Fatima & Roohi, 2021).

Several microorganismal species were found to depolymerase PE after physicochemical pretreatments, including UV irradiation, chemical oxidising agents, thermo-oxidation. Bacteria of the genus *Rhodococcus* are often involved in bioremediation, being able to degrade various complex substrates (Zampolli et al., 2022). It has been reported that some species of this genus can utilise pretreated PE by attacking it with alkane monooxygenases. However, recently a bacterium *Rhodococcus opacus* R7 has been reported that is able to grow on untreated PE as the sole carbon source. This strain utilises laccase-like multicopper oxidases (LMCOs) for this purpose. Further studies revealed that growth on PE in this strain activates the expression of alkane monooxygenases, cytochrome hydroxylases cyp450 and membrane transporters, apparently to transport intermediates into the cytoplasm. For today this strain is the only one reported to utilise untreated PE and included in the PAZy database as its activity is proven (Buchholz et al., 2023).

To date, only a few enzymes capable of attacking PE have been identified (Table 1.4). The most reported enzymes likely known for PE depolymerisation include laccases, manganese peroxidases, and lignin peroxidases, but as mentioned, they are active only after oxidation pretreatment (Zampolli et al., 2023).

Until recently, it was considered that the maximum molecular weight of PE that is suspected to be degraded in the degradation process is about 2000 Da. Later, a few organisms that can biodegrade long-chain PE (molecular weight > 2,000 Da) were isolated from different environmental sites such as mulch films, marine water, soil contaminated by crude oil, sewage sludge, and landfills (Ru et al., 2020).

Table 1.4 Enzymes associated with polyethylene (PE) biodegradation

Group of enzymes	**Description**	**References**
Manganese peroxidase (MnP)	Attacks oxidised polyethylene containing keto group	Iiyoshi et al., 1998
Lignin peroxidase (LiP)	Performs H_2O_2 dependent oxidative breakdown of lignin, also active on PE	Khatoon et al., 2019
Laccase	Catalyses the oxidation of both aromatic (mostly) and non-aromatic compound of lignin; performs oxidative cleavage of the amorphous region of high-density PE	Othman et al., 2021
Soybean peroxidase	With the presence of hydrogen peroxide enzyme has been shown to reduce the hydrophobicity of the PE surface	Zhao et al., 2004
alkane hydroxylases *(alkB alkB1, alkB2, alkM genes)*	Add one or two atoms of oxygen to form alcohols, ketones, carboxylic groups, and aldehydes by a free radical reaction, that further oxidised to fatty acids and catabolized via the bacterial β-oxidation pathway	Kumar et al., 2021
		Ratajczak et al., 1998
Laccase-like multicopper oxidases LMCO2, LMCO3 (from Rhodococcus *opacus* R7)	Introduce oxygen atoms via oxidative attack, form hydroxyl and carbonyl groups	Zampolli et al., 2023

1.4.1.3. Biodegradation of polypropylene

Polypropylene (PP), alternatively polypropene as well as PE has no hydrolysable bonds, its C-C backbone is very stable (Fig.1.7). Polypropylene is the second-most is the second most prevalent plastic (after polyethylene) and unfortunately also very poorly biodegradable without pretreatment (Zhang Y. et al., 2021).

Polypropylene is used as a chemically resistant container and to produce laboratory ware such as centrifuge tubes, pipette tips, Eppendorf test tubes, etc. (Suresh et al., 2025). Prolypropylene microplastic is commonly found in cosmetics and personal care product (in toothpastes, scrubs). unfortunately, it can persist for a very long time in the environment. (Othman et al., 2021).

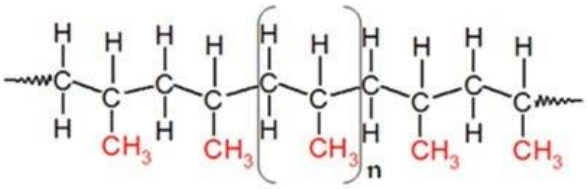

Fig.1.7 Chemical structure of polypropylene (Mandal & Šapčanin, 2023)

For today, only pretreated with γ-irradiation, UV irradiation, thermo-oxidation PP showed susceptibility to biodegradation (Ru et al., 2020). Several microorganisms from different environmental showed the potential to degrade PP (Table 1.5), among them bacteria isolated from waste dumping sites, mangrove environments (Auta et al., 2018) and even from Antarctica (Habib et al., 2020).

Table 1.5 Microorganisms associated with polypropylene biodegradation (putatively, after pretreatment), adapted from (Ru et al., 2020; Jadaun et al., 2022, Rana et al., 2022, Habib et al., 2020)

Strain	**Isolated source**	**Tested PP**
Yarrowia lipolytica 78–003	–	PP pellets
Rhodococcus sp. ADL36, *Pseudomonas* sp. ADL15	Antarctica	–
Pseudomonas stutzeri; Bacillus subtilis; Bacillus flexus	Plastic-dumping site	PP film
Stenotrophomonas panacihumi	Soil of waste storage yard	PP film
Aneurinibacillus aneurinilyticus, Brevibacillus agri; Brevibacillus sp.; Brevibacillus brevis	Landfills and sewage	PP film and pellets
Bacillus sp. 27, *Rhodococcus* sp. 36	Mangrove environments	PP microplastic
Lysinibacillus sp. JJY0216	Soil	PP film

Regrettably, no particular enzymes have been identified to attack PP, and the understanding of the microbial degradation mechanism of PP is quite limited (Jadaun et al., 2022). At the time of writing this review, no information about enzymes with proven activity against PP has been deposited in PAZy – The Plastics-Active Enzymes Database (Buchholz et al., 2022). In comparison to some other types of microplastics, the knowledge regarding the degradation and removal of polypropylene remains scarce.

1.4.1.4. Biodegradation of polyvinyl chloride

Out of all the major types of synthetic plastics, polyvinyl chloride (PVC) has the highest concentration of plasticiser, (up to 50%). Since plasticisers can serve as a source of carbon nutrients for numerous bacteria and fungi, PVC that has been plasticised may be prone to fungal or bacterial degradation (Webb et al., 1999). For example, various fungi were discovered to cause damage to several plasticised PVC bathroom products, including, bath mats, and shower curtains (Khatoon et al., 2019).

PVC without plasticisers is extremely hydrophobic and biodegradation resistant. Chemical structure of PVC is shown in Fig. 1.8.

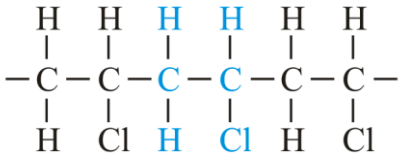

Fig. 1.8 Chemical structure of polyvinyl chloride (Chemistry glossary. glossary.periodni.com)

As with other plastics, bacteria capable of biodegrading PVC have been reported, but this is most common for plasticised PVC. They are most often found in areas contaminated with plastic, but species from marine environments have also been reported (Ru et al., 2020). Among them *Mycobacterium*, *Acinetobacter*, *Pseudomonas* and *Bacillus* are able to attack PVC and introduce morphological and physicochemical changes (Ru et al., 2020; Zhang et al., 2022).

When PVC is disposed of by incineration, HCl is released (Fig.1.8), which is harmful to human health and ecosystems (Kaushal et al., 2021). Therefore, it is extremely important to find a suitable method of biodegradation for this type of plastic. Similar to PE, the C-C bonds of PVC can potentially be attacked by alkane monooxygenases, lacases, manganese peroxidases and lignin peroxidases, but as with PE, pretreatment is required (Temporiti et al., 2022; Amobonye et al., 2023).

Table 1.6 Microorganisms associated with polyvinyl chloride (PVC) biodegradation (adapted from Ru et al., 2020)

Microorganism	**Isolated source**	**Tested PVC**
Mycobacterium sp. NK0301	Garden soil	Plasticised PVC film
Chryseomicrobium imtechense; Lysinibacillus fusiformis; Acinetobacter calcoaceticus; Stenotrophomonas pavanii	Landfill leachate	Plasticised PVC curtain
Acanthopleurobacter pedis; Bacillus cereus; Pseudomonas otitidis; Bacillus aerius	Plastic disposal sites	PVC film
Bacillus sp. AIIW2	Marine environment	Un-plasticised PVC film
Pseudomonas citronellolis	Plastic disposal site	Plasticised PVC film

Microorganisms capable of degrading both PVC and plasticisers are not known these days. Thus, unfortunately no key enzymes associated with the initiation of the process and cleavage of C-C backbone of PVC were found (Ru et al., 2020; Othman et al., 2021).

Recently, three PVC active esterases were isolated from marine bacteria *Vibrio sp*. (T-1.3), *Alteromonas sp.* (BP-4.3), *Cobetia sp*. (S-237) (Khandare et al., 2025). It is stated in the article that PVC film used in the study was plasticisers-free, however the procrdure itself includes bleaching

steps, which in its turn could alter the surface of the film, introducing functional groups, while intact PVC itself does not contain any ester bonds to be a substrate for esterases, and unfortunately there is no explanation of this phenomenon in the article.

1.4.1.5. Biodegradation of polyethylene terephthalate

Polyethylene terephthalate (PET) is petro-polymer (polyester) (Fig 1.9), which is synthesised by the condensation polymerisation of bis(2-hydroxyethyl) terephthalate (BHET) or esterification reaction between terephthalic acid (TPA) and ethylene glycol (EG). Unfortunately, physical methods of polymer processing deteriorate the mechanical properties of PET and after 6 processing cycles it cannot be reused anymore. PET is mainly used to produce PET bottles, film and various fibres in textile industry (Sun, 2024).

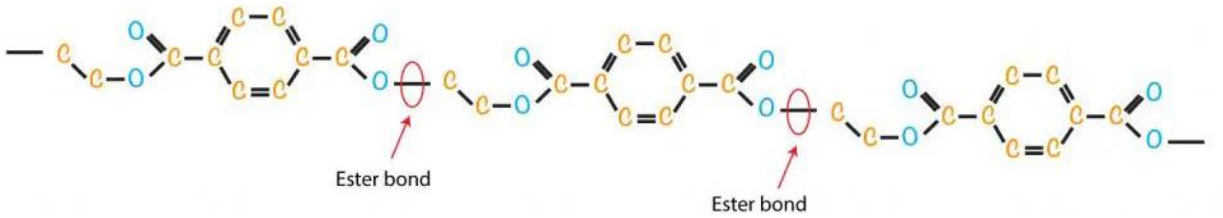

Fig. 1.9 Chemical structure pf PET with highlighted hydrolysable ester bonds, targets for hydrolytic enzymes. Adapted from (RS Science. https://rsscience.com/).

It can be said that PET is the most amenable petro-polymer to scientists' attempts to find the key to its biodegradation. By now, there is a considerable number of enzymes that have an affinity for PET. PET polymer molecules can arrange themselves in both highly crystalline structures and more amorphous (low- crystalline) manner. Given that enzymes prefer to attack flexible amorphous regions, the biodegradation efficiency of PET plastic decreases with the increase in the degree of crystallinity (Sun., 2024). The majority of enzymes associated with PET degradation are cutinases, lipases and carboxylesterases. They can act on amorphous but not crystalline PET. These enzymes break the ester bond in the polymer to either produce bis(2-hydroxyethyl) terephthalate (BHET), mono(2-hydroxyethyl) terephthalate (MHET) or terephthalic acid (TPA) and ethylene glycol (EG) (Appendix A) (Kawai et al., 2019). It was noticed that-PET degrading enzymes have a highly polar surface that favours binding to more hydrophilic regions of the substrate (Hou & Majumder, 2021).

Cutinases are mainly produced by saprophytic microorganisms that use cutin as a carbon source, or by plant pathogenic microorganisms invade into host. They belong serine esterases from α/β hydrolase superfamily (Sun, 2024). Their active pocket is large enough to accommodate substrates with high molecular weight (Maurya et al. 2020).

The first enzyme that was discovered to degrade PET was *Thermobifida fusca* cutinase *(*hydrolase) with the efficiency up to 50% of low-crystalline PET at 55 °C after 3 weeks (Müller et al. 2005). Following this, in 2009 Ronkvist et al., compared the PET-hydrolysing activities of three cutinases from different microorganisms, *Thermomyces insolens, Pseudomonas mendocina* and *Fusarium solani.* In this study *Thermomyces insolens* cutinase showed the highest efficiency (at 70°C), whereas cutinases from *Pseudomonas mendocina* and *Fusarium solani* showed lower results and were called PET surface-modifying enzymes, rather than PET hydrolases (Ronkvist et al., 2009).

In 2012 the Leaf branch compost cutinase was described by Sulaiman and colleagues. The enzyme can effectively hydrolyse low-crystalline PET package film at elevated temperatures (50°C). Although the organism is unknown, the gene was isolated from leaf-branch compost metagenomic library (Sulaiman et al., 2012).

By this time, many PET active cutinases have been described. The full list can be found in the PAZy (The Plastics-Active Enzymes) database (Buchholz et al., 2022).

One more important discovery was made by Yoshida et al. in 2016. The research group investigated *Ideonella sakaiensis* 201-F6, bacteria with enzymes for two sequential stages of PET degradation: PETase and MHETase. PETse is similar in characteristics to cutinases, but its active site is wider than in reported cutinases, which may be the reason for the high specificity toward the PET substrate. MHETase catalyses subsequent breakdown of the resulted intermediates into terephthalic acid and ethylene glycol – feedstock for the PET synthesis (Sun, 2024).

Esterases are a broad subclass of hydrolases with broad substrate specificity, which makes them attractive candidates to be applied in plastic biodegradation (Romano et al. 2015). Several known PET degrading esterases are deposited in the PAZy (The Plastics-Active Enzymes) database (Buchholz et al., 2022), however, the biochemical characteristics of enzymes are constantly being refined and esterases can be classified as one or another type of hydrolase.

For some identified PET-degrading enzymes, classification does not go beyond the class **hydrolases**. This may be due to the lack of information of the characteristics of the enzymes or the absence of features that would allow them to be precisely assigned to a particular subclass. Examples of PET-active hydrolases are in Table 1.7.

Table 1.7 PET degrading polyester hydrolase adapted from (Sun., 2024)

Enzyme	**Source**
PHL7, PES-H1 and PES-H2	Compost metagenome
Ple628 and Ple629	Marine microbial consortium
Enzyme 403	*Ketobacter* sp.
Enzyme 711	*Thermobifida cellulosilytica*
GlacPETase	Glacier metagenome
SIBER-1	*Microbispora* sp.

In PAZy database, there are 125 enzymes with proven PETase activity by the time of writing this review. Among them are bacterial, fungal, archaeal and even mentioning of human enzymes with PETase activity. It was identified, that well known mammal-origin natural phase II metabolic isozyme glutathione S-transferase P1-1 (hGSTP1-1) is capable of degrading amorphous PET under physiological conditions (Huang et al., 2024).

1.4.1.6. Biodegradation of polyurethane

Polyurethane (PUR) is a common name for plastic derived from the condensation of poly-alcohols (polyols) (–OH) and di– or polycyanates (–NCO) with the linkages of urethane bonds (Buchholz et al., 2022).

After PET, polyurethanes represent the second most common class of plastics capable of hydrolytic cleavage. This makes polyurethanes an attractive target to study enzymatic processing. They are used in the production of soft foams (e.g. mattresses, sponges), rigid foams (insulation and building materials), thermoplastics (sports shoes) and various coatings (sealants, paints and adhesives).

There are two types of PUR: polyester and polyether PUR (Fig. 1.10). PUR synthesised from polyester polyol is polyester PUR, and that synthesised from polyether polyol is polyether PUR. Although most of manufacturing PUR is polyether polymer, polyester PUR possesses higher biodegradability due to the presence of ester bonds in addition to urethane bond (Nakajima-Kambe et al., 1999).

The primary PUR bond – urethane (carbamate) bond includes C-N and C-O bonds, can be hydrolysed by urethanolytic enzymes or esterolytic enzymes, respectively. Among urethanolytic enzymes that catalyse hydrolysis of C-N bond within urethane bond are urethanases, amidases and ureases; among esterolytic enzymes active against C-O bonds are esterases, cutinases and lipases (Raczyńska et al., 2024).

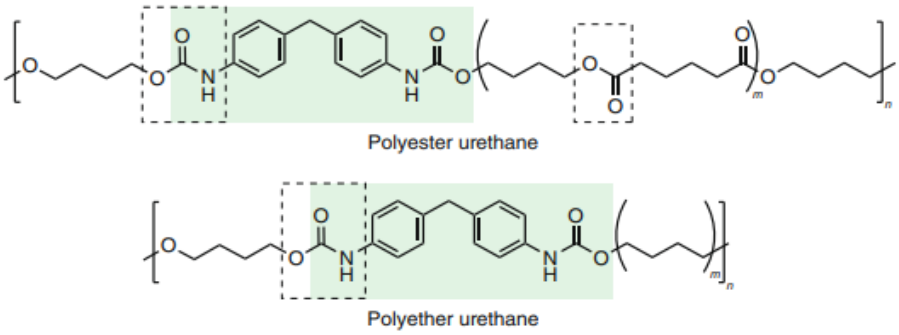

Fig 1.10. Chemical structure of PUR with hydrolysable bonds in squares. Adapted from Chen et al., (2020).

In this process, C–O bonds are more susceptible to biodegradation than C–N bonds, that is why only PUR active esterases (that mostly act on ester bonds and less often on C–O part of urethane bond) have been reported. However, it should be noted that esterases are sometimes capable of attacking amide bonds as well (Raczyńska et al., 2024). Furthermore, ester PUR is more hydrophilic, which also facilitates biodegradation, allowing water molecules and enzymes to penetrate into the polymer structure. Among the most effective PUR active enzymes are *Pseudomonas chloroaphis* polyurethanases (lipases) PueA, PueB ; PulA lipase from *Pseudomonas fluorescens*, and lipases PueA and PueB from *Pseudomonas protegens* Pf-5. Among the most effective urethanases, that catalyse degradation of PUR monomer, are recently discovered UMG-SP-2 urethanase and *Lysinibacillus fusiformis* urethanase, more known bacterial enzymes associated with the process of degradation are listed in Table (Appendix B). At the time of writing this review, there are 35 enzymes with proven PUR activity in the PAZY database (Buchholz et al., 2022).

1.5. Methods of identification of the potential of the environment to biodegrade (micro)plastics

Assessing the potential of the environment for biodegradation of microplastics is a complex task. Metagenomics is one of the most powerful tools to uncover microbial diversity and functions as it bypasses the need to cultivate microorganisms, over 90% of which are not amenable to cultivation (Chaudhary et al., 2019). To study the plastic degrading potential of microorganisms following metagenomics approaches can be applied (Purohit et al., 2020).

Microbial community analysis

Analysis of the composition of microbial community of the plastisphere, performed by sequencing of amplicons of marker genes, such as the 16S rRNA gene for bacteria and the ITS region for fungi can reveal the members potentially involved in plastic biodegradation. Alternatively, marker gene sequences can be extracted from whole metagenome sequencing results and further analysed (Kim et al., 2016). Microbial community analysis alone does not provide direct information about plastic degrading enzymes, functional gene abundance prediction based on microbial community composition using PICRUSt (Phylogenetic Investigation of Communities by Reconstruction of Unobserved States) analysis can reveal metabolic characteristics of the community (Kim et al., 2022). Research is being conducted to determine the dependence of the prevalence of certain taxa of microorganisms for each specific type of plastic (Purohit et al., 2020).

Targeted gene sequencing (gene-targeted metagenomics)

Targeted gene sequencing can be applied not only to aforementioned assessment of the bacterial community, based on 16S rRNA gene variations, but also to various functional genes, for detection

of their presence, polymorphisms and large rearrangements in them. This is useful data to reconstruct the evolutionary trajectory of these genes or to search for variants with improved catalytic activity, identify patterns of critical polymorphisms, which would be an excellent support for protein engineering of these enzymes for further targeted applications. Integrating targeted gene sequencing with heterologous expression and screening them for activity, could facilitate the selection of the most efficient enzyme variants (Kim et al., 2022). However, this type of analysis does not provide the possibility to search for *de novo* enzymes.

Functional metagenomics

Functional metagenomics is a highly suitable method to identify enzymes with target function that *de novo*. However, for the method to work effectively a lot of details need to be taken into account. Due to the heterogeneity of metagenomic DNA, the selection of the expression system must be done very carefully (Schmeisser et al., 2007). At any step from transcription to post-translational modifications and activity, the conditions for the enzyme may not be suitable and the target gene may escape attention. Another important point to consider is that plastic biodegradation enzymes are mostly exoenzymes, thus, the design of the experiment should include either a mechanism for exporting the expressed protein to the outside of the cell, or the use of alternative substrates that could be incorporated into cells without the initial breakdown and that correctly reflect the target activity, if present (e.g., tributyrin for PET) (Sulaiman et al., 2012).

Whole metagenome sequencing

In the context of searching for target genes, this method of screening is sequence-based rather than function-based and is fully dependent on the sequences of previously characterised plastic degrading enzymes**.** For this approach, databases of plastic degrading enzymes were created to facilitate their search in whole metagenome data. Plastic DB is a database of both microorganisms and enzymes involved in the degradation of both biodegradable and recalcitrant plastics (Kim et al., 2022). RemeDB is another database that aggregates various enzymes for the biodegradation of hydrocarbons, dyes and plastics (Subramanian et al., 2020). RemeDB and Plastic DB provide the ability to identify the sequences of these enzymes in full metagenomic sequence data (Subramanian et al., 2020; Kim et al., 2022). Using these databases, profiling plastic degradation-related genes in the plastisphere is possible. That is, it is possible to collect knowledge about which genes are most typical for sites with one or another prevalent plastic pollutant.

In order to move beyond reference-based approach and attempt to search for novel plastic-degrading enzymes in metagenomic sequences, it is important to collect metagenomic DNA from diverse sources and, through comparative analysis, identify genes that are more characteristic of plastisphere-associated microbiota. Also, HMM and BLAST searches based on already characterised

enzymes allow one to identify distant homologues of identified genes with potentially similar function and possibly greater efficacy (Kim et al., 2022).

1.6. Potential sources of microbiota (genes) are capable of plastic biodegradation

The idea behind it is intuitive and straightforward: to identify microorganisms capable of degrading a particular substrate, one should focus on environments where this substrate has been abundant for an extended period.

This aligns with the Principle of Microbial Infallibility, proposed by Martin Alexander in 1964 that postulates that microorganisms will always find a metabolic way to take advantage of available energy sources (Alexander, 1964). This points to such environments as landfills, recycling plants and other plastic-rich sites as promising reservoirs for plastic-degrading microorganisms. As an example, it can be mentioned that Yoshida with colleagues discovered *Ideonella sakaiensis* bacterium capable of efficiently utilising PET, in PET contaminated soil near a recycling facility in Japan (Yoshida et.al., 2016). According to the statistics collected by Gambarini et.al (2021), most of the putative plastic degraders were isolated from soils (27.8%), plastic waste landfill sites (9.6%) and composts (5.3%), while 15.9% were obtained from microbial culture collections (Fig.1.11).

The work of Zrimec and colleagues (2021) showed that the more plastic in the environment, the higher the abundance of genes responsible for its degradation. This emphasises the important role of the plastisphere – a microbial ecosystem that forms on the surface of plastics – as a promising source of genes involved in the biodegradation of synthetic polymers.

However, as mentioned above, despite the fact that polyethylene is the most widely used plastic today, a broad range of enzymes capable of efficiently degrading it has not yet been identified. This suggests that prevalence is an important factor, but not the main determinant of xenobiotic biodegradation efficiency.

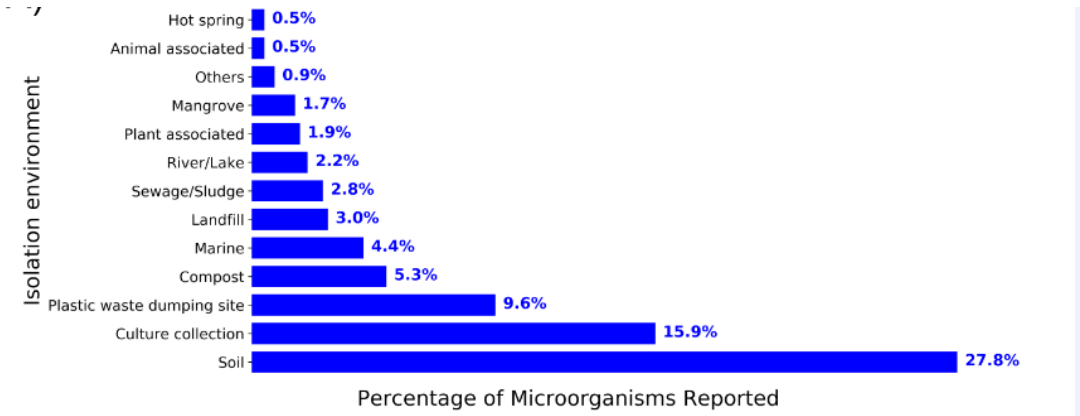

Fig.1.11 Environments from which microorganisms with plastic-degrading capabilities were isolated (Gambarini et.al 2021).

1.7. Considerations for PCR analysis of metagenomic DNA

Despite the fact that the metagenomic approach has opened a lot of opportunities in the genomics of microorganisms, its compositeness and heterogenicity impose certain limitations and pitfalls. One of the sources of incorrect results is selection of an unsuitable method of DNA extraction. To avoid it, the physico-chemical characteristics of the specimen must be taken into account to promote efficient disruption of cell walls and membranes, and removal of contaminants (Hugerth & Andersson, 2017). Insufficient extraction efficiency or excessively aggressive techniques will lead to distorted profile when assessing community composition. Thus, extraction efficiency is the first source of bias (Fig.1.12). Metagenomic DNA is often extracted from multi-component substances, e.g. soil, faeces. It is important that the method addresses the need to clean samples from a wide variety of impurities. Residual amounts of impurities will inhibit subsequent reactions (e.g. amplification) carried out with the DNA sample (Alaeddini, 2012).

Metagenomic DNA is highly heterogeneous in GC content while PCR is more likely to amplify regions with lower GC content, which can introduce bias into the results. This circumstance should be concidered when choosing denaturation conditions (Aird et al., 2011).

Another factor that should be taken into account is metagenomic DNA concentration in reaction. To find the most suitable DNA concentration, there are three points to be balanced: 1) the target gene in metagenomic DNA may be present in extremely low quantities, e.g. in single copy, 2) high concentrations of DNA inevitably inhibit polymerase activity (Alaeddini, 2012), 3) increasing the number of cycles increases the presence of PCR artefacts such as chimeric DNA (Wintzingerode et al., 1997).

Due to the diversity of DNA in metagenomic samples, there is an increased risk of formation of chimeric DNA, that are molecules containing partial sequences from two or more biological sequences. Such chimeras can compromise the results by indicating the presence of a sequence that is not actually present in the metagenomic DNA (Wintzingerode et al., 1997).

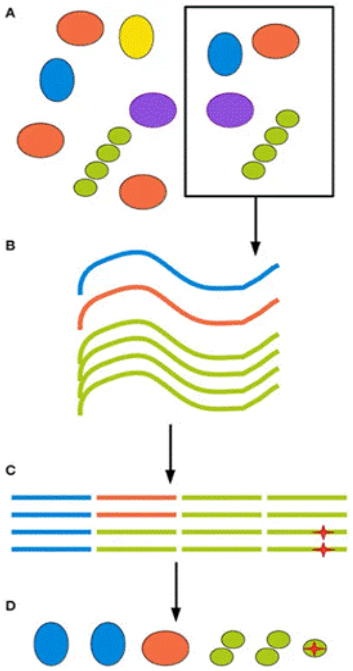

Fig. 1.12 Experimental steps that can contribute to the total bias. (A) Not all microorganisms inhabiting the collection site may be present in the collected sample, and those that are collected may be in skewed proportions. (B) The efficiency of DNA extraction is different for different groups of microorganisms. (C) Amplification and sequencing both introduce biases and point mutations (red stars), as well as possible chimerism. (D) The result may give a distorted view of the original microbiota adapted from (Hugerth & Andersson, 2017).

1.8. Prospects

At the moment, there is an active accumulation of fundamental understanding of plastic biodegradation processes. Projects related to the implementation of the knowledge gathered by this time are beginning to appear. Some of the current developments focus on the upcycling capability of plastics. This is due to the fact that such plastics as PET experience a loss of mechanical properties during static thermomechanical processing (Wu et al., 2019).

In a paper published in 2020 by a French research group, an improved version of Leaf Branch Compost Cutinase with a modified active centre was developed. The ICCG variant with higher thermostability was selected from several variants for further studies with an efficiency of 90% in 10 hours of treatment (in comparison with 45% of wild type). After depolymerisation, resulting monomers (terephthalic acid, TPA) purified, used to synthesise PET again and blown into bottles, closing the circular economy loop (Tournier et al., 2020). The development of the LCC^{ICCG} enzyme variant gave rise to the opening of a plastic recycling (PET waste circularity) plant based on Carbios biotechnological company (Principal scheme of the processes in Fig. 1.13).

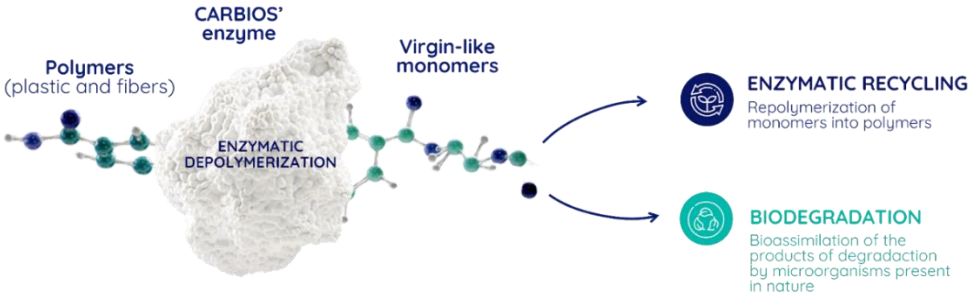

Fig.1.13 Principal scheme of the processes at the Carbios biotechnology plant. After depolymerisation, the monomers can be either fully biodegraded or recycled (Carbios, official website https://www.carbios.com/).

Another example of the big scale implementation of plastic biodegradation technology is Breaking^{TM}, founded in 2024 incubated in Colossal Biosciences with research of Harvard University's Wyss Institute. As stated on the official website, they have developed a bacteria called X-32 that can degrade various types of plastic, including polyolefins, polyesters and polyamides, in 22 months without pretreatment. The company is currently working to improve the efficiency of X-32 using synthetic biology and machine learning, with plans to commercialise the technology in 2025, further details are not disclosed so far (Wyss Institute, 2024, https://wyss.harvard.edu).

By the time of writing this review, no other than the above-mentioned attempts to bring the plastics bioprocessing process to a big-scale level have been found in open sources, which proves the relevance and necessity of research in this field.

Enzyme genes for plastic upcycling, in particular for converting them into valuable substances are of great interest (Veluru, & Seeram, 2024) As mentioned above, terephthalic acid is a product of depolimerisation of PET (Appendix A) (Tournier et al., 2020). Among valuable substances that can be obtained from TPA are gallic acid, pyrogallol, catechol, muconic acid and vanillic acid. From styrene, polysterene monomer, mandelic acid can be obtained in 4 enzymatic reactions with the yield of 70%. Conventional method to synthesise widely used in cosmetics mandelic acid involves toxic cyanide, thus alternative biological approach would be highly beneficial (Veluru, & Seeram, 2024).

Biodegradation pathways for the majority of plastics remain largely unexplored, and even for those for which pathways are known, such as PUR and PET, their implementation is slow and limited. Although the number of studies in this area is steadily increasing every year, research is still at its naive stage.

2. RESEARCH MATERIALS AND METHODS

2.1. Samples collection sites

Samples analysed in this study were collected from different both environmental and artificial sites. In total 47 samples were in operation; different groups were involved in different stages of the study.

Among groups: **KR** samples collected from Kariotiškės landfill. Kariotiškės landfill is a former municipal waste disposal site that was opened in 1987 and closed in 2008 and, according to estimations, accumulated 3 million tons of differnt wastes, plastic as well. Nowadays it is still and covered by ground. The exact collections spots are marked on the satellite map (Fig. 2.1 a)). In this study 9 samples collected on this site were analysed: KR1(T), KR1(B), KR2(T), KR2(B), KR3(T), KR3(B), KR4(T), KR4(B) and KR5. For these samples and samples below: “T” in the brackets indicates that the sample was collected from the top of the ground; “B” indicates that the sample was taken at a depth of 10 cm. If no letter is indicated next to a sample, it was collected from the top layer.

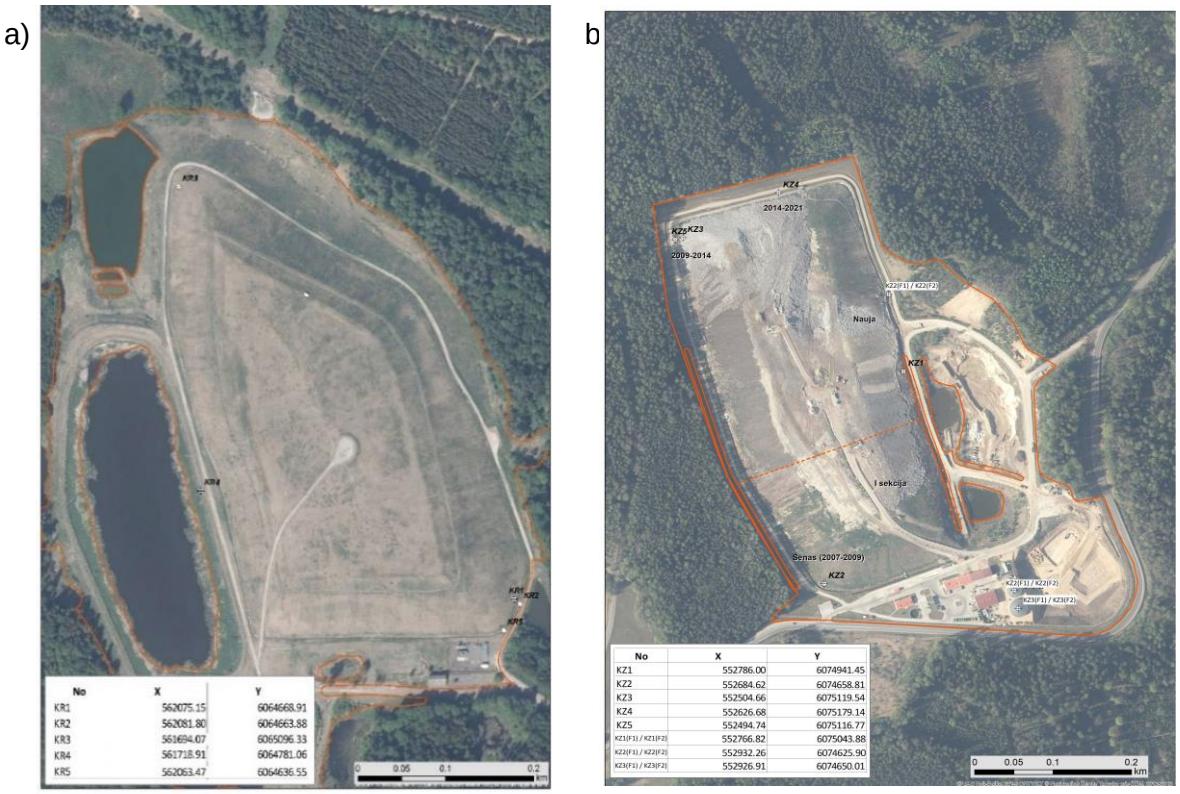

Fig 2.1 Sattelite maps with marked sample collection spots (a) Kariotiškės landfill (b) Kazokiškės landfill.

(**KZ**) samples were collected form active Kazokiškės municipal dump site. It was opened in 2007 and has already accumulated more than 2 million tons of garbage. The exact coordinates of

collection spots are marked on the satellite map (Fig 2.1 b). In total, 8 samples were analysed: KZ1, KZ2, KZ3, KZ4(T), KZ4(B), KZ5(T), KZ5(B).

Fig. 2.2 Drainage channel along the Kazokiškės landfill (KZ1(F1) and KZ1(F2) samples collection spot).

(KZ(F)) Samples marked as KZ2(F1), KZ2(F2) and KZ3(F1), KZ3(F2) on Fig.2.1(b) were derived from filtration and sedimentation tanks that collect leachate from the landfill site. Samples KZ2(F1) and KZ3(F1) (not included in the legend of the figure) were collected from the same tanks but at different times:

KZ2(F1) / KZ2(F2) – from filtration tank №1. Samples collection took place straight after filtration and after 4 weeks of sedimentation, respectively.

KZ3(F1) / KZ3(F2)– from filtration tank №2. Samples collection took place after 3– and 12-weeks post-filtration sedimentation, respectively.

Samples KZ1(F1) and KZ1(F2) were derived from the drainage channel (Fig 2.2; Fig 2.1.(b)), sample KZ1(F1) – six months earlier.

(C) clean site soil samples were collected from a garden in Molėtai district. It is assumed that there the level of xenobiotics contamination is minimal. Such samples as C1(T), C1(B), C2(T), C2(B), C3(T), C3(B), C4(B).

(P) samples were collected at Energesman waste sorting plant. 5 samples were analysed: P1, P2, P3, P4 and P5. P1 is a mud sampled from the floor near the heating chambers (Fig**.** 2.3 (b)); P2 and P3 – collected from the chambers with grinded waste plastic that was incubated for 28 days at increased temperature (55 – 70 °C); P4, P5 – plastic fragments collected immediately after the shredding process.

Regarding the thermal pretreatment of plastic particles (P2, P3 samples) there are several reasons to implement this. It is proven that increased temperatures promote the initiation of microbial biodegradation of plastic pieces by increasing the availability of bonds for enzyme attack (James-Pearson et al., 2023). That is due to the fact that thermal effects change the degree of crystallinity of petropolymers and its morphological features. This occurs at the so-called glass transition temperature. At these temperatures, the material converts from a hard state to a soft semi-molten state, more susceptible to biodegradation. For example, this is characteristic of PET, which under normal conditions is resistant to biodegradation because its ester bonds are hidden under aromatic groups. In Chapter 1.4.1.5 it is mentioned that the optimal temperature of *Thermobifida fusca* hydrolase is 55 °C. This is due to the fact that many organisms that compost organic matter/degrade plastic are thermophiles (Wei & Zimmermann, 2017). Also, during intensive heating (70–80°C), oxidised groups such as carboxyl, carbonyl and hydroxyl may be formed (Kotova et al., 2021). This is also very important for plastics that require pre-treatment to introduce oxygen into the structure in order to enable the action of enzymes, such as PE, PP and PVC.

a) b)

Fig. 2.3 Energesman waste sorting plant, a), b) specimen sampling sites.

D samples (2) were collected from Dusia lake, sediment, (collection spots are marked in yellow squares on sattelite map (Appendix C. Fig.C1 (a)), Dus2 and Dus3 correspond to D1 and D2 samples, respectively); **K** sample was sediment collected from the Kalesninkai pond (exact coordinates not provided is this study); **(S) S** samples (3) are sediments that were collected from Simnas fishery reservoir (collection spots are marked in yellow squares on sattelite map (Appendix C. Fig.C1. (b)), samples SŠ2, SŠ3 and SŠ4 correspond to S1, S2 and S3 respectively). **R** samples (3) are sedimentsthat were collected from road runoff near the Gubesėlė River (sample collection spots are shown in satellite map (Appendix C. Fig.C2), GS2, GS4 GS6 correspond to R1, R2 and R3 respectively). **BP** samples (4) were collected from beaver dam at Nevėža Lake (Vilnius region), (BP1(T), BP1(B),

BP2(T), BP2(B)) two from the top (T) and two from the bottom part (B), in an urbanized, inhabited area along the lake shore. Exact coordinates can be provided upon request by colleagues who have provided samples.

2.2. Materials used in the work

Reagents used in the work:

- DNA fragment size standard Gene Ruler™ DNA Ladder Mix (SM0331) (Thermo Fisher Scientific);
- EDTA disodium salt dihydrate (Sigma Aldrich);
- Electrophoretic DNA loading dye TriTrack (6X) (Thermo Fisher Scientific);
- Ethanol (alc. 96%; Vilniaus degtine);
- Ethidium bromide (Sigma Aldrich);
- Glacial acetic acid (Merck);
- Isopropanol (Merck);
- NaOH (Sigma Aldrich);
- Nuclease-free water (Thermo Fisher Scientific);
- PCR Master Mix DreamTaq Green (2X) (Thermo Fisher Scientific);
- Primers (listed in Table 2.1) (Linea Libera, Eurofins);
- TopVision Agarose (Thermo Fisher Scientific);
- Tris base (Sigma Aldrich);

Commercial kits used in work:

- ZymoBIOMICS ™ DNA Miniprep Kit for genomic DNA isolation (Zymo research™);
- GeneJET Gel Extraction Kit (Thermo Scientific™);

Equipment used in work

- Biological Safety Cabinet Class2 Safe 2020 (Thermo Scientific™);
- Electronic table scales (Kern);
- Electrophoresis imaging system DNA Bio-Imaging System (MiniBIS Pro);
- Homogenizer, Bullet Blender® Homogenizer (Next Advance);
- Horizontal gel electrophoresis chamber system Mini-Sub Cell GT Horizontal Electrophoresis System (Bio-Rad);
- Horizontal gel electrophoresis chamber system Wide Mini-Sub Cell GT Cell (Bio-Rad);
- Microtubes 1.5 ml, 2 ml (Nerbe plus);
- Spectrophotometer (NanoDrop 2000);

- Spectrophotometer (Thermo Scientific™ NanoDrop™ One Microvolume UV-Vis);
- PCR tubes 0.2 ml (Nerbe plus);
- Pipetes (Eppendorf Research, Thermo scientific);
- Pipete tips (Nerbe Plus);
- Power source (Consort E865);
- Table centrifuge (Eppendorf 5424);
- Thermocycler (PTC Tempo, BIORAD);
- Thermo–Shaker TS-100C (biosan);
- Transilluminator-UV (Biometra TI 1);
- Vortex mixer (Velp SCIENTIFICA);

2.3. Preparation of reagents used in work

50X TAE buffer

To prepare 100 ml of the 50X TAE buffer solution, 24.20 g of Tris base was dissolved in 70 ml of distillate H_2O. 10 ml of 0.5 M EDTA and 5.71 ml of glacial acetic acid were added to the solution and mixed well. After, the volume was adjusted to 100 ml and mixed thoroughly. The solution was stored at room temperature.

1X TAE buffer

To prepare 0.5 L of the solution, 10 ml of 50X TAE buffer was dissolved in 490 ml of distillate H_2O and mixed thoroughly. The solution was stored at room temperature.

Agarose gel for horizontal electrophoresis of DNA

To prepare 100 ml of the agarose gel of desired concentration (the concentrations used in the study ranged from 1% to 3% depending on the expected fragment length and the purposes) the required amount (in the range of 1–3 g) of agarose powder was added to 100 ml of 1X TAE buffer, mixed and left for 3–5 minutes to allow agarose hydration and then was boiled until the agarose was completely dissolved (the solution became transparent without inclusions). The flask with the gel was left to cool to a temperature of about 45 – 50 °C, followed by addition of Ethidium bromide in the amount 50 µg (5 µl of 10 mg/ml solution) per 100 ml of the gel to obtain the final concentration 0.5 µg/ml and mixed thoroughly. The warm gel was poured into the prepared mold and left still until solidifying.

2.4. Methods

2.4.1. Isolation of metagenomic DNA

The peculiarities of metagenomic DNA isolation from composite samples are described in Chapter 1.11. In this study ZymoBIOMICS DNA Miniprep Kit (Zymo Research, Cat. No. D4300) was used to isolate the DNA from the samples. This kit was chosen for the following reasons: it is reported that it is designed to avoid bias at the DNA isolation stage, preserve DNA integrity (size of resulted fragments around 15 – 20 kb), thoroughly purify DNA from contaminants, and ensure good yield when used appropriately. The full protocol is available at: https://zymoresearch.eu/products/zymobiomics-dna-miniprep-kit. The recommended procedure was changed regarding the characteristics of the samples to obtain a greater yield of the product:

- In several cases, the recommended mass/volume of starting material was exceeded;
- The homogenisation step was prolonged to 8 min for all samples;
- At variance with the protocol recommendations, the samples were incubated for 5 minutes with a mixture of ethanol and a Binding Buffer instead of 1 minute;
- The incubation of nuclease-free water on the IICR column during elution step was prolonged to 10 min instead of 1 min.

The concentration of the isolated genomic DNA was measured with a NanoDrop™ 2000 spectrophotometer. The isolated DNA samples were stored at – 20 °C.

2.4.2. PCR analysis as a screening approach

PCR analysis can be used as a screening method to identify microbiota capable of degrading various xenobiotics (Neethu et al., 2019). Analysis can be designed for a narrow spectrum of homologous genes or, for that stringent primers are applied, or, conversely, involve degenerate primers to detect a wide variety of gene variants.

PCR procedure

Sets of applied primers and PCR conditions are listed in (Appendix D) Metagenomic DNA isolated using the method described above was used as DNA potentially containing templates. In this study, it was decided not to adjust all the samples to a uniform concentration, but rather to monitor samples with high DNA concentrations (above 150 ng/µl) for inhibition of the reaction. It was found that the amplification efficiency for samples with relatively high DNA concentration 250 ng/µl (250 ng per 50 µl reaction) was not noticeably reduced. However, it was observed that samples with an initial DNA concentration of less than 3 ng/µl yielded almost no product.

Unfortunately, it was not possible to obtain positive controls for tracking PCR efficiency due to the high cost of synthesising or purchasing all strains/cloned genes that could serve as positive template. Negative controls (without DNA addition) were present in all PCRs

Reactions were carried out using a Master Mix™ DreamTaq, a commercially available mixture which contains Taq polymerase as an enzyme, as well as premixed nuclease-free water, buffer, dNTPs, dye and density component.

Conditions for PCR reactions were chosen based on the data provided in the literature (for the primers adopted from previously published studies) or developed in this study (for the primers that were designed in this study). In addition to the main stages, single stages of preliminary denaturation and final elongation were applied to all PCRs. The number of cycles increased to 35 – 40. For negative control, an equal volume of water instead of metagenomic DNA was added.

50 µl PCR mixture consisted of:

- 22 µl of nuclease-free water;
- 1 µl of Forward primer;
- 1 µl of Reverse primer;
- 1 µl of metagenomic DNA;
- 25 µl of 2X DreamTaq DNA Polymerase Master Mix.

Final concentration of each primer in the reaction was 2 µM (pmol/µl). PCR reactions were performed in BIORAD T100 and BIORAD PTC Tempo thermocyclers under the conditions described in Appendix D.

Some PCR products used in this study were generated during a bachelor's thesis project. In the Results section, it is indicated which of the previously obtained results are used in current work.

DNA electrophoresis procedure

DNA electrophoresis was performed to evaluate the results of PCR.

Electrophoresis agarose gel was prepared as described above and immersed in a horizontal electrophoresis chamber system Wide Mini-Sub Cell GT Cell (Bio-Rad) filled with 1X TAE buffer solution. The MasterMix used for PCR contained convenient dyes visible under room light, which are separated during electrophoresis in the same direction as DNA to track the migration of fragments of the desired length, and density reagent, which makes it possible to load the products directly from the PCR tube without prior mixing with the loading dye. For post-PCR results assessment, 6 µl of samples were loaded. For isolation of amplicons from the gel, in each case the volume of the loaded mixture was determined separately for the best yield.

As a fragment lengths standard, 3.5 µl of Gene Ruler™ DNA Ladder Mix (SM0331) were loaded. For this, it was mixed with loading dye and nucleases free water in the ratio 1:1:4, respectively. Electrophoresis was carried out at a voltage of 10 V per 1 cm of gel length. After, the gel was

visualised under UV light in an Electrophoresis imaging system (MiniBIS Pro (DNA Bio-Imaging System)). Results were analysed manually.

2.4.3. Primer design

The primers that were designed in this study are indicated in (Appendix D) The tools that were used for this were: NCBI primer design tool Primer-BLAST and OligoArchitect™ online (Sigma Aldrich). Among criteria were: increased annealing temperature, absence or minor presence of secondary structures and primer-dimers, extended length (26 – 30nt). Primer pair PHL7_F/R was constructed based on sequence with accession number LT571446.1, CE_Ubrb_F/R on sequence with accession number SIP63154.1; VpSty_F/R from reference sequence MF781075.1.

2.4.4. Amplicon sequencing

By obtaining an electrophoretic profile of the PCR results, it is possible to make a preliminary conclusion on whether the desired gene is present in the metagenomic DNA sample. However, without confirmation by sequencing, one must be cautious about the positivity of the result.

In this study, two approaches to the sequencing of PCR amplification products were applied: isolation of a specific amplicon from an electrophoresis agarose gel, which ensures that only the product of the expected length is sequenced; and sequencing of all amplification products from a PCR mixture without prior extraction from the gel.

The second method allows sequencing of all DNA fragments amplified with primers to the target gene and would be useful if more than one product is observed in the electrophoretic pattern (even under optimal conditions minimising the possibility of non-specific annealing of primers). Sequencing PCR products without prior gel extraction, including those obtained from multiplex PCR, is a common practice (Hojgaard et al., 2024). It is generally used after the absence of non-specific amplification has been confirmed to reduce the number of steps in sample preparation and minimise DNA loss. However, in this case, such technique may potentially provide information about genetic variability of the target gene, which gives significant differences in length (e.g. indels, duplications), amplification of homologous genes if they have similar sequences in the primer annealing sites. The choice of approach also depends on the required depth of analysis and technical capabilities.

2.4.4.1. PCR product extraction from the agarose gel

To extract the DNA from an agarose gel after electrophoretic separation, bands of the required sizes were cut out with scalpel of the gel while visualising them with Transilluminator-UV (Biometra

TI 1). The scalpel was constantly rinsed in distilled water to reduce the risk of cross-contamination of amplicons. Appropriate safety measures were taken when working with direct UV light. To reduce DNA damage, UV exposure time was minimised. Gel pieces containing DNA were kept for a short time (up to 48 h) at +4°C. DNA was extracted from the gel using a commercial kit GeneJET Gel Extraction Kit (Thermo Scientific™) in accordance with the protocol with several modifications: during the stages of membrane binding and DNA elution, the solutions were passed through the membrane twice; the incubation time of the elution buffer on the membrane was extended to 10 minutes. The full protocol is available at: https://www.thermofisher.com/order/catalog/product/K0701. Concentrations were measured with a Thermo Scientific™ NanoDrop™ One Microvolume UV-Vis spectrophotometer.

2.4.4.2. Library preparation and sequencing (extraction from the gel approach)

DNA of 134 bands successfully isolated amplicons were distributed into 54 pools that contained them from 1 to 3. Prior that, concentration of all DNA samples was adjusted (where possible) to required numbers: 10 – 20 ng/µl, for amplicons >1kb <5kb, 5 ng/µl, for amplicons >200 bp <1kb and 1 ng/µl for amplicons <200 bp. After that, they were pooled in the ratio of 1:1 (for 2) or 1:1:1 (for 3). Ther rules that were followed for mixing: the difference between (among) amplicons in size in 1 pool fell in the range of 200 – 600 bp; pooled amplicons were not from the same class of enzymes. Prior to full-scale sequencing, pilot experiment was done to develop a scheme for mixing amplicons into pools that would yield high-quality results.

Further preparations and sequencing were carried out by sequencing facility UAB Seqvision. DNA sequencing was performed on the Oxford Nanopore platform. The used protocol implied sequencing of one strand of DNA molecules. More details can be found in Appendix E.

2.4.4.3. Analysis of obtained sequences

Primary data analysis was done by the mentioned sequencing facility by Junior Scientist, Technical Specialist Jonas Juozapaitis. Consensus sequence generation was carried out using amplicon_sorter, tool designed for analysis of short Oxford Nanopore reads with default parameters (Vierstraete & Braeckman, 2022). This is important for the further interpretation of the results. The detailed procedure can be found in Appendix E. The data for subsequent analysis after primary processing was obtained from sequencing facility in fasta format.

Sequences of expected length were extracted from the data. In addition to fragments of the expected length, which represented peaks, shorter fragments and longer reads were also present

(Fig.2.4, indicated by red boxes). Shorter reads are artefacts of the stage of DNA extraction from the gel. During this stage, part of the DNA is fragmented due to the breaks during UV exposure, mechanical damage, such as intense vortexing, damage when cutting out a fragment, or excessive heating during the gel melting stage. Longer read are artefacts caused by multiplexing. Small fraction of reads were misassigned due to barcode or base-calling errors. This is a limitation of technology.

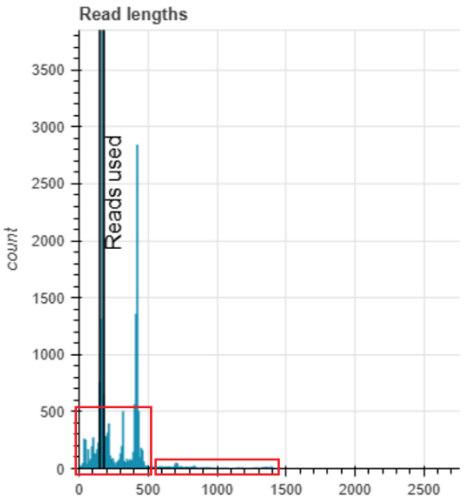

Fig. 2.4. Example of the graph of lengths distribution in pool. There are two main peaks with expected fragment lengths of approximately 170 bp and 420 bp.

The output of amplicon_ sorter tool is a file containing the consensus sequences found for the selected peak. There may be one or more consensus sequences due to the heterogeneity of the metagenomic DNA (Fig.2.5).

```
>consensus_Amplicon_14.selected_0_0(1678)
TCGAGCACATCCGCGGCCACCATTGAGACAACCACGCCAGCCGGCGGGGCCCAGCGCTGCCGCAACCAAGCGCTCCCGGTGACGGCGCTGGACTCC
GCCGCTTGATCGAGCCTGTCGCTCGACGAACGAAGGGAGCGTCACCATGCCTACCTCGACTGCGATGCCTAGTGCTAGGCCGACTGCGACGTTCGA
GACCAGCCAGGAACGCCGCTGGACGATCACGAATCCCCGACTGCGGCTGAAGCCCACGTACGGGACGAGAGGTGTTGTGCAGGGCGGCTGGTGGCC
GCGGATGTGCTCGA
>consensus_Amplicon_14.selected_0_1(92)
CCGTAGTGCTCGACGTAGTTGACGGCCTCCAGCAGGCAGAACCCGATGACCGCCTGCCCGATGAGCCACGGCAGCACGACGATGCCGAACCACACG
ATCAGGACGGCGTACAGCACCACGGTCAGCGCCCATGCGTTGAGCACGTCGTTGCGCAAGCTCCACGGCGTCGTGCCGATCCGCCTGAACCGGGCG
CGCTCGAGTTGCCAAGCCGATCGCACGCCGCCGGTCACCGAACGACGGATGAACGCGTAAAGCGATTCCCCCAGTTGCGAACTCGCGGGGTCTTCC
GGGGTGGCGACCCTGGCGTGGTGGC
```

Fig. 2.5. Example of fasta format file with 2 consensuses. Red squares indicate the number of sequences (molecules) included in the construction of this consensus.

Amplicon_sorter combines sequences into a consensus based on their nucleotide similarity and length (Fig 2.6). Grouping begins with a set of reads that are at least 93% similar to each other. From this starting subgroup, the first draft consensus is formed, to which the remaining reads are then added. A sequence is added if it has at least 95% similarity to the current consensus and differs in length by no more than 5%. If, after several iterations, there are still unassigned reads, the threshold can be gradually reduced to 85%, but this does not always happen and depends on the data. sequences that cannot be assigned to any consensus are recorded as “unique”. Consensuses are merged into one

if two conditions are met: they must be 96% identical to each other in sequence and differ in length by no more than 8%. Otherwise, they are considered different (Vierstraete & Braeckman, 2022).

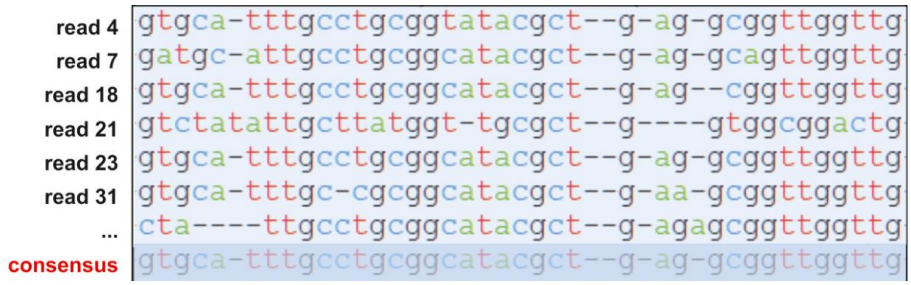

Fig. 2.6. Principle of constructing a consensual sequence of amplicon_sorter tool, (adapted from Verstraete & Braeckman, 2022).

As can be seen from the methodology for combining sequences into consensuses, this method is not well suited for determining the strain or even species (for species with low divergence) identity of sequences, as it may 'average out' single-nucleotide substitutions that are crucial for strain identification. However, species with ≥ 5% divergence in the target gene are reliably separated into distinct consensus groups.

This approach was chosen over reference-based methods due to the experimental design. Working with metagenomic DNA implies that the sample may contain undescribed or unsequenced taxa. Even with stringent primers, there can still be substantial divergence between taxa. In some cases, only a small, conserved motif may match the original target sequence, which is important to be captured but would likely be missed by reference-based approaches.

Consensuses were analysed with BLASTx (Basic Local Alignment Search Tool x) tool available from the Galaxy Web service (usegalaxy.org server) that performed protein homology search (Afgan et al., 2018). It identifies potential protein products encoded by a nucleotide query. For this, it translates nucleotide query and searches protein databases for homologs. The search parameters were default, the number of hits to display was reduced to 5 – 10. The Results section contains tables with the most significant search hits (regarding e-value) or the most significant in each context. BLASTx was used as a primary tool of analysis due to the fact that protein sequences are more conserved than DNA sequences.

In cases required clarification of similarity between the obtained and the target sequences for which the primers were developed, pairwise alignment was performed using the NCBI BlASTn Web service with default parameters. BLASTn finds regions of local similarity between nucleotide sequences.

2.4.4.4. Sequencing of PCR product mixtures

Sequencing of mixed PCR amplicons was performed at the Department of Biochemistry and Molecular Biology by Senior researcher, Dr. Aleksandras Konovalovas on the Oxfrod Nanopore Technologies platform.

A distinctive feature of this approach was that all PCR products from each sample were combined to create a single pool of amplicons per sample. Post-pooling, the samples were cleaned with magnetic beads to remove salts, dyes, primers, dNTPs, resulting in concentrated DNA that was subjected to sequencing and primary data analysis. More details can be found in Appendix E.

2.4.4.5. Analysis of results of sequencing of PCR product mixtures

Obtained after primary analysis fasta files contained amplicons with specified length and coverage (cov) (Fig 2.9).

```
>NODE_39_length_173_cov_475.108696
GATCGTGTCGAGGTCGGCCCCGATGATCAGCGTCGGCACGGTGACGCTGCTCCAGTTCTT
GTTGAGGTGCCACGGGGTGAGCGGGATGGCGGCCTTCAGGTCGGGACGCTGGGAGGCCAG
ACGCAGGGTGCCGCCGCCGCCCATGGAGTGGCCCATGACCGCCAGTCGGCTGC
```

Fig. 2.9. Example of obtained fasta file.

However, it should be noted that a significant portion of the sequences were found to be of low complexity, which could be either sequencing or PCR artefacts (Fig. 2.10.). It is important to emphasise that some of them were present in significant quantities (coverage outlined in red) and, if this is a PCR artefact, it could appear as a pronounced band on the electrophoretic profile.

```
>NODE_8_length_347_cov_7724.740909
ATTCCATTCCATTCCATTCCATTCCATTCCATTCCATTCCATTCCATTCCATTCC
ATTCCATTCCATTCCATTCCATTCCATTCCATTCCATTCCATTCCATTCCATTCC
ATTCCATTCCATTCCATTCCATTCCATTCCATTCCATTCCATTCCATTCCATTCC
ATTCCATTCCATTCCATTCCATTCCATTCCATTCCTTCCATTCCATTCCATTCCA
TTCCATTCCATTCCATTCCATTCCATTCCATTCCATTCCATTCCATTCCATTCCA
TTCCATTCCATTCCATTCCATTCCATTCCATTCCATTCCATT
```

Fig. 2.10 Example of artefact of analysis.

For determining the nature of the amplicons/ NCBI blastn Web service with default parameters was used. For searching for sequences containing used primers EMBOSS:primersearch tool available through Galaxy (server https://usegalaxy.org) was used. For multiple alignment of the amplicons with similar nature, proven with BLASTn search, Clustal Omega tool was used. For visualisation of the alignments, Jalview Version: 2.11.4.1 Desktop version was used.

3. RESULTS

3.1. Isolation of metagenomic DNA

Metagenomic DNA was isolated from samples with varying efficiency depending on the sample type. Liquid, sandy samples and those composed of plastic particles were poorer in DNA than soil samples. The range of derived concentrations was from 3 ng/µl to 268 ng/ µl. The A260/280 ratio was within the acceptable range of 1.5–2.2, while the A260/230 ratio in most cases was much lower than normal, which can be explained by the multicomponent nature of the soil, presence of humic acid, other aromatic compounds and presence of residual amounts of salts in it (Hu et al., 2010).

3.2. PCR analysis and amplicon sequencing

PCR analysis was performed for 47 samples that belonged to different groups: Clean garden soil samples **(C)** group; closed Kariotiškės landfill (**KR**) group; open Kazokiškės landfill (**KZ**) group, Kazokiškės landfill filtered lecheate (**KZ**(**F**)); samples from Dusia lake sediment (**D**) , Kalesninkai (**K**) pond sediment, Simnas fishery reservoir sediment (**S**); road runoff near the Gubesėlė River (**R**), Samples from beaver dam (**BP**) and samples from Energesman waste sorting plant (**P**). Different groups of samples were involved at different stages of the analysis. PCR products from groups D, K, S, R, BP, and R were not sequenced due to the low detection rate of products.

Partial PCR analysis of samples from groups C, KR, KZ was carried out as part of the bachelor's thesis. In this section, electrophoresis gel images will be shown selectively, based on the applied importance of the amplified gene or the need to highlight a particular aspect. For P samples, electrophoresis gel images of all PCRs will be shown to highlight the diversity of genes and high potential of the samples. Tables include amplicons if they were detected at least once

DNA of 134 amplicons of 34 metagenomic DNA samples from groups C, KR, KZ, KZ(F) and P after PCRs with 18 pairs of primers for various genes were isolated from the electrophoresis agarose gel. Obtained DNA concentrations were measured with spectrophotometer and were in the range from 2.57 ng/µl to to 53.30 ng/µl. A260/280 ratio was in a wide range and often differed significantly (1.42– 11.29) from normal, but this did not significantly affect sequencing. The same applies to the A260/230 ratio: in the majority of cases, it was significantly lower than normal values of 2.0 – 2.2 and was > 0.1. This can be explained by the methodology of DNA extraction: the procedure included the step with guanidinum thiocyanate, chaotropic salt that is used (in combination with other component) to facilitate agarose solubilasation and binding the DNA to silica membranes of columns. This leads to the fact that trace amounts of the substance remain even after washing steps. Guanidine thiocyanate, in its turn, absorbs at 230 nm wavelength, that affects the ratio (Zapeda et al., 2022).

However, it appears that dilution during library preparation was sufficient, and trace amounts did not affect the performance of enzymes of library preparation and sequencing itself, as demonstrated by the informativeness of the data obtained.

Below in this section the results of PCR analysis and blastx homology search of sequences of the amplicons are presented. The data obtained in the bachelor's thesis marked accordingly. All the rest data was obtained as a part of the master's thesis.

3.2.1. Genes of hydrolases

As mentioned in chapter 1.5.2., hydrolases are one of the key enzymes in the biodegradation of plastics. Their job is to break down a chemical bond in the presence of water, resulting in the break-down of a larger molecule into smaller molecules. Hydrolases are active on such plastics as PET and PUR since they have hydrolysable ester and urethane bonds (Chapters 1.4.1.5., 1.4.1.6.). The results for some hydrolases analysed in this study are given below.

***Fusarium solani* cutinase**

Primer pair Cut4_F/Cut4_R was used to detect cutinase gene from *Fusarium solani* (Alexandrakis et al., 1998). *Fusarium solani* it is a phytopathogenic fungus that uses cutinase to invade its host. In the chapter on PET biodegradation (1.4.1.5), this enzyme is mentioned as an enzyme that modifies the surface of PET, in particular, increases its hydrophilicity (Alisch-Mark et al., 2006). The results of PCR and electrophoretic analysis for all groups of samples are shown in Table 3.1 and Table 3.2. The picture of electrophoretic analysis for group P samples is Fig. 3.1.

The data in this table was obtained as a part of bachelors' thesis

Table 3.1 Results of PCR and electrophoretic analysis samples with Cut4_F/Cut4_R pair of primers for *Fusarium solani* cutinase, expected product size was 189 bp

Sample	Amplicon (bp)	Sample	Amplicon (bp)	Sample	Amplicon (bp)
C1(T)	zone 250–1200	**KR1(B)**	–	**KZ1**	–
C1(B)	–	**KR2(T)**	**180**/ zone 500–1000	**KZ2**	zone 500– 1000
C2(T)	350/500/600/800	**KR2(B)**	**180**/500/600/900/1100	**KZ3**	450/900
C2(B)	**180**/800	**KR3(T)**	–	**KZ4(T)**	–
C3(T)	250/500/700/800	**KR3(B)**	**180**/600/800/900/1600	**KZ4(B)**	zone 600– 1200
C3(B)	500/700/800	**KR4(T)**	zone 400–1200	**KZ5(T)**	zone 450– 1200
C4(B)	**180**/250/500/700	**KR4(B)**	**180**/250/zone 300–1000/1500	**KZ5(B)**	–
KR1(T)	300/500/800/100	**KR5**	–	**KZ1(F1)**	350/1000

'Zone' refers to a smear of PCR products of varying lengths in specified range without distinct bands in a defined size range, most likely resulting from non-specific primers annealing. In this and the following tables, products similar to the expected size are highlighted in ***bold.***

The rest of the data was obtained as a part of master's thesis

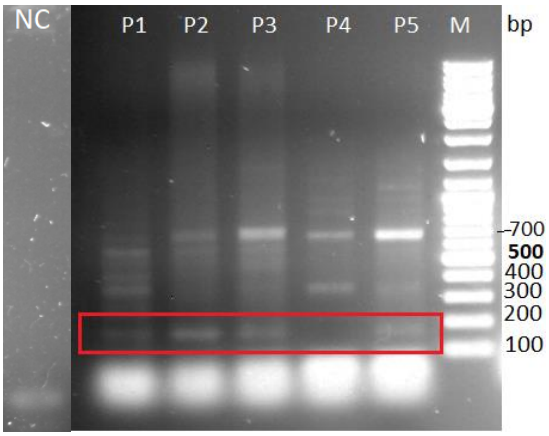

Fig. 3.1 Electrophoresis gel image after PCR with primers for c*ut4* gene (*Fusarium solani* cutinase) for group P samples. NC - negative control. M - Gene Ruler™ DNA Ladder Mix (SM0331). Expected size of product ~ 189 bp.

Table 3.2 Results of PCR and electrophoretic analysis of the samples with Cut4_F/Cut4_R pair of primers for *Fusarium solani* cutinase, expected product size was 189 bp

Sample	Amplicon (bp)	Sample	Amplicon (bp)	Sample	Amplicon (bp)
KZ1F	600/800/1000/1200	**S1(S)**	**190**/ zone 250– 900	**BP2(T)**	450/650
KZ2F	350/1100	**S2(S)**	450/550/800/900	**BP2(B)**	400/500/750
KZ2F2	–	**S3(S)**	zone 300–600/750	**P1**	**180**/zone 320–600
KZ3(F1)	–	**R1(S)**	260	**P2**	**180**/ 700
KZ2(F1)	450/600/1000/1200	**R2(S)**	zone 300–750	**P3**	**180**/700
D1(S)	350/400/730/780/900	**R3(S)**	500/800	**P4**	350/700
D2(S)	1000	**BP1(T)**	**180**/250–550	**P5**	**180**/350/700
K(S)	**190**/zone 250–900	**BP1(B)**	–		

Based on the number of products with lengths different from the expected ones, it can be said that the specificity of PCR was insufficient. Without sequencing, it was not possible to draw correct conclusions about the identity of the amplicons and whether the results were positive.

Amplicons of expected size from the samples P1, P2, P3, P5, C2B, C4, KR2T, KR2B, KR3B were sequenced. The results of blastx search for obtained sequences are in Table 3.3.

Table 3.3 Results of blastx search of sequences of amplicons of expected size after PCR for c*ut4* gene (*Fusarium solani* cutinase). Top e-value hit for each sample is provided (each sample contained only one consensus)

Sample	Seq. len.	Ident. (%)	Align. Len. (aa)	E-value	Bit score	Protein ID	Annotation
P1	170	100	56	1.13E-31	119	Q99174.1	Cutinase [Fusarium solani-melongenae], cutinase [Fusarium petroliphilum
P2	170	100	56	1.13E-31	119	Q99174.1	Cutinase [Fusarium solani-melongenae], cutinase [Fusarium petroliphilum
P3	171	100	56	3.23e-32	120	Q99174.1	Cutinase [Fusarium solani-melongenae], cutinase [Fusarium petroliphilum

Table 3.3 *continued*

P5	170	100	56	1.13E-31	119	Q99174.1	Cutinase [Fusarium solani-melongenae], cutinase [Fusarium petroliphilum
C4	171	100	56	8.94E-32	119	AAA33335.1	cutinase [Fusarium solani]

In this table and in all tables below with the results of blastx search: ***Seq. len.*** *– length of the query sequence (nt);* ***Ident, %*** *– percentage of simularity of aligned region between query amplicon converted to amino acid sequence and protein from database;* ***Align. len. (aa)*** *– alignment length, the length of amino acid sequence involved in alignment; standard blastx analysis in Galaxy with 25-colums extended table doesn't include query cover to reduce computing resources consumed, instead, it was decided to use alignment length (in amino acids) to evaluate the size of product involved in the alignment ;* ***E-value*** *– expectation value (acceptable values ≤ 0.001);* ***Bitscore*** *– bit score.*

Homology search revealed, that the amplicons from samples P1, P2, P3, P5 and C4 were obtained from *Fusarium solani* cutinase template (Table 3.3). However, the size of the product differed from the expected one, specified in the original article (Alexandrakis et al.,1998). To find the reason, it was decided to verify the size of the expected amplicon by PCR simulation. For this purpose, the Galaxy primersearch tool was used. The test confirmed that the correct expected amplicon size was 170 bp. The rest testes products appeared to be products of unspecific amplification.

Thermobifida fusca **cutinase 2**

The next analysed cutinase was cutinase 2 gene (*cut2*) from thermophilic actinomycete *Thermobifida fusca.*, This enzyme effectively hydrolyses the ether bonds of PET, and one of the reasons for that, apart from its good affinity to the substrate, may be that its optimal temperature (55 °C) is close to the glass transition temperature of PET (Muller et al., 2005). Table 3.4 presents the results of PCR and electrophoretic analysis for the samples analysed as a part of master's thesis. The rest of the samples from the groups C, KZ, KR, that were analysed as a part of bachelor's thesis, did not yield any amplification product in triplicate. The image of electrophoretic analysis of PCR products for group P samples is below (Fig 3.2).

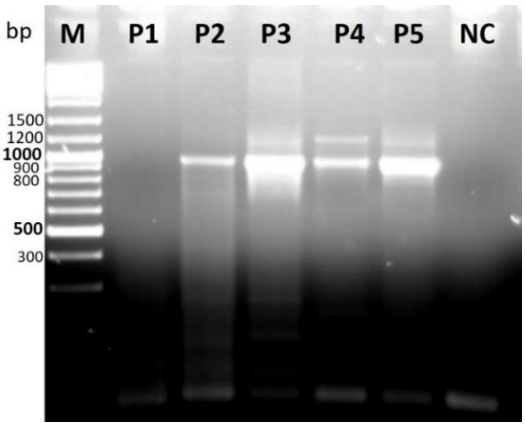

Fig 3.2 Electrophoresis gel image after PCR with primers for c*ut2* gene (*Thermobifida fusca* cutinase 2) for group P samples. NC - negative control. M - Gene Ruler™ DNA Ladder Mix (SM0331). Expected size of the product ~ 930 bp.

Table 3.4 Results of PCR and electrophoretic analysis of the samples with Cut2_F/Cu2_R pair of primers for *Thermobifida fusca* cutinase *cut2* gene. The expected size of target product was 930 bp

Sample	Amplicon (bp)	Sample	Amplicon (bp)	Sample	Amplicon (bp)
KZ1F	–	**S1(S)**	–	**BP2(T)**	–
KZ2F	–	**S2(S)**	–	**BP2(B)**	–
KZ2F2	–	**S3(S)**	–	**P1**	–
KZ3(F1)	–	**R1(S)**	–	**P2**	200/300/500/**930**
KZ2(F1)	–	**R2(S)**	–	**P3**	200/300/**930**/1100
D1(S)	–	**R3(S)**	–	**P4**	280/**930**/1100
D2(S)	–	**BP1(T)**	–	**P5**	**930**/1100
K(S)	–	**BP1(B)**	–		

Amplicons of expected size from the samples P2, P3, P4, P5 were subjected to sequencing. The results of blastx search of sequences are in Table 3.5.

Table 3.5 Results of sequencing of amplicons of expected size after PCR for c*ut2* gene (*Thermobifida fusca* cutinase 2). Each sample contained only one consensus, but resulted in several different top hits

Sample	Seq. len.	Ident. (%)	Align. len. (aa)	E-value	Bit score	Protein ID	Annotation
P2	930	100	301	0	531	WP_011291330.1	cutinase [Burkholderia cepacia], cutinase [Thermobifida fusca], BTA-hydrolase 1 [Thermobifida fusca]
	930	100	263	0	523	ALF04778.1	BTA-hydrolase, partial [synthetic construct]
	930	100	261	0	520	ADV92526.1	cutinase 1, partial [Thermobifida cellulosilytica]
P3	930	100	301	0	531	WP_011291330.1	cutinase [Burkholderia cepacia], cutinase [Thermobifida fusca], BTA-hydrolase 1 [Thermobifida fusca]
	930	100	263	0	523	ALF04778.1	BTA-hydrolase, partial [synthetic construct]
	930	100	261	0	520	ADV92526.1	cutinase 1, partial [Thermobifida cellulosilytica]
P4	930	100	301	0	531	WP_011291330.1	cutinase [Burkholderia cepacia], cutinase [Thermobifida fusca], BTA-hydrolase 1 [Thermobifida fusca]
	930	100	263	0	523	ALF04778.1	BTA-hydrolase, partial [synthetic construct]
	930	100	261	0	520	ADV92526.1	cutinase 1, partial [Thermobifida cellulosilytica]
P5	930	100	301	0	531	WP_011291330.1	cutinase [Burkholderia cepacia], cutinase [Thermobifida fusca], BTA-hydrolase 1 [Thermobifida fusca]
	930	100	301	0	520	ADV92526.1	cutinase 1, partial [Thermobifida cellulosilytica]

Sequencing revealed that all examined amplicons from P2, P3, P4, P5 samples were of the nature of *Thermobofida fusca* cutinase (BTA-hydrolase 1) (the term hydrolase is used as a synonym to cutinase for this enzyme depending on the study, due to the fact that cutinases belong to the

alpha/beta serine hydrolases (see chapter 1.5.2.5)). However, instead of the target cutinase 2 amplicons, cutinase (hydrolase) cutinase 1 was found. This is not surprising, considering that *Thermobofida fusca* cutinase 2 (CAH17554.1) possesses 93% similarity with *Thermobifida fusca* cutinase 1 (CAH17553.1) (Fig.3.3). "*They are located sequentially in the genome, likely due to a gene duplication event, however they do not appear to be in an operon*" (Chen et al., 2008). The e-value of 0 for these alignments indicates absolute similarity of the amplicons to the mentioned proteins.

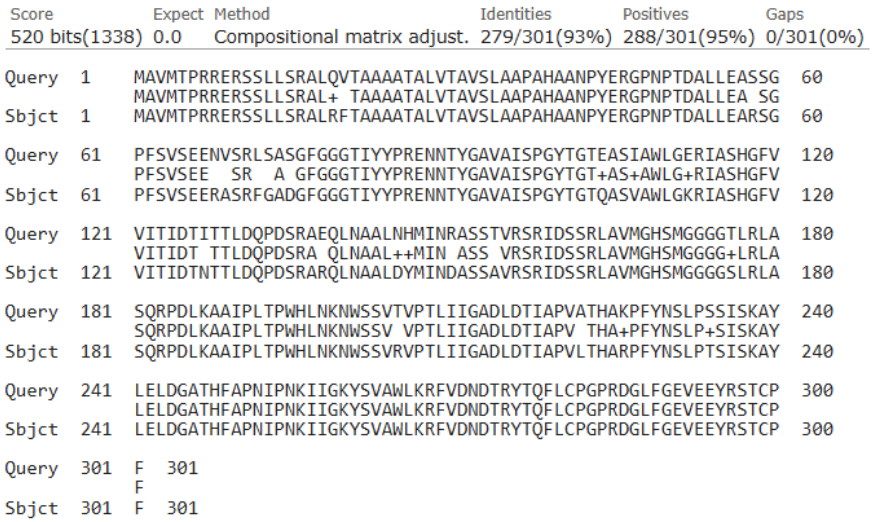

Score	Expect	Method	Identities	Positives	Gaps
520 bits(1338)	0.0	Compositional matrix adjust.	279/301(93%)	288/301(95%)	0/301(0%)

```
Query  1    MAVMTPRRERSSLLSRALQVTAAAATALVTAVSLAAPAHAANPYERGPNPTDALLEASSG  60
            MAVMTPRRERSSLLSRAL+ TAAAATALVTAVSLAAPAHAANPYERGPNPTDALLEA SG
Sbjct  1    MAVMTPRRERSSLLSRALRFTAAAATALVTAVSLAAPAHAANPYERGPNPTDALLEARSG  60

Query  61   PFSVSEENVSRLSASGFGGGTIYYPRENNTYGAVAISPGYTGTEASIAWLGERIASHGFV  120
            PFSVSEE  SR  A GFGGGTIYYPRENNTYGAVAISPGYTGT+AS+AWLG+RIASHGFV
Sbjct  61   PFSVSEERASRFGADGFGGGTIYYPRENNTYGAVAISPGYTGTQASVAWLGKRIASHGFV  120

Query  121  VITIDTITTLDQPDSRAEQLNAALNHMINRASSTVRSRIDSSRLAVMGHSMGGGGTLRLA  180
            VITIDT TTLDQPDSRA QLNAAL++MIN ASS VRSRIDSSRLAVMGHSMGGGG+LRLA
Sbjct  121  VITIDTNTTLDQPDSRARQLNAALDYMINDASSAVRSRIDSSRLAVMGHSMGGGGSLRLA  180

Query  181  SQRPDLKAAIPLTPWHLNKNWSSVTVPTLIIGADLDTIAPVATHAKPFYNSLPSSISKAY  240
            SQRPDLKAAIPLTPWHLNKNWSSV VPTLIIGADLDTIAPV THA+PFYNSLP+SISKAY
Sbjct  181  SQRPDLKAAIPLTPWHLNKNWSSVRVPTLIIGADLDTIAPVLTHARPFYNSLPTSISKAY  240

Query  241  LELDGATHFAPNIPNKIIGKYSVAWLKRFVDNDTRYTQFLCPGPRDGLFGEVEEYRSTCP  300
            LELDGATHFAPNIPNKIIGKYSVAWLKRFVDNDTRYTQFLCPGPRDGLFGEVEEYRSTCP
Sbjct  241  LELDGATHFAPNIPNKIIGKYSVAWLKRFVDNDTRYTQFLCPGPRDGLFGEVEEYRSTCP  300

Query  301  F  301
            F
Sbjct  301  F  301
```

Fig. 3.3 Alignment of amino acid sequences of cutinase 1 (query) and cutinase 2 (subject).

Leaf Branch Compost Cutinase

One more cutinase called Leaf Branch Compost Cutinase (LCC) was the target of this study. As mentioned in chapter 1.4.1.5., LCC is one of the most effective known enzymes capable of PET cleavage. The host organism of the protein is unknow, the gene was isolated from leaf and branch compost. The original article states that the temperature in this compost is maintained at around 70 °C during the year and then gradually decreases to 50 °C (Sulaiman et al., 2012), so it can be suggested that this enzyme belongs to thermophilic microorganism.

There were three PCR repeats with primers for the gene encoding LCC. The product of the expected size was detected only once in 2 samples from P group (Fig. 3.4, red squares), however the concentration of them wasn't sufficient for extraction. The weak signal may indicate that the product is non-specific. There also were several samples in which different products were amplified, but their sizes differed significantly from target, hence they were not considered as positive.

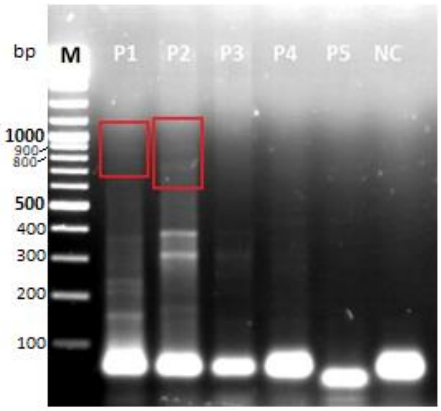

Fig 3.4 Electrophoresis gel image after PCR with primers for *lcc* gene (Leaf Branch Compost Cutinase) for group P samples. NC - negative control; M - Gene Ruler™ DNA Ladder Mix (SM0331). Expected size of product ~ 880 nt.

Thermobifida fusca cutinase 1

Another analysed hydrolase (cutinase) from *Thermobifida fusca* was cutinase 1. In comparison with the results of PCR for cutinase 2, in this case, many amplification products were formed in many samples (Table 3.6). One of the reasons may be that the primers in this PCR were shorter (28 nt) than for Cut2 (34 nt). This fact once again proves the complexity and unpredictability of working with metagenomic DNA. Images of electrophoretic analysis of obtained PCR products for P group are below (Fig 3.5). Table 3.6 presents the results of PCR for all tested samples.

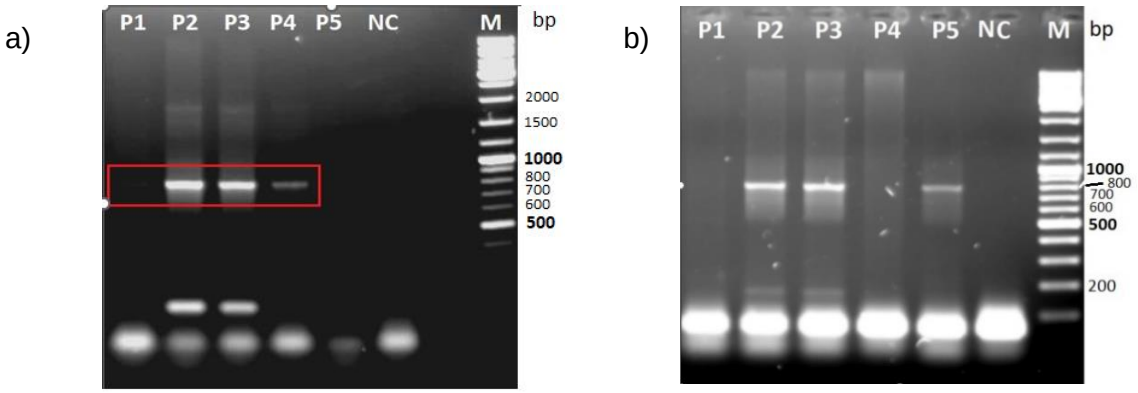

Fig 3.5 Electrophoresis gel image after PCR with primers for *cut1* gene (*Thermobifida fusca* cutinase 1); b) P group of samples, primers annealing temperature 62 °C; c) same as b), but annealing temperature 66 °C. NC- negative control; M - Gene Ruler™ DNA Ladder Mix (SM0331). Expected size of product ~ 808 bp.

Table 3.6 Results of PCR and electrophoretic analysis of the samples with pair of primers for *Thermobifida fusca cut1* gene. The expected size of target product was 808 bp

Sample	Amplicon	Sample	Amplicon	Sample	Amplicon
C1(T)	–	**KZ1**	–	**S1(S)**	–
C1(B)	350/680	**KZ2**	280/**800**	**S2(S)**	230/500
C2(T)	500/680	**KZ3**	1500	**S3(S)**	–

Table 3.6 *Continued*

C2(B)	500/680	**KZ4(T)**	–	**R1(S)**	–
C3(T)	400/700/100/1300	**KZ4(B)**	–	**R2(S)**	–
C3(B)	500/950	**KZ5(T)**	600	**R3(S)**	**–**
C4(B)	–	**KZ5(B)**	–	**BP1(T)**	**–**
KR1(T)	400	**KZ1(F2)**	–	**BP1(B)**	400
KR1(B)	300/400/600	**KZ2(F2)**	–	**BP2(T)**	–
KR2(T)	500/700	**KZ3(F2)**	–	**BP2(B)**	400
KR2(B)	–	**KZ2(F1)**	N/A	**P1**	**800**
KR3(T)	**780**	**KZ1(F1)**	–	**P2**	150/**800**/1800
KR3(B)	750/1400/1500/1800	**KZ3(F1)**	–	**P3**	150/**800**/1800
KR4(T)	**750**/1300/1500	**D1(S)**	230	**P4**	**800**/1800
KR4(B)	280	**D2(S)**	**–**	**P5**	**800**
KR5	–	**K(S)**	**–**		

Amplicons of similar to expected size and which were possible to extract in sufficient concentration from the samples KR3T, KR4T, KZ2, P1, P2, P3, P4, P5 were subjected to sequencing with subsequent blastx protein homology search (Table 3.7).

Table 3.7 Results of blastx search for obtained sequences of amplicons after PCR for *cut1* gene (*Thermobifida fusca* cutinase 1). Top hits based on e-value are provided for all consensuses*

Sample	Seq len.	Ident. (%)	Align. len. (aa)	E-value	Bit score	Protein ID	Annotation
P1_1	808	100	261	0	540	WP_061783624.1	alpha/beta hydrolase [Thermobifida fusca
	809	93.87	261	0	509	6AID_A	cutinase [Thermobifida alba]
2	808	100	261	0	523	WP_011291330.1	cutinase [Burkholderia cepacia], cutinase [Thermobifida fusca], BTA-hydrolase 1 [Thermobifida fusca]
	808	100	261	0	523	WP_011291330.1	cutinase [Burkholderia cepacia], cutinase [Thermobifida fusca], BTA-hydrolase 1 [Thermobifida fusca]
P2	808	99.62	262	0	539	CAH17554.1	BTA-hydrolase 2 [Thermobifida fusca]
P3_1	808	100	261	0	540	WP_061783624.1	alpha/beta hydrolase [Thermobifida fusca]
	808	100	261	0	523	WP_011291330.1	cutinase [Burkholderia cepacia], cutinase [Thermobifida fusca], BTA-hydrolase 1 [Thermobifida fusca]
	808	99.62	262	0	521	5LUI_A	cutinase 1 [Thermobifida cellulosilytica]
2	808	99.62	262	0	539	CAH17554.1	BTA-hydrolase 2 [Thermobifida fusca]
P4	808	100	261	0	523	WP_011291330.1	cutinase [Burkholderia cepacia], cutinase [Thermobifida fusca], BTA-hydrolase 1 [Thermobifida fusca]
P5_1	808	100	261	0	523	WP_011291330.1	cutinase [Burkholderia cepacia], cutinase [Thermobifida fusca], BTA-hydrolase 1 [Thermobifida fusca]

Table 3.7 *Continued*

2	808	100	261	0	540	WP_061 783624.1	alpha/beta hydrolase [Thermobifida fusca]
KR4T_ 1	748	60.30	68	1.48E -26	87	WP_038 044226.1	serine hydrolase [Thermocrispum agreste]
2	869	61.54	117	1.92E -29	122	WP_105 343052.1	alpha/beta hydrolase [Mycobacterium sp. ITM-2016-00318]
3	869	89.58	96	1.31E -50	177	WP_105 343052.1	alpha/beta hydrolase [Mycobacterium sp. ITM-2016-00318]

* Only the first consensus per sample is labeled with the sample name (e.g., P1_1); subsequent ones are numbered (2, 3, 4, etc.). If no number is indicated, only one consensus was obtained for that sample. Consensus construction principles are detailed in Chapter 2.4.4.3. Some consensuses had multiple significant hits, which are listed in the table

Protein homology search revealed that the amplicons from sample P1, P4 and P5 had absolute similarity with tartgeted *Thermobifida fusca* cutinase (hydrolase) 1. Samples P2 and P3 also possessed maximum similarity with targeted enzyme, however they could also be cutinases (hydrolases) 2 with 99.62 % of similarity in aligned amino acid region of 262 (786 bp). Bit scores for those search hits were even higher than for hydrolase 1. As for the KR4T sample, homology search found relatively high similarity between the sequence of amplicon and serine hydrolase of *Thermocrispum agreste* and alpha/beta hydrolase of *Mycobacterium* sp. *ITM-2016-00318. Thermobifida fusca* cutinases belong to the alpha/beta serine hydrolases subclass of enzymes. Therefore, it can be assumed that this sequence is the product of specific amplification. It should also be noted that this may be a new, previously uncharacterised enzyme with potential activity against PET. More detailed sequence analysis, cloning and characterisation of the protein can be carried out. Primers were designed to amplify the entire gene, hence it can be cloned for expression in only a few steps.

PHL7 hydrolase

One more targeted cutinase/hydrolase in this study was recently discovered hydrolase PHL7 (Sonnendecker et al., 2022). PHL7 is a thermostable polyester hydrolase isolated from compost metagenome and is active against amorphous PET, converting them into terephthalic acid and ethylene glycol. Optimal enyzyme temperature is elevated, as for the previous ones, and is 70 °C, which apparently determines its effectiveness. It is also noteworthy that this hydrolase was isolated using the methodology applied in the current study: amplification products obtained with degenerate primers specific to the enzyme group of interest were cloned and their activity was assessed.

Electrophoretic profile of PCR products for P samples is in Fig 3.6.

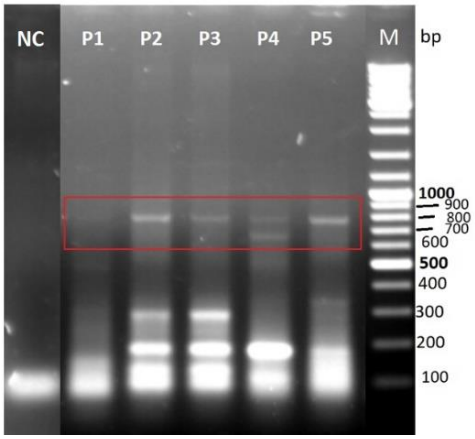

Fig 3.6 Electrophoresis gel image after PCR with primers for *phl7* gene (PHL7 enzyme) P group of samples. NC- negative control; M - Gene Ruler™ DNA Ladder Mix (SM0331). Expected size of product ~ 780 nt.

Results for all examined samples are in the Table 3.9.

Table 3.8 Results of PCR and electrophoretic analysis of the samples with Phl7_F/Phl7_R pair of primers for the gene encodes PHL7. The expected size of target product was ~ 780 bp

Sample	Amplicon	Sample	Amplicon	Sample	Amplicon
C1(T)	–	**KR3(B)**	–	**KZ1(F2)**	450
C1(B)	–	**KR4(T)**	–	**KZ2(F2)**	–
C2(T)	–	**KR4(B)**	–	**KZ3(F2)**	–
C2(B)	–	**KR5**	–	**KZ2(F1)**	–
C3(T)	–	**KZ1**	–	**KZ1(F1)**	450
C3(B)	–	**KZ2**	–	**KZ3(F1)**	–
C4(B)	–	**KZ3**	**–**	**P1**	**780**
KR1(T)	–	**KZ4(T)**	–	**P2**	180/280/**780**
KR1(B)	–	**KZ4(B)**	–	**P3**	180/280/**780**
KR2(T)	–	**KZ5(T)**	–	**P4**	180/690/**780**
KR2(B)	–	**KZ5(B)**	–	**P5**	330/**780**
KR3(T)	**780**				

Amplicons similar to expected size from the samples KR3T, P1, P2, P3, P4, P5 were subjected to sequencing (Table 3.9).

Table 3.9 Results of blastx search of amplicons of expected size after PCR for *phl7* gene (PHL7 hydrolase). Top hits based on e-value are provided for all consensuses

Sample	Seq. len.	Ident. (%)	Align. Len. (aa)	E-value	Bit score	Protein ID	Annotation
P1	789	100	261	0	524	WP_011291330.1	cutinase [Burkholderia cepacian], [Thermobifida fusca], BTA-hydrolase 1 [Thermobifida fusca
	789	100	262	0	522	5LUI_A	cutinase 1 [Thermobifida cellulosilyt-ica]

Table 3.9 *continued*

P2_1	789	100	261	0	524	WP_011291330.1	cutinase [Burkholderia cepacian] [Thermobifida fusca], BTA-hydrolase 1 [Thermobifida fusca]
P2_2	788	100	261	1.66E-161	459	WP_061783624.1	alpha/beta hydrolase [Thermobifida fusca]
	788	99.55	261	6.06E-161	458	CAH17554.1	BTA-hydrolase 2 [Thermobifida fusca]
P3_	789	100.00	261	0	524	WP_011291330.1	cutinase [Burkholderia cepacian] [Thermobifida fusca], BTA-hydrolase 1 [Thermobifida fusca]
P4 (690 bp)	691	90.82	196	3.23E-110	327	5LUI_A	Structure of cutinase 1 from [Thermobifida cellulosilytica]
	691	85.2	196	6.22E-103	308	5LUK_A	double variant of cutinase 2 from Thermobifida cellulosilytica
P4 (780 bp)	786	93.28	119	1.06e-117	505	ADV92528.1	cutinase 1, partial [Thermobifida fusca]
P5_1	807	100.00	259	0	519	WP_011291330.1	cutinase [Burkholderia cepian], BTA-hydrolase 1 [Thermobifida fusca]
2	819	99.61	254	0	524	CAH17554.1	BTA-hydrolase 2 [Thermobifida fusca]
3	789	100.00	261	0	541	WP_061783624.1	alpha/beta hydrolase [Thermobifida fusca]
KR3T	789	100.00	261	0	524	WP_011291330.1	cutinase [Burkholderia cepacian] [Thermobifida fusca], BTA-hydrolase 1 [Thermobifida fusca]
	789	100.00	262	0	522	ADV92526.1	cutinase 1, partial [Thermobifida cellulosilytica]

Sequences from samples P2, P3 and P5 turned out to be either cutinase 1 from *Thermobifida fusca* (alternatively *Burkholderia cepacia)* or with almost the same probability (e-value 1.66E-161, identity 99.55%) cutinase 2; for P1 and KR3T all the e-value hits suggested the cutinase 1 protein origin. As for sample P4, an intriguing phenomenon is observed on the electrophoresis gel image (Fig.3.6), which may have biological meaning. Two bands of equal intensity are visible on the lane, with a difference of approximately 100 bp. The longer one, that corresponds to the expected size, had the highest similarity with *Thermobifida fusca* cutinase 1/2, the shorter one (691 bp) has showed the highest similarity with *Thermobifida* cellulosilytica enzymes, however, the similarity in nucleotides was 93% (alignment is in Appendix F) The difference in size can be explained by the fact that this gene belongs to another closely related organism that has not been characterised previously, and cloning and expression of this gene could provide information about its activity.

The fact that the rest of amplicons show almost absolute identity to the hydrolase of another organism can be explained by the fact that *Thermobifida fusca* cutinase 1 gene and PHL7 gene share 67% similarity, (with cutinase 2 – 63.5%) (Appendix G). The ends of the genes turned out to be conservative enough so that the primers designed for *phl7* annealed to *cut1/2*. The absence of the

target gene among the results may be explained by potential strong prevalence of bacteria of the genus *Thermobifida* in the samples (that can be tested with 16S rRNA gene sequencing), which prevented the *phl7* gene from manifesting itself at various stages of the analysis, or by the complete absence of this gene in the samples.

Lysinibacillus fusiformis SCO2 urethanases

The next analysed enzyme was a urethane hydrolase (alternative name glutamyl–tRNA– amidotransferase) from *Lysinibacillus fusiformis* SCO2. Originaly this strain was isolated from murine intestine and showed higher activity than all other urethanases known at that time. Although it does not participate in the depolymerisation of PUR like the PueA mentioned below, it hydrolyses polyurethane monomer to ammonia, ethanol and carbon dioxide, and this is important because urethane as an intermediate of PUR degradation is a carcinogenic substance from 2A group (Jia et al., 2020).

Amplification products were visualised in agarose gel. Electrophoresis gel image for samples from group P is Fig 3.7.

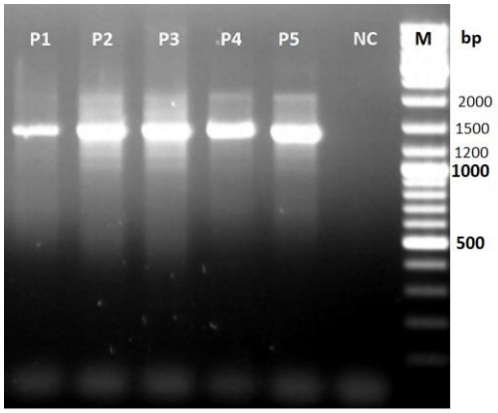

Fig. 3.7. Gel electrophoresis image of PCR products obtained using primer pair Lf_ureF/Lf_ureR with P group of samples. NC - negative control. M - Gene Ruler™ DNA Ladder Mix (SM0331). expected size of the target product was ~1400 bp.

PCR results for all tested samples are in Table 3.10.

Table 3.10 Results of PCR and electrophoretic analysis of the samples with Lf_ureF/Lf_ureR pair of primers for urethanase (glutamyl–tRNA amidotransferase) gene. The expected size of the target product was ~1400 bp

Sample	Amplicon	Sample	Amplicon	Sample	Amplicon
C1(T)	–	**KR3(B)**	–	**KZ1(F2)**	–
C1(B)	–	**KR4(T)**	–	**KZ2(F2)**	–
C2(T)	–	**KR4(B)**	–	**KZ3(F2)**	–
C2(B)	–	**KR5**	–	**KZ2(F1)**	–
C3(T)	**1400**	**KZ1**	–	**KZ1(F1)**	–
C3(B)	–	**KZ2**	–	**KZ3(F1)**	–

Table 3.10 *continued*

C4(B)	–	**KZ3**	**–**	**P1**	**1400**
KR1(T)	–	**KZ4(T)**	–	**P2**	**1400**/2000
KR1(B)	–	**KZ4(B)**	–	**P3**	**1400**/2000
KR2(T)	–	**KZ5(T)**	–	**P4**	**1400**/2000
KR2(B)	–	**KZ5(B)**	–	**P5**	**1400**/2000
KR3(T)	–				

The amplicons from samples C3T, P1, P2, P3, P4, P5 were sequenced, the results of homology search are in the table below.

Table 3.11 Results of blastx search of sequences of amplicons of expected size after PCR for the gene of *Lysinibacillus fusiformis* SCO2 uretanase. Top hits based on e-value are provided for all consensuses

Sample	Seq. len.	Ident. (%)	Align. Len. (aa)	E-value	Bit score	Protein ID	Annotation
	1418	100	472	0	593	WP_083225424.1	hypothetical protein [Lysinibacillus sp. AR18-8]
P1_1	1418	100	472	0	593	OCX55545.1	glutamyl-tRNA amidotransferase [Lysinibacillus sp. AR18-8]
	1419	100	472	0	932	WP_036121982.1	Asp-tRNA(Asn)/Glu-tRNA(Gln) amidotransferase GatCAB subunit A [Lysinibacillus fusiformis]
2	1419	100	472	0	396	KUF28214.1	glutamyl-tRNA amidotransferase [Lysinibacillus sp. F5]
P2	1419	99.58	472	0	900	WP_081010925.1	urethanase [Lysinibacillus fusiformis]
	1419	99.56	472	0	900	WP_081010925.1	urethanase [Lysinibacillus fusiformis]
P4	1419	99.79	472	0	899	WP_112117097.1	urethanase, partial [Lysinibacillus sp.]
P5_1	1419	100	472	0	932	WP_036121982.1	Asp-tRNA(Asn)/Glu-tRNA(Gln) amidotransferase GatCAB subunit A [Lysinibacillus fusiformis]
2	1419	99.56	472	0	900	WP_081010925.1	urethanase [Lysinibacillus fusiformis]
3	1258	100	266	0	233	SPT98690.1	glutamyl-tRNA(Gln) amidotransferase subunit A [Lysinibacillus capsici]
	1419	100	472	0	900	WP_115673857.1	amidase [Lysinibacillus capsici]
C3T	1419	99.15	472	0	895	WP_081010925.1	urethanase [Lysinibacillus fusiformis]

Sequencing confirmed the high similarity between PCR products and genes of urethanases of *Lysinibacillus* genus species for samples C3T, P1, P2, P4 and P5. Unfortunately, the data for P3 sample could not be obtained due to technical reasons.

3.2.2. Genes of alkane hydroxylases

A comprehensive study of alkane hydroxylases is very important, as they are one of the few enzymes capable of attacking extremely recalcitrant PE. In this section, the results of PCR analysis for alkane hydroxylases genes and blastx analysis of the sequences of obtained amplicons will be provided.

TS2S/Deg1RE pair of primers

The first applied pair of primers was TS2S/Deg1RE, constructed for conservative region of *Pseudomonas oleovorans* GPo1 *alkB* and *Acinetobacter* sp. ADP1 *alkM* alkane hydroxylases genes (primers are not degenerate) (Olivera et al., 2009). Electrophoresis gel image after PCR with pair of primers for P group of samples is shown in the figure Fig.3.8.

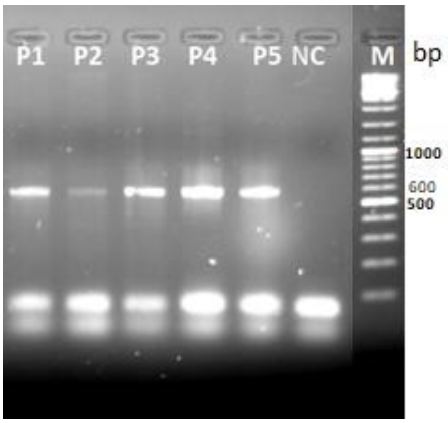

Fig 3.8 Electrophoresis gel image after PCR with primers TS2S/Deg1RE for P group of samples. NC- negative control; M - Gene Ruler™ DNA Ladder Mix (SM0331). Expected size of product ~ 550 bp.

This pair of primers was used as a part of bachelor's thesis for samples from the groups C, KZ, KR as well, however, the repeats that were done during master's thesis work revealed more bands of expected size.

Table 3.12 shows the results of PCR, the data is presented in approximate amplicon lengths.

Table 3.12 Results of PCR and electrophoretic analysis of the samples with TS2S_Deg1RE pair of primers for *alkM, alkB* alkane hydroxylases genes. The expected size of target product was ~ 550 bp

Sample		Sample	Amplicon	Sample	Amplicon
C1(T)	–	**KZ1**	–	**S1(S)**	–
C1(B)	–	**KZ2**	**550**	**S2(S)**	**550**
C2(T)	–	**KZ3**	**550**	**S3(S)**	**550**
C2(B)	**550**	**KZ4(T)**	**550**	**R1(S)**	–
C3(T)	**550**	**KZ4(B)**		**R2(S)**	–
C3(B)	–	**KZ5(T)**	–	**R3(S)**	–
C4(B)	–	**KZ5(B)**	**550**	**BP1(T)**	–
KR1(T)	–	**KZ1(F2)**	350	**BP1(B)**	–
KR1(B)	**550**	**KZ2(F2)**	–	**BP2(T)**	–

Table 3.12 *continued*

KR2(T)	–	**KZ3(F2)**	–	**BP2(B)**	–
KR2(B)	**550**	**KZ2(F1)**	–	**P1**	**550**
KR3(T)	**550**	**KZ1(F1)**	–	**P2**	**550**
KR3(B)	**550**	**KZ3(F1)**	350	**P3**	**550**
KR4(T)	**550**	**D1(S)**	–	**P4**	**550**/1200
KR4(B)	**550**	**D2(S)**	–	**P5**	**550**
KR5	–	**K(S)**	–		

Amplicons of similar to expected size from the samples C2B, C3T, KR1B, KR2B, KR3B, KZ2, KZ3, KZ4T, KZ5B P1, P2, P3, P4, P5 were subjected to sequencing. The results of blastx analysis are in Appendix H.

Homology search revealed that all the sequenced amplicons were of the origin of alkane-1-monooxygenase (alkane hydroxylases class of enzymes). AlkB belongs to the membrane fatty acid desaturase (FADS)-like superfamily. Members of this group are non-heme diiron monooxygenases that desaturate or hydroxylate fatty acyl aliphatic chains (Guo et al., 2023). Another synonym from the tables (here and below) is rubredoxin-dependent monooxygenase follows from the fact that AlkB indeed utilises rubredoxin as an electron transfer partner (rubredoxin is encoded by *alkG* on the same operon as *alkB* itself) (Guo et al., 2023).

Analysis revealed that putative sequences may belong to a wide range of microorganisms with varying degrees of certainty. Not all samples had homologues with 100% identity, which may mean that these sequences had not been sequenced earlier or were not included in the database used for search. However, it is important to mention that among the e-value hits there were almost no micro-organisms that the primers were targeting originally.

To summarise the data from the table, results with the highest e-value can be highlighted.

For sample **P1**, the highest homology was observed with alkane monooxygenases belonging to species *Corynebacterium frenei*, *Corynebacterium xerosis* and *Clostridium paraputrificum*. For **P2** sample species *Corynebacterium frenei*, *Pseudomonas* sp, *Dietzia* sp. For **P3** the same species as for P2. For P**4** and **P5 -** *Corynebacterium variabile*. For **C2B** – *Actinobacteria* bacterium and *Pedobacter* sp. For **C3T** *Stenotrophomonas* sp. For **KR1B** and **KR2B** enzymes that belong to *Nocardioides* sp. For **KR3B -** *Stenotrophomonas* sp. For **KZ2** sample – *Nocardioides* sp. For sample **KZ3** – *Pedobacter* sp enzyme showed the highest homology. For **KZ4T** – Nocardioides sp, However for **KZ5B** sample the e-value of the hits was not low enough to be recognised as reliable homology.

AlkB484F/ AlkB824R pair of primers

The next pair of primers that was used to detect alkane hydroxylases genes was AlkB484F and AlkB824R. These degenerate primers were designed for alkane hydroxylase gene *alkB* for wide group of microorganisms, e.g. genera of *Alcanivorax*, *Rhodococcus*, *Mycobacterium*, *Acinetobacter*,

Gordonia and such species as *Prauserella rugosa, Thalassolituus oleivorans, Oleiphilus messinensis, Pseudomonas fluorescens,* and many more (59 alkB unique gene sequences from pure cultures) (Olivera et al., 2009). Table 3.13 and Table 3.14 present the amplicons that were detected during electrophoretic analysis of PCR products with mentioned primers. Fig. 3.9 presents the PCR product electrophoretic profile for P samples.

The data in the table was obtained as a part of the bachelor's thesis.

Table 3.13 Results of PCR and electrophoretic analysis of the samples with AlkB484F/AlkB824R pair of primers. The expected sizes of the target products were 340 bp

Sample	Amplicon	Sample	Amplicon	Sample	Amplicon
C1(T)	220/**340**	KR1(B)	**340**	**KZ1**	220/**340**
C1(B)	220/**340**	KR2(T)	220/**340**	**KZ2**	–
C2(T)	220/**340**	KR2(B)	220/**340**	**KZ3**	–
C2(B)	220/**340**	KR3(T)	220/**340**	**KZ4(T)**	220
C3(T)	220/**340**	KR3(B)	220/**340**	**KZ4(B)**	220/**340**
C3(B)	220/**340**	KR4(T)	220/**340**	**KZ5(T)**	–
C4(B)	220/**340**	KR4(B)	–	**KZ5(B)**	–
KR1(T)	220/**340**	KR5	–	**KZ1(F1)**	–

The data below was obtained as a part of the master's thesis.

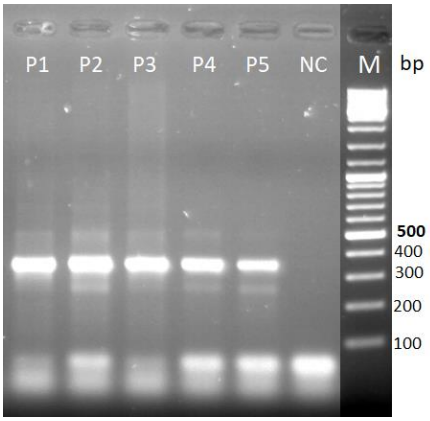

Fig 3.9. Gel electrophoresis image of PCR products obtained with primers AlkB484F _ AlkB824R for P group of samples. NC- negative control; M - Gene Ruler™ DNA Ladder Mix (SM0331). Expected size of product ~ 340 bp.

Table 3.14 Results of PCR and electrophoretic analysis of the samples with AlkB484F/AlkB824R pair of primers. The expected sizes of the target products were, 340 bp

Sample	Amplicon (bp)	Sample	Amplicon (bp)	Sample	Amplicon (bp)
KZ1F	-	**S1(S)**	-	**BP2(T)**	220/**340**
KZ2F	-	**S2(S)**	220/**340**	**BP2(B)**	220/**340**
KZ2F2	-	**S3(S)**	220/**340**	**P1**	280/**340**/480
KZ3(F1)	-	**R1(S)**	-	**P2**	280/**340**/480
KZ2(F1)	-	**R2(S)**	-	**P3**	280/**340**/480
D1(S)	-	**R3(S)**	-	**P4**	280/**340**/480
D2(S)	-	**BP1(T)**	**340**	**P5**	280/**340**/480
K(S)	-	**BP1(B)**			

Amplicons of similar to expected size from the samples P1, P2, P3, P4 were subjected to sequencing. The results of blastx analysis of obtained sequences are in Appendix I.

Analysis of sequences proved the alkane hydroxylase origin of all examined amplicons. Indeed, this set of degenerate primers allowed the amplification of the genes from wide range of microorganisms and may be suitable for screening samples for alkane hydroxylases genes, in particular alkane 1-monooxygenase.

Comparing the results for the previous pair of primers (T2S2/Deg1RE) and this one, it can be said that the newly detected homologues with the lowest e-value for sample **P1** belong to the species *Mycolicibacterium thermoresistibile.* For **P2** samples – the highest similarity with enzyme of Mycolicibacterium *hassiacum.* For **P3** – *Mycolicibacterium thermoresistibile, Mycolicibacterium hassiacum,* and *Rhodococcus gordoniae.* For sample **P4** this pair of primers yielded a product with high homology to enzyme from *Mycolicibacterium hassiacum* and *Mycolicibacterium phlei.*

MonF/ MonR pair of primers

The next set of degenerate primers was initially designed to detect alkane hydroxylases (*alkB* gene) that originate from *Alcanivorax dieselolei, Alcanivorax venustensis, Alcanivorax jadensis, Pseudomonas putida* GPo1. Table 3.16 and table in Table 3.18 contain the results of PCR with subsequent electrophoretic analysis and present the lengths of detected amplicons. Fig. 3.10 represents the results of PCR for P samples.

The data in this table was obtained as a part of bachelor's thesis.

Table 3.15 Results of PCR analysis of the samples with MonF/ MonR pair of primers. The expected size of the target product was ~ 420 bp

Sample	Amplicon (bp)	Sample	Amplicon (bp)	Sample	Amplicon (bp)
C1(T)	300/**420**/585	**KR1(B)**	**420**	**KZ1**	**420**/585
C1(B)	300/**420**/585	**KR2(T)**	**420**	**KZ2**	**420**/585
C2(T)	300/**420**/585	**KR2(B)**	300/**420**	**KZ3**	**420**/585
C2(B)	300/**420**/585	**KR3(T)**	300/**420**/470	**KZ4(T)**	–
C3(T)	300/**420**	**KR3(B)**	300/**420**/470	**KZ4(B)**	**420**/585
C3(B)	300/**420**	**KR4(T)**	300/**420**	**KZ5(T)**	**420**/585
C4(B)	300/**420**	**KR4(B)**	300/**420**	**KZ5(B)**	–
KR1(T)	300/**420**	**KR5**	**420**	**KZ1(F1)**	–

The data below was obtained as a part of the master's thesis.

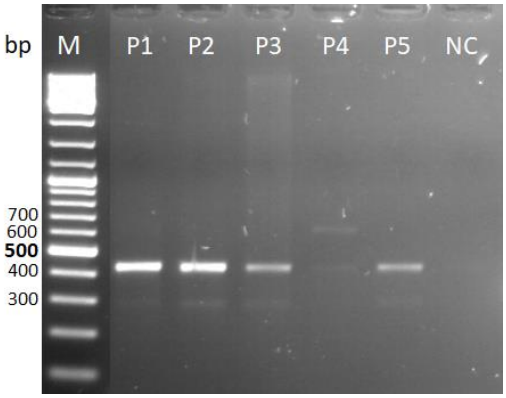

Fig. 3.10 Gel electrophoresis image of PCR products obtained with MonF/ MonR pair of primers for P group of samples. NC- negative control; M - Gene Ruler™ DNA Ladder Mix (SM0331). Expected size of product ~ 340 nt.

Table 3.16 Results of PCR analysis of the samples with MonF/MonR pair of primers. The expected size of the product was ~ 420 bp

Sample	Amplicon (bp)	Sample	Amplicon (bp)	Sample	Amplicon (bp)
KZ1F	–	**S1(S)**		**BP2(T)**	–
KZ2F	–	**S2(S)**	290/**420**	**BP2(B)**	–
KZ2F2	–	**S3(S)**	290/**420**	**P1**	300/**420**
KZ3(F1)	–	**R1(S)**	–	**P2**	300/**420**
KZ2(F1)	–	**R2(S)**	**420**	**P3**	300/**420**
D1(S)	–	**R3(S)**	–	**P4**	420/**620**
D2(S)	–	**BP1(T)**	–	**P5**	300/**420**
K(S)	–	**BP1(B)**	–		

Amplicons of similar to expected size from the samples C1T, C2T, C3T, C3B, KR1T, KR2B, KR2T, KR5, P1, P2, P3, P4, P5 were subjected to sequencing. The results of blastx analysis of obtained sequences are in Appendix J.

Homology search confirmed the origin of the amplicons from alkane monooxygenase genes for all samples, but interestingly, among the most reliable matches, there were no genes belonging to the microorganisms for which these primers were originally designed. The degeneracy of the primers allowed them to anneal to conservative regions of alkane monooxygenase genes belonging to a very wide range of microorganisms.

Comparing the results for the previous pairs of primers (T2S2/Deg and AlkB484F/AlkB824R) and this one, it can be said that the newly detected homologues with the lowesr e–value for sample P1 belong to *Gordonia iterans*. For **P2** sample no new homologues were found. For **P3** and **P4** – *Clostridium paratrificum.* In **P5** among new findings are *Pseudomonas brassicacearum* and *Pseudomonas veronii*. For **C1** sample, e-value hit was enzyme from *Curvibacter* sp. For **C2T** – *Rhodococcus aetherivoran, Pedobacter* sp., and *Pimelobacter simplex.* For **C3T** – Pedobacter sp., *Nocardioides cavernae* and *Marmoricola* sp. For **KR1T** – *Nocardioides seonyuensis* and *Marmoricola* sp. For samples **KR2B** there were not enough reliable hits. As for sample **KR3B**, *Acetobacteraceae* family

bacterium enzyme has the lowest e-value. For **KZ1** sample – enzyme of Mycolibacterium sinensis. For sample **KZ3** – the enzyme from *Nocardioides* sp. was the closest homologue.

A1k1_F/Alk1_R pair of primers

One more set of stringent primers for alkane hydroxylases (A1k1_F/Alk1_R) was applied in this study. These stringent primers were designed to detect *alkB* gene from *Amycolatopsis rugosa, Pseudomonas fluorescens CHA0, Rhodococcus erythropolis, Burkholderia cepacian and alkB1* from *Pseudomonas aeruginosa* PG201, *Rhodococcus sp.* 1BN, *Pseudomonas aeruginosa* PAO1. However, in the current study, they generated products that gave the same blastx analysis results as those for the primer pairs discussed above, so it was decided not to include the data in the results.

3.2.3. Laccase-like multicopper oxidases from *Rhodococcus opacus* R7

Among the targets for PCR, there was also a gene for a unique enzyme that can attack PE without pre-treatment. This gene is laccase-like multicopper oxidase LCMO2 from *Rhodococcus opacus* R7 (Zampolli et al., 2023) that is described in some details in Chapter 1.5.2.2. was isolated during transcriptome analysis after growth of *R. opacus* R7 on PE powder and showed the highest activity at 65°C. Such elevated temperatures can make plastic more amorphous, which facilitates biodegradation. Unfortunately, none of the tested samples from groups C, KZ, KR and P yielded in PCR product.

3.2.4. Styrene monooxygenases' (SMOs) genes

In this section the results of analysis of styrene monooxygenase genes will be discussed.

***Rhodococcus* spp. StyA2B**

Styrene monooxygenases (SMOs) oxygenate the vinyl side chain of styrene to styrene oxide. This initiates the degradation process. SMOs usually include 2 components: epoxidase (StyA) and reductase (StyB). StyB uses NADH to reduce the FAD cofactor which is utilized by the StyA to activate molecular oxygen and to catalyse the epoxidation of styrene. However, a rarer one-component variant occurs. In this case, both domains (StyA and StyB) are fused in one protein (Tischler et al., 2012). Primer set StyA2B_F1/StyA2B_R2 designed to detect such unique one-component systems. The genes that were used as references to design primers for conservative regions of SMOs belonged to *Rhodococcus opacus* MR11, *Rhodococcus rhodochrous* 172, *Rhodococcus rhodnii* 135.

As in the original article, in this study, when amplifying with these primers under optimal conditions, quite a lot of non-specific products were formed. However, the article states that the product of the expected size was indeed the target product (Tischler et al., 2012).

Amplification on samples P1 and P2 showed a product of exactly the size reported as positive (Fig. 3. 11). A number of other samples also demonstrated products with lengths similar to target (Table 3.17)

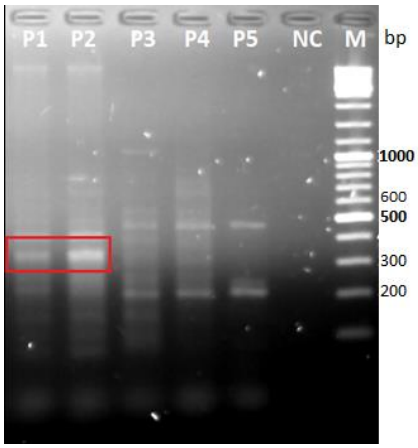

Fig. 3.11 Gel electrophoresis image of PCR products obtained with primers StyA2B_F1/StyA2B_R2 for P group of samples. NC- negative control; M - Gene Ruler™ DNA Ladder Mix (SM0331). Expected size of product ~ 360 nt.

This pair of primers was used as a part of bachelor's thesis for samples from the groups C, KZ, KR as well, however, the repeats that were done during master's thesis work revealed more bands of expected size.

Table 3.17 Results of PCR and electrophoretic analysis of the samples with StyA2B_F1/ StyA2B_R2 pair of primers. The expected size of the target product was ~ 360 bp

Sample	Amplicon (bp)	Sample	Amplicon (bp)	Sample	Amplicon
C1(T)	–	**KR2(B)**	500	**KZ4(B)**	170/220/360
C1(B)	200	**KR3(T)**	200/320/**360**/500	**KZ5(T)**	–
C2(T)	–	**KR3(B)**	200/320/**360**/500/ 600	**KZ5(B)**	zone with bright peak **300**–**400**
C2(B)	550	**KR4(T)**	zone with bright peak **300**–**400**	**KZ1(F1)**	120/220/**360**/420/5 10
C3(T)	300/550	**KR4(B)**	–	**P1**	210/**360**/400
C3(B)	–	**KR5**	–	**P2**	**360**/400
C4(B)	200/**400**	**KZ1**	220	**P3**	210/450
KR1(T)	–	**KZ2**	–	**P4**	210/450
KR1(B)	zone with bright peak **300**–**400**	**KZ3**	150/220/**330**	**P5**	210/450
KR2(T)	550	**KZ4(T)**	–		

Part of the amplicons of samples where the products of similar to expected size were detected, were sequenced. Among them: C4, KR1B, two KR3T from different PCR repeats, two KR3B from different repeats, KR4T, KZ3, KZ5B, KZ1(F1), P1 and P2.

Table 3.18 Results of blastx search of amplicons of expected size after PCR for styrene monooxygenase gene

Sample	Seq. len.	Ident. (%)	Align. Len. (aa)	E-value	Bit score	Protein ID	Annotation
P2_1	356	70.73	55	8.95E-21	38.1	WP_189021159.1	flavin reductase [Paenarthrobacter histidinolovorans]
	356	70.73	55	9.18E-21	38.1	WP_039239282.1	monooxygenase component B [Arthrobacter sp. MWB30]
	356	70.73	55	9.18E-21	38.1	WP_079582600.1	flavin reductase [Arthrobacter sp. 31Cvi3.1E]
	356	70.73	55	9.41E-21	38.1	WP_110505927.1	flavin reductase [Paenarthrobacter ni,otinovorans]
2	360	66.39	122	1.66E-48	170	WP_012256439.1	NAD(P)/FAD-dependent oxidoreductase [Chloroflexus aurantiacus]
3	358	65.55	119	1.79E-38	146	WP_118927463.1	styrene monooxygenase/indole monooxygenase family protein flavin reductase [Nocardioides immobilis]
	358	64.71	119	1.99E-36	140	WP_026058503.1	styrene monooxygenase/indole monooxygenase family protein flavin reductase [Streptomyces sp. SS]

The sequencing followed by blastx analysis revealed ambiguous results. For several samples, the analysis revealed strong homology with enzymes from the oxidoreductase class, that may have biological significance in the context of styrene monoxygenases. For example, for sample P1, it was luciferase like monooxygenaselass flavin-dependent oxidoreductase of *Comamonas* sp., for sample KR1B it was aldo/keto reductase of *Chloroflexi* bacterium, for KR3B - flavin reductase of *Anaerolineales* bacterium (not included in the table). However, subsequent pairwise nucleotide alignment with the target sequence did not detect any significant similarity, even though they were indeed flanked with primers. Thus, the results for all samples except P2 were recognised as negative. This supports the fact that single-component systems are rare and PCR only is not enough to makeconclusions about the presence of the gene in the sample.

***Variovorax paradoxus* StyA2B**

Another primers set that was applied in this study was designed for 2-component styrene monooxygenase system of *Variovorax paradoxus***.** It consists of an epoxidase protein (*Vp*StyA1) and a two-domain protein (*Vp*StyA2B) harboring an epoxidase (A2) and a FAD-reductase (B) domain (Tischler et al., 2018). The primers developed in this work targeted the conservative region of the second protein, the *Vp*StyA2B protein fragment.

The article describing this system states that styA2B is mainly found in *Actinobacteria* (e.g., *Amycolatopsis, Arthrobacter, Gordonia, Mycobacterium, Nocardia*, etc.), as well as in *Variovorax* (β-proteobacteria). In other non-Actinobacteria, no *styA2B*-like genes have been identified. The closest homologues of the two-domain proteins of *Variovorax* have been found in *Delftia* (Tischler et al,.

2018). Electrophoresis gels images after two repeats of PCR for P group of samples are shown in Fig.3.12. Table 3.19 shows the results for all the tested samples; the data is presented in approximate amplicon lengths.

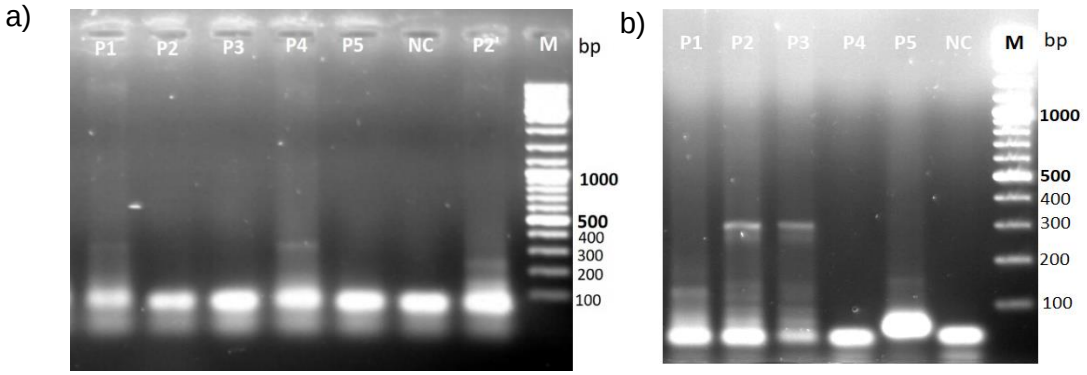

Fig. 3.12 Gel electrophoresis image of PCR products obtained using primer pair VpStyA F/R. a) and b) obtained under the same conditions for P group of samples, repeats. P2' is also P2 sample, but DNA isolated at a different time. NC - negative control. M - Gene Ruler™ DNA Ladder Mix (SM0331). The expected product size was ~ 230 bp.

Table 3.19 Results of PCR and electrophoretic analysis of the samples for the gene of *Variovorax paradoxus* styrene monooxygase StyA2B with VpStyA2B_F/R pair of primers. The expected size of the target product was ~ 230 bp

Sample	Amplicon	Sample	Amplicon	Sample	Amplicon
C1(T)	**230**	**KR3(B)**	–	**KZ1(F2)**	–
C1(B)	**–**	**KR4(T)**	–	**KZ2(F2)**	
C2(T)	**230**	**KR4(B)**	–	**KZ3(F2)**	–
C2(B)	**230**	**KR5**	N/A	**KZ2(F1)**	–
C3(T)	**230**	**KZ1**	**230**	**KZ1(F1)**	500
C3(B)	**230**	**KZ2**	–	**KZ3(F1)**	–
C4(B)	**230**	**KZ3**	–	**P1**	150/310
KR1(T)	**–**	**KZ4(T)**	**230**	**P2**	150/310
KR1(B)	**–**	**KZ4(B)**	–	**P2'**	**230**
KR2(T)	**230**	**KZ5(T)**	–	**P3**	150/310
KR2(B)	**230**	**KZ5(B)**	–	**P4**	310
KR3(T)	–			**P5**	150

N/A – data not available; P2' is P2 sample, but DNA isolated at a different time.

The amplicons from part of the samples where the product of similar to expected size were detected, were sequenced. Among them: C1T, C2T, C2B, C3T, C4, C3B, KR2B, KR2T, KZ1(F1) (500 bp), P2' and P2 (300 bp). Appendix K contains detailed results of blastx analysis. Unfortunately, it was not possible to obtain the data for the amplicon from the sample KR2T.

Homology search revealed that amplicons from samples C1T, C2T, C2B, C3T, C4, C3B, KR2B were of the origin of target gene, however grom various different organisms. Sequences from samples C1T, KZ1(F1), (500bp) and P2 (300 bp) were not related to initial target.

Summarising the data, it can be concluded that for sample **P2**, the hits for homology search were enzymes belonging to such species as *Delfia acidovorans*, *Skermania* sp, *Variovorax* sp and *Azoarcus* sp. For sample **C2T** the closest homologs of amplicons were from species *Mesorhizobium* sp, *Rhodococcus* sp. and *Variovoras paradoxus*. For **C2B** samples flavin reductase enzymes from *Mycobacterium tuberculosis*, *Variovorax* sp, and *Mezorisobium* sp. For sample **C3T** – *Variovorax paradoxus*, *Variovorax gossypii*, *Rhodococcus* sp. For – **C3B** *Delfia* sp. and *Mesorhizobium soli*. For amplicons from sample **C4** the closes homologs were from species *Glaciimonas soli* and several species from *Variovoras* genus. Finally, for **KR2B** sample the lowest e–value showed enzymes from *Glaciimonas* soli.

In results table Appendix K there are several names used for the same enzyme, including names flavin reductase and alanine-phosphoribitol ligase. The name flavin reductase (or FAD-binding reductase) comes from the function of the protein VpStyA2B described above, while the name alanine-phosphoribitol ligase comes from an outdated annotation of the protein StyA2B (Lin et al., 2020).

3.2.5. *Ideonella sakaensis* PET-active enymes

In 2016, Yoshida et al. reported the discovery of a soil bacterium, *Ideonella sakaiensis* 201-F6, that produces extracellular enzymes capable of depolymerization of PET. These are very promising enzymes that are being researched and optimised for large-scale PET processing (Sevilla et al., 2023).

First PCR with the pair of primers for *Ideonella sakaensis* PETase yeilded the product of around expected size in several samples Table 3.20, while the following two attempts showed negative results for all samples. Samples from P group did not result in any product in all attemtpts.

Table. 3.20 Results of PCR and electrophoretic analysis of samples with IsPETaseF/R pair of primers for the gene of *Ideonella sakaiensis* PETase, expected product size was ~ 900 bp

Sample	Amplicon	Sample	Amplicon	Sample	Amplicon
C1(T)	**850**	**KR3(B)**	700	**KZ1(F2)**	–
C1(B)	–	**KR4(T)**	–	**KZ2(F2)**	–
C2(T)	**700–1000**	**KR4(B)**	–	**KZ3(F2)**	–
C2(B)	**900**	**KR5**	N/A	**KZ2(F1)**	–
C3(T)	**850**	**KZ1**	–	**KZ1(F1)**	–
C3(B)	–	**KZ2**	1100/1300	**KZ3(F1)**	–
C4(B)	–	**KZ3**	700/**900**/1500	**P1**	–
KR1(T)	–	**KZ4(T)**	–	**P2**	–
KR1(B)	700/**800**/**900**/1200/1700	**KZ4(B)**	–	**P3**	–
KR2(T)	–	**KZ5(T)**	1000/1300/1800	**P4**	–
KR2(B)	1000	**KZ5(B)**	–	**P5**	–
KR3(T)	N/A				

Amplicons of similar to expected size from samples C1T, C2B, C3T, KR1B, KR1B (900 bp), KR2B, and KZ3 were subjected to sequencing.

Unfortunately, all the tested PCR products were the results of unspecific primers annealing.

After blastx sequences analysis, it was noted that the annotations of some matches indicate a similar biological function of the amplicon with the target gene. However, subsequent pairwise nucleotide alignment did not reveal any significant similarity. Interestingly, but amplicon from the sample C3T that seemed pure and pronounced Table 3.20, (gel image not provided) also appeared to be completely different from the target product.

As mentioned in Chapter 1.4.1.5, *Ideonella sakaensis* is unique in that it contains two enzymes involved in PET utilisation: the aforementioned PETase and MHETase, an enzyme that catalyses the next stage of PET digestion. Results of 3 repeats of PCR with primers for *Ideonella sakaensis* MHETase were negative for all examined samples from all groups.

3.2.6. PUR-active lipases

Lipases certainly belong to the class of hydrolases, but PueA (poluretanase A) enzyme has already been classified as a specific polyurethanase due to its high PUR specificity, which is why it is discussed separately. This enzyme catalyses the hydrolysis of the ester and amide bonds, resulting formation of polyol and a carboxylic acid or amine and a carboxylic acid respectively (Stern et al., 2000). The primers for the gene of this enzyme were designed to capture 54-amino acid glycine-rich motif of *Pseudomonas chlororaphis* PueA polyurethanase (Langlois & Howard, 2002). Results of PCR with subsequent electrophoretic analysis are on the picture (Fig. 3.13).

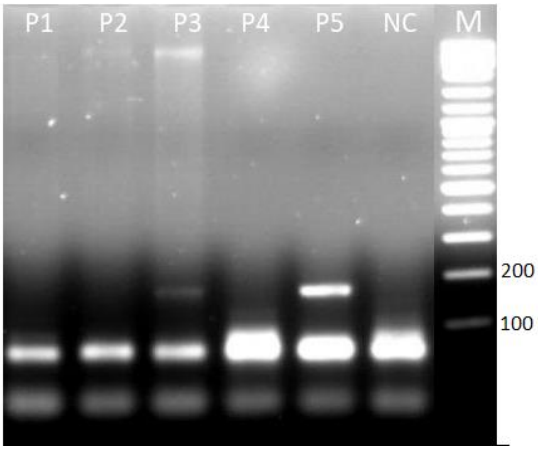

Fig. 3.13 Gel electrophoresis image of PCR products obtained with primers pueA_F/pueA_R for P group of samples. NC- negative control; M - Gene Ruler™ DNA Ladder Mix (SM0331). Expected size of product ~ 180 bp.

All samples from all groups were tested, but only 2 samples from P group gave positive results with amplicons ~ 180 bp in size. They were subjected to sequencing. The results of blastx homology search of obtained sequences are in Table 3.21.

Table 3.21 Results of blastx search of sequences of amplicons of expected size after PCR for pueA gene (*Pseudomonas chlororaphis* PueA polyurethanase)

Sam-ple	Seq. len.	Ident. (%)	Align. Len. (aa)	E-value	Bit score	Protein ID	Annotation
P3	182	94.74	54	2.86e-27	110	RBL67788.1	polyurethanase, partial [Pseudo-monas sp. MWU13-2625]
	182	94.74	54	1.29e-26	110	WP_011061486.1	polyurethanase A [Pseudomonas protegens]
P5	169	96.30	54	5.88E-26	108	WP_053151819.1	polyurethanase [Pseudomonas protegens]
	169	96.30	54	6.05E-26	108	ABM54447.1	polyurethanase A [Pseudomonas chlororaphis]

Amplicons from both samples showed a high degree of identity with polyurethanases from bacteria of the genus *Pseudomonas*, including *Pseudomonas chlororaphis.*

Ce_Ubr lipase

Interesting results were obtained while studying samples for genes encoding another enzyme that degrades PUR called Ce_Ubr. This enzyme was isolated from the bovine rumen microbiome and showed high activity against impranil (type of PUR). Further research revealed that the enzyme belongs to the carboxyl-ester hydrolase from lipolytic family IV (Ufarté et al., 2017). Results of gel electrophoresis of PCR product are in Fig. 3.14. Table 3.22 contains results of PCR for all tested samples.

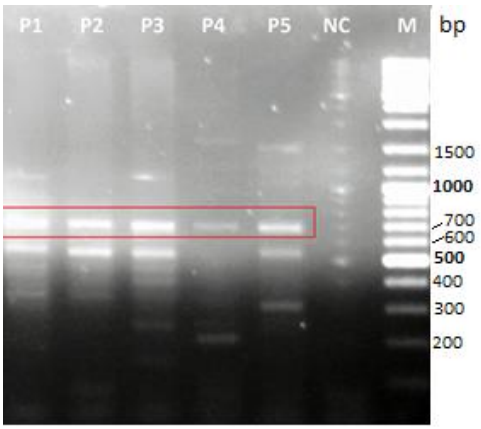

Fig. 3.14 Gel electrophoresis image of PCR products obtained using primer pairs Ce_UbrF/R for P group of samples. C - negative control. M - Gene Ruler™ DNA Ladder Mix (SM0331). Red squares indicate zones of target product. Expected product size ~780 bp.

Table 3.22 Results of PCR with Ce_UbrF/R pair of primers. Expected product size ~780 bp

Sample	Amplicon	Sample	Amplicon	Sample	Amplicon
C1(T)	–	**KR3(B)**	280/350/**750**	**KZ1(F2)**	–
C1(B)	–	**KR4(T)**		**KZ2(F2)**	–
C2(T)	–	**KR4(B)**	–	**KZ3(F2)**	–
C2(B)	200/300/500/600/**800**	**KR5**	–	**KZ2(F1)**	–
C3(T)	300/600/**800**	**KZ1**	–	**KZ1(F1)**	–
C3(B)	–	**KZ2**	–	**KZ3(F1)**	–
C4(B)	300/500/**800**	**KZ3**	**–**	**P1**	380/500/**700**
KR1(T)	–	**KZ4(T)**	–	**P2**	380/500/**700**
KR1(B)	500/600/**800**	**KZ4(B)**	700/**800**	**P3**	250/500/**700**
KR2(T)	–	**KZ5(T)**	–	**P4**	200/**700**
KR2(B)	500/700/**800**	**KZ5(B)**	**800**/700	**P5**	300/550/**700**
KR3(T)	500/**750**/1200				

Despite the fact that there were many products, some of them were quite distinct. For all samples from group P, pronounced amplicons approximately 100 bp shorter than the target were obtained (Fig.3.14). For a number of samples from other groups, well-resolved amplicons of the expected size were also obtained.

Bands of similar to expected size from samples C2B, C3T, C4, KR1B, KR2B, KR3T, KR3B, KZ4B, KZ5B, P1, P2, P3, P4, P5 were subjected to sequencing.

Interestingly, among the potential homologues to the obtained amplicons with a higher degree of confidence were enzymes with similar biological functions, and also these amplicons turned out to be the results of amplification from the same templates across tested samples. However, pairwise comparison of nucleotide sequences between amplicons and the target sequence revealed no significant similarity (only the regions to which the primers were designed were similar) (results not included). Table 3.23 shows several illustrative examples.

Table 3.23 Results of blastx search of sequences of amplicons of expected size after PCR for Ce_Ubr lipase gene

Sample	Seq. len.	Ident. (%)	Align. Len. (aa)	E-value	Bit score	Protein ID	Annotation
P2	700	98.36	122	5.44E-75	253	RIJ98969.1	hypothetical protein DCC46_10025 [Armatimonadetes bacterium]
P3	702	98.36	122	5.64e-75	253	RIJ98969.1	hypothetical protein DCC46_10025 [Armatimonadetes bacterium]
P4_1	705	94.36	124	2.33E-73	249	RIJ98969.1	hypothetical protein DCC46_10025 [Armatimonadetes bacterium]
2	679	84.11	214	5.72E-128	377	WP_167273306.1	aminotransferase [Paenibacillus lupini]

Table 3.23 *Continued*

P5	716	75.81	215	1.41E-118	352	WP_166144329.1	exo-alpha-sialidase [Paenibacillus sp. S3N08]
C2B	866	83.09	136	1.93E-76	239	RMG85740.1	aminotransferase class I/II-fold pyridoxal phosphate-dependent enzyme, partial [Chloroflexi bacterium]
KR1B	867	80.37	163	6.39E-93	283	HGS83889.1	aminotransferase class I/II-fold pyridoxal phosphate-dependent enzyme [Chloroflexi bacterium]
KR2B	867	78.53	163	1.01E-90	277	HGS83889.1	aminotransferase class I/II-fold pyridoxal phosphate-dependent enzyme [Chloroflexi bacterium]
KZ4B	867	80.98	163	4.66E-93	283	HGS83889.1	aminotransferase class I/II-fold pyridoxal phosphate-dependent enzyme [Chloroflexi bacterium]

Further analysis of the reasons for this phenomenon is required.

3.3. Sequencing of mixtures of amplicons

In addition to sequencing amplicons isolated from agarose gel, a pilot experiment was conducted to sequence all PCR products after all PCRs (the method is described in the corresponding chapter). For this purpose, samples from group P were selected. The aim was to obtain information about all amplicons formed as a result of primer annealing. Information about all genes to which primers are related could reveal homologues that are very different in length but relevant to the target sequence, for example, as a result of large gene rearrangements (large indels), or if the concentration was insufficient for detection by agarose gel electrophoresis. This would have provided a comprehensive picture of the representation of the gene of interest in sample.

The primary results of blastn analysis of the data obtained with this approach are consistentwith the results of sequencing involved the gel extraction method. The method requires sophisticated bioinformatic tools but putatively has great potential. Among the target products, genes for alkane monooxygenases originating from various microorganisms and *Thermobifida fusca* cutinases were widely represented. The polyurethanase genes *pueA* were also found, but initial analysis of the data did not reveal the any styrene monooxygenases genes, which were successfully detected in previously described analysis.

In general, the results are complex and inconclusive so far, though require further detailed examination.

4. DISCUSSION

The Results section provides the data for the main groups of enzymes involved in plastic biodegradation: hydrolases and oxidases. Over time, some enzymes become specificity for plastic substrates and start to be named after the type of plastic they degrade, for example PETase and PURase. This means that both the evolution of enzymes and the study of these enzymes are advancing.

A summary table for all sequencing results is below (Table 4.1). The results should be interpreted as follows: '+' indicates that the target gene was detected, while '–' indicated that it was not detected. The absence may be due to various reasons, not only because of its actual absence in the sample, as described in Chapter 1.11, among them the presence of residues of humic acid from the soil that inhibits PCR, or secondary DNA structures that were not separated during denaturation PCR step. To address these issues, additional DNA purification steps and a prolonged denaturation stage can be applied respectively.

Nevertheless, it can be confidently stated that the samples from group P contain a wide range of genes that are known to be involved in the biodegradation of (micro)plastics. This is not surprising, as these samples were collected at the Energesman waste processing plant. The fact that such places are good sources of microorganisms (and genes) capable of biodegradation of different types of plastics is discussed in Chapter 1.8.

As for the other sample groups, it was expected that the KZ/KZ(F) samples would also show a wide representation of the genes investigated in this study, due to the fact that they were collected from the active landfill site, however the results were similar to those of the control group from garden soil. In groups KR and C, a certain number of genes associated with plastic biodegradation were also found. This finding is unexpected for group C, given that the samples originated from garden soil.

As an explanation for the results of KZ/KZ(F) groups, it can be assumed that under the constantly changing conditions of an active landfill, such as the displacement of layers due to the work of levelling machines, the microbiota does not have an opportunity to stabilise. In this case, collecting samples of plastisphere (for example, to collect actual fragment of plastic with signs of decomposition) may be a good alternative method for searching for genes of interest.

The presence of the target genes in KR samples is not surprising, as they were collected from a closed landfill that began operating in 1987 and closed in 2008. The landfill is covered with a layer of soil, but apparently the huge amount of waste underneath affects the composition of the soil's microbiota.

Table 4.1 Summary table with results of target metagenome sequencing

Genes (primers)/ Sample groups	**Targets**													
	Hydrolases					**Alkane hydroxylases**			**LCMO2**	**Styrene mono-oxygenases**		**Polyu-reta-nase**	***Is*PETase**	***Is*ME-Tase**
	*Fs*Cut4	*Tf*Cut2/ *Tf*Cut1	LCC	Phl7	*Lf*Ure	TS2S/ Deg1RE	AlkB484/ AlkB824	Mon_F/R	LCMO2	StyA2B	*Vp*StyA2B	PueA	*Is*PETase	*Is*MHETase
C	+	–	–	–	+	+	N/A	+	–	–	+	–	–	–
P	+	+	–	*Tf* cutinase, rather than PHL7	+	+	+	+	–	+	+	+	–	–
KR	–	+	–	*Tf* cutinase, rather than PHL7	–	+	N/A	+	–	–	+	–	–	–
KZ/ KZ(F)	–	–	–	–	–	+	N/A	+	–	–	N/A	–	–	–

N/A – amplicon(s) were detected, but not sequenced;

"+" – amplicon from at least one sample from the group was target product;

"–" none of the samples in the group resulted in target product (either at the PCR stage, or the amplicons were the result of non-specific annealing of primers).

Clean soil – Molėtai forest, P – Energesman waste sorting facility, KR – Kariotiškės landfill, KZ / KZ(F) – Kazokiškės landfill samples, but not only KZ samples, but also filtrate samples from KZ(F) group.

Results for Ce_Ubr are not included due to their ambiguity.

It should also not be neglected that although the enzymes under investigation are involved in the biodegradation of plastics, they have their own natural substrate: for cutinases - plant cutin, for alkane oxygenases - natural alkanes. Styrene is less common in nature and is primarily of anthropogenic origin (of industrial emissions) thus has been present in the atmosphere before the issue of plastic pollution emerged. For urethanases the substrate is urethane, which is found in small quantities in wine, beer, and soy sauce as a by-product of fermentation (Jia et al., 2020). Therefore, it is very important to assess not only the presence of the genes, but also their specificity and effectiveness against plastic.

Thus, based on the data (Table 4.1), it can be said that alkane monooxygenases is a highly represented class of enzymes among all groups of samples, due to the fact that alkanes are widespread substances. However, knowledge about these enzymes is very valuable because they are currently one of the most promising candidates for solving the problem of PE degradation. PET-active hydrolases such as *Fusarium solani* cutinase, *Thermobifida fusca* cutinases 1 and 2, as well as PUR-active enzymes *Lisinobacilllus fusiformis* urethanase and *Pseudomonas chloraphis* PueA lipase, are the most popular in samples from group P. A rare type of single-component styrene monooxygenase was found only in the sample from group P, while the more prevalent two-component system was also more prevalent among the groups of samples.

The findings obtained in this study partially align with the results obtained in some previous studies; however, they differ in some aspects. For example, in a study based on whole metagenome sequencing of landfill metagenome samples from India (humid subtropical conditions) high prevalence and diversity of alkane monooxygenases was shown, which is consistent with the results of current study. Genes involved in styrene degradation (*styA*) showed lower representation (4 out of 10 samples) which is lower than for clean soil samples from group C, but higher than for all other plastic-contaminated sample groups in this study (Kumar et al., 2021).

However, the samples from India have shown much higher representation of PET-active enzymes (Kumar et al., 2021), whereas the same metric in this study was low for analysed landfills samples, but not for those from waste sorting plant.

Among the possible reasons can be the fact that as already mentioned, optimal temperatures for PET-degrading enzymes are elevated, whereas the average annual temperature in Lithuania, where the samples were collected is ~7 °C. This explanation can be applied to the high level of representation of these enzymes in samples from waste sorting plant: they were collected from closed, heated facility, moreover, 2 of them were additionally heated to 55–70 °C for 28 days (Chapter 2.1). Among other possible explanation might be the different waste composition due to cultural differences or variations in waste management practices.

In another study based on metatranscriptomic analysis, some of the results also match those obtained in the current study. In this study two groups of samples were analysed: rich in plastic samples collected from a closed landfill site in eastern Germany and sampled forest soil, potentially free from plastic contamination. The samples were cultivated for 53 days in the presence of PE film. The results regarding alkane hydroxylases (*alkB*) revealed a high presence of gene transcripts in response to PE in both types of samples with almost no difference between them (MacLean et al., 2024), which is consistent with the results of the current study regarding the prevalence of these genes. What is unique in this study is that PETases gene transcripts were detected only in the forest soil samples and were completely absent in the plastic-contaminated soil samples. Though this finding is not directly relevant to the current study, it suggests that the distribution of plastic degrading is difficult to predict, and it may be useful to broaden the search for such enzymes to include natural ecosystems in addition to sites heavily polluted with wastes (MacLean et al., 2024).

In the Results section, PCR results for some other groups of environmental samples (D, K, S, R, BP) are also presented. It was noticed that the detection rate of target-sized products was fairly low, putatively because of aquatic origin of the samples, therefore it was decided not to perform further PCRs and not to sequence the obtained products.

The problem of bias during PCR analysis is already described above (Chapter 1.11). Due to such instability of results, for some primer sets, repeats of PCRs were performed, since one test may be uninformative and lead to false false- negative results.

CONCLUSIONS

1) Metagenomic DNA from 47 environmental samples were isolated in concentrations from 3 ng/µl to 268 ng/ µl. The A260/280 ratio fell within range 1.5–2.2, while the A260/230 was significantly lower for the majority of samples, putatively due to the presence of residues of humic acid.

1) Amplification products of expected size were obtained after PCRs targeted to genes of alkane hydroxylases, styrene monooxygenases, PET-active cutinases, urethanase and PUR-active lipase, indicating their potential presence in metagenomic samples, with the highest abundance of genes of alkane monooxygenases (in all 10 groups of samples), and lowest abundance of PUR-active lipase and of *Thermobifida fusca* cutinase 2 (both found only in waste sorting plant samples). No amplification product was detected for the gene of laccase-like multicopper oxidase from *Rhodococcus opacus* R7.

2) The sequence of obtained amplicons proved the origin and identity of *Thefmobifida* genus cutinases, *Fusarium solani* cutinase, *Pseudomonas* genus pueA lipase, *Lysinibacillus* genus urethanase, *Variovorax* genus styrene monooxygenase. For *Rhodococcus* genus styrene monooxygenase the origin differed from the expected one. For alkane monooxygenases, the identity was proven, and the most common genera of origin were Corynebacterium, *Nocardioides*, *Mycolicibacterium, Clostridium*. Part of the PCR products tested turned out to be unspecific.

3) Analysis of metagenomic DNA revealed variating plastic biodegradation potential in all of them:

a) Samples collected at the waste-sorting plant show potential for the depolymerisation of PET and PUR, degradation of the PUR urethane monomer and styrene (PS monomer), as well as degradation of pretreated PE.

b) Samples of clean soil collected from the garden show potential for the degradation of pretreated PE and styrene (PS monomer), as well as for surface modification of PET.

c) The microbiota from the closed landfill harbors genes for enzymes active on PET, pretreated PE, and styrene.

d) A potential for the degradation of pretreated PE was identified in samples from the active landfill.

AUTHOR’S PERSONAL CONTRIBUTION

The author’s contribution in this paper consisted of the development of methodology and conceptualisation (together with supervisor and consultant), research, data analysis, initial draft writing.

ACKNOWLEDGMENTS

I would like to sincerely thank my Supervisor Prof. dr. **Eglė Lastauskienė** and Academic consultant PhD student, **Gintarė Jansonaitė** for their wise guidance of the work, their willingness to help and provide answers to questions that arose, as well as encouragement to find answers on my own and support throughout the process of writing my Master's thesis.

I would also like to thank Dr **Aleksandras Konovalovas** for his willingness and enthusiasm to try an unconventional sequencing approach and for his great efforts in bionformatic data analysis.

I would like to thank sequencing facility UAB **Seqvision** for rapid and high-quality sequencing of sample, and especially **Jonas Juozapait**is for detailed counselling on aspects of data processing.

I am also very thankful to **senior colleagues** in the laboratory for their willingness to provide advice on methodological difficulties.

I am sincerely grateful to **Vilnius University** for the opportunity to study in the Master's program.

VILNIUS UNIVERSITY
LIFE SCIENCES CENTER

Alena Koida

Master's thesis

Analysis of (micro)plastic biodegradation-associated genes in environmental microorganisms

ABSTRACT

Due to insufficient plastic waste management, plastic pollution has become one of the greatest challenges of the 21st century. Microplastics and nanoplastics formed from larger plastic parts are even more problematic due to the resistance to natural degradation, increased surface area and ubiquity. Their harmful effects on aquatic and terrestrial ecosystems as well as human health have been proven. Due to the variability of microbial metabolism, microorganisms have begun to modify their metabolism to degrade plastic to use it as a carbon source. Large scale application of these enzymes could be a sustainable solution to mitigate global plastic pollution due to environmental friendliness. However, sufficient fundamental knowledge has not yet been accumulated.

The aim of this study is to explore different both natural and artificial sources for microorganismal genes that encode enzymes that are associated with degrading various types of (micro)plastics.

For that, metagenomic DNA was isolated from 47 environmental samples and subjected to PCR analysis. Samples from water bodies showed a low amplification rate, thus were excluded from further testing. After PCR analysis of 34 samples for the genes that encode alkane hydroxylases, styrene monooxygenases, PET-active cutinases, urethanase and PUR-active lipase, 134 amplicons were subjected to sequencing.

Sequencing revealed that the microbiome of the waste treatment plant is capable of depolymerising PET and PUR, degrading of urethane and styrene, as well as degrading of pretreated PE. The microbiota from the closed landfill harbors genes for enzymes active on PET, pretreated PE, and styrene. A potential for the degradation of pretreated PE was identified in samples from the active landfill. Surprisingly, samples of soil collected from the garden showed potential for the degradation of pretreated PE and styrene, as well as for surface modification of PET.

These results prove that prolonged contact of microbiome with contaminants may increase the prevalence and diversity of genes associated with plastic biodegradation but also suggest that it may be reasonable to broaden the focus of search to different environments to find new enzymes.

LIST OF REFERENCES

1. Aird, D., Ross, M. G., Chen, W. S., Danielsson, M., Fennell, T., Russ, C., Gnirke, A. (2011). Analyzing and minimizing PCR amplification bias in Illumina sequencing libraries. Genome Biology, 12(2), R18. https://doi.org/10.1186/gb-2011-12-2-r18
2. Alaeddini, R. (2012). Forensic implications of PCR inhibition—A review. Forensic Science International: Genetics, 6(3), 297–305. https://doi.org/10.1016/j.fsigen.2011.08.006
3. Alariqi, S. A., Kumar, A. P., Rao, B. S. M., and Singh, R. P. (2006). Biodegradation of γ-sterilised biomedical polyolefins under composting and fungal culture environments. Polym. Degrad. Stab. 91, 1105–1116. doi: 10.1016/ j.polymdegradstab.2005.07.004
4. Aliya, S., Alhammadi, M., Ilangovan, S., Han, S., Tamang, S., Son, B., Lee, H. U., & Huh, Y. S. (2025). Microplastics: An emerging environmental risk factor for gut microbiota dysbiosis and cancer development? Environmental Chemistry and Ecotoxicology, 7, 706–728. https://doi.org/10.1016/j.enceco.2025.03.005
5. Amplicon Sequencing. (2025). https://www.genewiz.com/public/services/next-generation-sequencing/amplicon-sequencing-services [Accessed 15 May, 2025]
6. Akutsu, Y., Nakajima-Kambe, T., Nomura, N., and Nakahara, T. (1998). Purification and properties of a polyester polyurethane-degrading enzyme from Comamonas acidovorans TB-35. Appl. Environ. Microbiol. 64, 62–67. doi: 10. 1128/aem.64.1.62-67.1998
7. Alshehrei F (2017) biodegradation of low density polyethylene by fungi isolated from Red Sea water. Int J Current Microbiol App Sci 6(8):1703–1709
8. Alexander,M., 19651903158, English, Journal article, doi:10.1146/annurev.mi.18.100164.001245, 0066-4227, 18, Annual Review of Microbiology, (217–252), Biochemical ecology of soil microorganisms., (1964))
9. Alexandrakis, G., Jalali, S., & Gloor, P. (1998). Diagnosis of Fusarium keratitis in an animal model using the polymerase chain reaction. British Journal of Ophthalmology, 82(3), 306–311. doi:10.1136/bjo.82.3.306
10. Amobonye, A. E., Bhagwat, P., Singh, S., & Pillai, S. (2023). Biodegradability of polyvinyl chloride. In A. Sarkar, B. Sharma, & S. Shekhar (Eds.), Biodegradability of conventional plastics (pp. 201–220). Elsevier. https://doi.org/10.1016/B978-0-323-89858-4.00017-8
11. An, L., Liu, Q., Deng, Y., Wu, W., Gao, Y., & Ling, W. (2020). Sources of Microplastic in the Environment. In Microplastics in Terrestrial Environments (pp. 143-159). Springer. doi: 10.1007/698_2020_449
12. Asiandu A, Wahyudi A, Widiya Sari S (2021) A review: plastics waste biodegradation using plastics-degrading bacteria. J Environ Treat Tech 9(1):148–157
13. Auta, H. S., Emenike, C. U., Jayanthi, B., and Fauziah, S. H. (2018). Growth kinetics and biodeterioration of polypropylene microplastics by Bacillus sp. and Rhodococcus sp. isolated from mangrove sediment. Mar. Pollut. Bull. 127, 15–21. doi: 10.1016/j.marpolbul.2017.11.036
14. Bergmann, M., Mützel, S., Primpke, S., Tekman, M. B., Gerdts, G., & others. (2019). White and wonderful? Microplastics prevail in snow from the Alps to the Arctic. Science Advances, 5(8), eaax1157. doi: 10.1126/sciadv.aax1157
15. Branson, Y., Söltl, S., Buchmann, C., Wei, R., Schaffert, L., Badenhorst, C. P. S., Reisky, L., Jäger, G., & Bornscheuer, U. T. (2023). Urethanases for the enzymatic hydrolysis of low molecular

weight carbamates and the recycling of polyurethanes. Angewandte Chemie International Edition, 62(2), e202216220. https://doi.org/10.1002/anie.202216220
16. Suresh Brydson, J. A. (2017). Plastics materials (8th ed.). Elsevier.
17. Buchholz, H.L. Zhang, P. Perez-Garcia, L-L. Nover, J. Chow, W. R. Streit, J. Pleiss (2022);Plastics degradation by hydrolytic enzymes: the Plastics-Active Enzymes Database - PAZy, https://doi.org/10.1002/prot.26325
18. Carbios. https://www.carbios.com/en/enzymatic-recycling/ [Accession 1 March, 2025]
19. Carpenter, E. J., & Smith Jr, K. L. (1972, March 17). Plastics on the Sargasso sea surface. Science, 175(4027), 1240-1241. https://doi.org/10.1126/science.175.4027.1240
20. Chamas, A., Moon, H., Zheng, J., Qiu, Y., Tabassum, T., Jang, J. H., Abu-Omar, M., Scott, S. L., & Suh, S. (2020). Degradation Rates of Plastics in the Environment. ACS Sustainable Chemistry & Engineering, 8, 3494-3511. Retrieved from https://pubs.acs.org/doi/10.1021/acssuschemeng.9b06635
21. Chaudhary, D. K., Khulan, A., & Kim, J. (2019). Development of a novel cultivation technique for uncultured soil bacteria. Scientific Reports, 9, Article 6666. https://doi.org/10.1038/s41598-019-43182-x
22. Chen, G., Feng, Q., & Wang, J. (2020). Mini-review of microplastics in the atmosphere and their risks to humans. Science of The Total Environment, 703, 135504. https://doi.org/10.1016/j.scitotenv.2019.135504.
23. Çobanoğlu, H., Belivermiş, M., Sıkdokur, E., Kılıç, Ö., & Çayır, A. (2021). Genotoxic and cytotoxic effects of polyethylene microplastics on human peripheral blood lymphocytes. Chemosphere, 272, 129805.
24. Danso, D., Schmeisser, J., Streit, W. R., & Plastics, M. D. (2019a). New insights into the function and global distribution of polyethylene terephthalate (PET)-degrading bacteria and enzymes in marine and terrestrial ecosystems. Applied and Environmental Microbiology, 85(16), e01095-19. https://doi.org/10.1128/AEM.01095-19
25. Danso, D., Chow, J., & Streit, W. R. (2019b). Plastics: environmental and biotechnological perspectives on microbial degradation. Applied and environmental microbiology, 85(19), e01095-19.
26. Dresler, K., van den Heuvel, J., Müller, R.-J., & Deckwe, W.-D. (2006). Production of a recombinant polyester-cleaving hydrolase from Thermobifida fusca in Escherichia coli. Bioprocess and Biosystems Engineering, 29, 169–183. https://doi.org/10.1007/s00449-006-0069-9
27. Geyer, R. (2020). A brief history of plastics. In M. Streit-Bianchi, M. Cimadevila, & W. Trettnak (Eds.), Mare Plasticum – The Plastic Sea. Springer. https://doi.org/10.1007/978-3-030-38945-1_2
28. Fackelmann, G., & Sommer, S. (2021). Microplastics and the gut microbiome: How chronically exposed species may suffer from gut dysbiosis. Marine Pollution Bulletin, 167, 112402. https://doi.org/10.1016/j.marpolbul.2021.112402
29. Fatima, M., & Roohi. (2021). A brief overview on current and potential applications of thermoplastic starch. Acta Scientific Pharmaceutical Sciences, 5(12), 50–57.
30. Fotopoulou, K. N., & Karapanagioti, H. K. (2019). Degradation of various plastics in the environment. Hazardous chemicals associated with plastics in the marine environment, 71-92.
31. Jia, Y., Zhou, J., Du, G., Chen, J., & Fang, F. (2020). Identification of an urethanase from Lysinibacillus fusiformis for degrading ethyl carbamate in fermented foods. Food Bioscience, 36, 100666. https://doi.org/10.1016/j.fbio.2020.100666

32. Gambarini V, Pantos O, Kingsbury JM, Weaver L, Handley KM, Lear G. 2021. Phylogenetic Distribution of Plastic-Degrading Microorganisms. mSystems 6:10.1128/msystems.01112-20. https://doi.org/10.1128/msystems.01112-20
33. Gasperi, J., Wright, S. L., Dris, R., Collard, F., Mandin, C., Guerrouache, M., Langlois, V., Kelly, F. J., & Tassin, B. (2018). Microplastics in air: Are we breathing it in?. Current Opinion in Environmental Science & Health, 1, 1-5. doi:10.1016/j.coesh.2017.10.002
34. Glossary of Chemistry Terms. https://glossary.periodni.com/dictionary.php?en=polyvinyl [Accessed 2 May, 2025]
35. Guo, X., Zhang, J., Han, L., Lee, J., Williams, S. C., Forsberg, A., Xu, Y., Austin, R. N., & Feng, L. (2023). Structure and mechanism of the alkane-oxidizing enzyme AlkB. Nature communications, 14(1), 2180. https://doi.org/10.1038/s41467-023-37869-z
36. Goldman, A. S. (2010). ChemInform abstract: organometallic chemistry: carbon-carbon bonds get a break. Nature 463, 435–436. doi: 10.1038/463435a
37. Iiyoshi, Y., Tsutumi, Y., and Nishida, T. (1998). Polyethylene degradation by lignin degrading fungi and manganese peroxidase. J. Wood Sci. 44, 222–229. doi: 10.1007/bf00521967
38. Habib, S., Iruthayam, A., Abd Shukor, M. Y., Alias, S. A., Smykla, J., & Yasid, N. A. (2020). Biodeterioration of Untreated Polypropylene Microplastic Particles by Antarctic Bacteria. Polymers, 12(11), 2616. https://doi.org/10.3390/polym12112616
39. Hegde, K., & Veeranki, V. D. (2013). Production optimization and characterization of recombinant cutinases from Thermobifida fusca sp. NRRL B-8184. Applied Biochemistry and Biotechnology, 170(3), 654–675. https://doi.org/10.1007/s12010-013-0219-x
40. Heris, Y. S. (2024). Bacterial biodegradation of synthetic plastics: A review. Bulletin of the National Research Centre, 48, 87. https://doi.org/10.1186/s42269-024-01241-y Hahladakis, J. N. (2020). Delineating and preventing plastic waste leakage in the marine and terrestrial environment. Environmental Science and Pollution Research, 27, 12830-12837. https://doi.org/10.1007/s11356-020-08014-6
41. Hojgaard, A., Osikowicz, L. M., Eisen, L., & Eisen, R. J. (2020). Evaluation of a novel multiplex PCR amplicon sequencing assay for detection of human pathogens in Ixodes ticks. Ticks and tick-borne diseases, 11(6), 101504. https://doi.org/10.1016/j.ttbdis.2020.101504
42. Hu, Y., Liu, Z., Yan, J., Qi, X., Li, J., Zhong, S., Yu, J., & Liu, Q**.** (2010). A developed DNA extraction method for different soil samples. Journal of Basic Microbiology, 50(4), 401–407. https://doi.org/10.1002/jobm.200900373
43. Huang, Y., Zhao, Y., Wang, J., Zhang, M., Jia, W., & Qin, X. (2019). LDPE microplastic films alter microbial community composition and enzymatic activities in soil. Environmental Pollution, 254(Part A), 112983. https://doi.org/10.1016/j.envpol.2019.112983
44. Huang, X., Li, Y., Shu, Z., Huang, L., Liu, Q., & Jiang, G. (2024). High-efficiency degradation of PET plastics by glutathione S-transferase under mild conditions. Environmental Science & Technology, 58(30), 13358–13369. https://doi.org/10.1021/acs.est.4c02132
45. Huerta Lwanga, E., Gertsen, H., Gooren, H., Peters, P., Salánki, T., van der Ploeg, M., & Geissen, V. (2017). Microplastics in the terrestrial ecosystem: implications for Lumbricus terrestris (Oligochaeta, Lumbricidae). Environmental Science & Technology, 51(12), 7064-7073. doi: 10.1021/acs.est.7b00176
46. Hugerth, L. W., & Andersson, A. F. (2017). Analysing microbial community composition through amplicon sequencing: From sampling to hypothesis testing. Frontiers in Microbiology, 8, Article 1561. https://doi./10.3389/fmicb.2017.01561

47. Ho, B. T., Roberts, T. K., and Lucas, S. (2018). An overview on biodegradation of polystyrene and modified polystyrene: the microbial approach. Crit. Rev. Biotechnol. 38, 1–13. doi: 10.1080/07388551.2017.1355293
48. Hou, L., & Majumder, E. L.-W. (2021). Potential for and distribution of enzymatic biodegradation of polystyrene by environmental microorganisms. Materials, 14(3), 503. https://doi.org/10.3390/ma14030503
49. Jadaun, J. S., Bansal, S., Sonthalia, A., Rai, A. K., & Singh, S. P. (2022). Biodegradation of plastics for sustainable environment. Bioresource Technology, 347, 126697. https://doi.org/10.1016/j.biortech.2022.126697
50. Jia, Y., Zhou, J., Du, G., Chen, J., & Fang, F. (2020). Identification of an urethanase from Lysinibacillus fusiformis for degrading ethyl carbamate in fermented foods. Food Bioscience, 35, 100666. https://doi.org/10.1016/j.fbio.2020.100666
51. Junaid, M., Siddiqui, J. A., Sadaf, M., Liu, S., & Wang, J. (2022). Enrichment and dissemination of bacterial pathogens by microplastics in the aquatic environment. Science of The Total Environment, 830, 154720. https://doi.org/10.1016/j.scitotenv.2022.1547201
52. Joo, S., Cho, I. J., Seo, H., Son, H. F., Sagong, H. Y., Shin, T. J., Choi, S. Y., Lee, S. Y., & Kim, K. J. (2018). Structural insight into molecular mechanism of poly(ethylene terephthalate) degradation. Nature Communications, 9, Article 382. https://doi.org/10.1038/s41467-018-02881-1
53. Khatoon, N., Jamal, A., and Ali, M. I. (2019). Lignin peroxidase isoenzyme: a novel approach to biodegrade the toxic synthetic polymer waste. Environ. Technol. 40, 1366–1375. doi: 10.1080/09593330.2017.1422550
54. Khandare, S. D., Chaudhary, D. R., & Jha, B. (2025). Isolation and purification of esterase enzyme from marine bacteria associated with biodegradation of polyvinyl chloride (PVC). Biodegradation, 36(4). https://doi.org/10.1007/s10532-024-10101-5
55. Kim, D. W., Ahn, J. H., & Cha, C. J. (2022). Biodegradation of plastics: mining of plastic-degrading microorganisms and enzymes using metagenomics approaches. Journal of Microbiology, 60(10), 969-976.
56. Kohno, T., Sugimoto, Y., Sei, K., & Mori, K. (2002). Design of PCR primers and gene probes for general detection of alkane-degrading bacteria. Microbes and Environments, 17(3), 114–121. https://doi.org/10.1264/jsme2.17.114
57. Kotova, I. B., Taktarova, Y. V., Tsavkelova, E. A., Egorova, M. A., Bubnova, I. A., Malakhova, D. V., Shirinkina, L. I., Sokolova, T. G., & Bonch-Osmolovskaya, E. A. (2021). Microbial degradation of plastics and approaches to make it more efficient. Microbiology, 90(6), 671–701. https://doi.org/10.1134/S0026261721060084
58. Kumar, R., Pandit, P., Kumar, D., Patel, Z., Pandya, L., Kumar, M., Joshi, C., & Joshi, M. (2021). Landfill microbiome harbour plastic degrading genes: A metagenomic study of solid waste dumping site of Gujarat, India. Science of The Total Environment, 779, 146184. https://doi.org/10.1016/j.scitotenv.2021.146184
59. Kumar, S., Rajesh, M., Rajesh, K. M., Suyani, N. K., Rasheeq, A. A., & Pratiksha, K. S. (2020). Impact of Microplastics on Aquatic Organisms and Human Health: A Review. International Journal of Environmental Science and Natural Resources, 26(2), IJESNR.MS.ID.556185 (2020) 0059. https://doi.org/10.19080/IJESNR.2020.26.556185
60. Langlois, P., & Howard, G. T. (2002). A single glycine-rich repeat of *Pseudomonas chlororaphis* Polyurethanase A mediates secretion of a GST fusion protein in *Escherichia coli*. *International*

Biodeterioration & Biodegradation, *50*(2), 121-126. https://doi.org/10.1016/S0964-8305(02)00069-0

61. Lucas, N., Bienaime, C., Belloy, C., Queneudec, M., Silvestre, F., & Nava-Saucedo, J. E. (2008). Polymer biodegradation: Mechanisms and estimation techniques. Chemosphere, 73, 429-442.

62. Luo, Y., Chuah, C., Al Amin, M., Khoshyan, A., Gibson, C. T., Tang, Y., Naidu, R., & Fang, C. (2022). Assessment of microplastics and nanoplastics released from a chopping board using Raman imaging in combination with three algorithms. Journal of Hazardous Materials, 431, Article 128636. https://doi.org/10.1016/j.jhazmat.2022.128636

63. MacLean, J., Bartholomäus, A., Blukis, R., Liebner, S., & Wagner, D. (2024). Metatranscriptomics of microbial biofilm succession on HDPE foil: Uncovering plastic-degrading potential in soil communities. Environmental Microbiome, 19(1), 95. https://doi.org/10.1186/s40793-024-00621-

64. Magnin, A., Pollet, E., Perrin, R., Ullmann, C., Persillon, C., Phalip, V., et al. (2019b). Enzymatic recycling of thermoplastic polyurethanes: synergistic effect of an esterase and an amidase and recovery of building blocks. Waste Manag. 85, 141–150. doi: 10.1016/j.wasman.2018.12.024

65. Mandal, Š., & Sapcanin, A. (2023). Polymeric materials in gluing techniques. Journal of Sustainable Technologies and Materials, 3, 36–48. https://doi.org/10.57131/jstm.2023.4.6

66. Maroof, L., Khan I., Yoo, H. S., Kim, S., Park, H-T., Ahmad, B., Azam, S. (2021). Identification and characterization of low-density polyethylene degrading bacteria isolated from soils of waste disposal sites Environ. Eng. Res. 26(3): 200167.

67. Maurya, A., Bhattacharya, A., & Khare, S. K. (2020). Enzymatic remediation of polyethylene terephthalate (PET)–based polymers for effective management of plastic wastes: An overview. Frontiers in Bioengineering and Biotechnology, 8, Article 602325. https://doi.org/10.3389/fbioe.2020.602325

68. Menéndez-Pedriza, A., & Jaumot, J. (2020). Interaction of environmental pollutants with microplastics: A critical review of sorption factors, bioaccumulation and ecotoxicological effects. Toxics, 8(2), 40. https://doi.org/10.3390/toxics8020040

69. Meyer-Cifuentes, I. E., Werner, J., Jehmlich, N., Will, S. E., Neumann-Schaal, M., & Öztürk, B. (2020). Synergistic biodegradation of aromatic-aliphatic copolyester plastic by a marine microbial consortium. Nature Communications, 11, 5790. https://doi.org/10.1038/s41467-020-19555-2

70. Mohanan, N., Montazer, Z., Sharma, P. K., Levin, D. B. (2020). Microbial and Enzymatic Degradation of Synthetic Plastics. Frontiers in Microbiology, 11, 580709.

71. Müller, R.-J., Schrader, H., Profe, J., Dresler, K., & Deckwer, W.-D. (2005). Enzymatic degradation of poly(ethylene terephthalate): Rapid hydrolyse using a hydrolase from T. fusca. Macromolecular Rapid Communications, 26(17), 1400–1405. https://doi.org/10.1002/marc.200500410

72. Muthukumar, A., & Veerappapillai, S. (2015). Biodegradation of plastics–a brief review. International Journal of Pharmaceutical Sciences Review and Research, 31(2), 204-209.

73. Napper, I. E., Davies, B. F. R., Clifford, H., Elmore, A. C., Gajurel, A. P., & Thompson, R. C. (2020). Reaching new heights in plastic pollution—preliminary findings of microplastics on Mount Everest. One Earth, 3(5), 621-630. https://doi.org/10.1016/j.oneear.2020.10.020

74. Nakajima-Kambe, T., Shigeno-Akutsu, Y., Nomura, N., & et al. (1999). Microbial degradation of polyurethane, polyester polyurethanes and polyether polyurethanes. Applied Microbiology and Biotechnology, 51, 134–140. https://doi.org/10.1007/s002530051373

75. Nakamiya K, Sakasita G, Ooi T, Kinoshita S (1997) Enzymatic degradation of polystyrene by hydroquinone peroxidase of Azotobacter beijerinckii HM121. J Ferment Bioeng 84:480–482. https://doi.org/10.1016/S0922-338X(97)82013-2
76. Othman, A.R., Hasan, H.A., Muhamad, M.H. et al. Microbial degradation of microplastics by enzymatic processes: a review. Environ Chem Lett 19, 3057–3073 (2021). https://doi.org/10.1007/s10311-021-01197-9
77. Oelschlägel, M., Zimmerling, J., & Tischler, D. (2018). A review: The styrene metabolizing-cascade of side-chain oxygenation as biotechnological basis to gain various valuable compounds. Frontiers in Microbiology, 9, 490. https://doi.org/10.3389/fmicb.2018.00490
78. Plastic-eating bacteria. https://rsscience.com/plastic-eating-bacteria/ [Accession May 10, 2025]
79. Purohit, J., Chattopadhyay, A., Teli, B. (2020). Metagenomic Exploration of Plastic Degrading Microbes for Biotechnological Application. Current Genomics, 21, 253-270.
80. Rahman, A. Sarkar, O.P. Yadav, et al. (2020), Potential human health risks due to environmental exposure to microplastics and knowledge gaps: A scoping review, Science of the Total Environment, https://doi.org/10.1016/ j.scitotenv.2020.143872,
81. Raczyńska, A., Góra, A., & André, I. (2024). An overview on polyurethane-degrading enzymes. Biotechnology Advances, 77, 108439. https://doi.org/10.1016/j.biotechadv.2024.108439
82. Rana, A. K., Thakur, M. K., Saini, A. K., Mokhta, S. K., Moradi, O., Rydzkowski, T., Alsanie, W. F., Wang, Q., Grammatikos, S., & Thakur, V. K. (2022). Recent developments in microbial degradation of polypropylene: Integrated approaches towards a sustainable environment. Science of The Total Environment, 826, 154056. https://doi.org/10.1016/j.scitotenv.2022.154056
83. RS Science. Plastic-eating bacteria: The future of plastic biodegradation. RS Science. https://rsscience.com/plastic-eating-bacteria/ [Accessed 2 May, 2025]
84. Revel M., Châtel A., Mouneyrac C. (2018) Micro(nano)plastics: A threat to human health? Current Opinion in Environmental Science & Health 1, 17-23. https://doi.org/10.1016/j.coesh.2017.10.003
85. Rillig, M. C. (2012). Microplastic in terrestrial ecosystems and the soil?. Environmental Science & Technology, 46(12), 6453-6454. https://doi.org/10.1021/es302011r
86. Rillig, M. C., Ingraffia, R., & de Souza Machado, A. A. (2017). Microplastic incorporation into soil in agroecosystems. Frontiers in plant science, 8, 1805.
87. Rochman, C. M., Browne, M. A., Halpern, B. S., Hentschel, B. T., Hoh, E., Karapanagioti, H. K., Rios-Mendoza, L. M., Takada, H., Teh, S., & Thompson, R. C. (2013). Classify plastic waste as hazardous. Nature, 494(7436), 169–171. https://doi.org/10.1038/494169a
88. Ronkvist, Å. M., Xie, W., Lu, W., & Gross, R. A. (2009). Cutinase-catalyzed hydrolysis of poly(ethylene terephthalate). Macromolecules, 42(14), 5128-5138. https://doi.org/10.1021/ma9005318
89. Schmidt, J., Wei, R., Oeser, T., Dedavid, E., Silva, L. A., Breite, D., et al. (2017). Degradation of polyester polyurethane by bacterial polyester hydrolases. Polymers 9:65. doi: 10.3390/polym9020065
90. Schmeisser, C., Steele, H., & Streit, W. R. (2007). Metagenomics, biotechnology with non-culturable microbes. Applied microbiology and biotechnology, 75(5), 955–962. https://doi.org/10.1007/s00253-007-0945-5
91. Sommer, F., Dietze, V., Baum, A., Sauer, J., Gilge, S., Maschowski, C., & Gieré, R. (2018). Tire Abrasion as a Major Source of Microplastics in the Environment. Aerosol and Air Quality Research, 18, 2014-2028. doi: 10.4209/aaqr.2018.03.0099

92. Sonnendecker, C., Oeser, J., Richter, P. K., Hille, P., Zhao, Z., Fischer, C., Lippold, H., Blázquez-Sánchez, P., & others. (2021). Low carbon footprint recycling of post-consumer PET plastic with a metagenomic polyester hydrolase. ChemSusChem, 14(18), 3882–3891. https://doi.org/10.1002/cssc.202101062
93. Stern, R. V., & Howard, G. T. (2000). The polyester polyurethanase gene (pueA) from Pseudomonas chlororaphis encodes a lipase. FEMS Microbiology Letters, 185(2), 163–168. https://doi.org/10.1111/j.1574-6968.2000.tb09056.x
94. Sun Shengwei. 2024. Recent advances in screening and identification of PET-degrading enzymes. Environmental Reviews. 32(3): 294-314. https://doi.org/10.1139/er-2023-0107
95. Subramanian, S. H. S., Balachandran, K. R. S., Rangamaran, V. R., & Gopal, D. (2020). RemeDB: Tool for rapid prediction of enzymes involved in bioremediation from high-throughput metagenome data sets. Journal of Computational Biology, 27(7), 1020–1029. https://doi.org/10.1089/cmb.2019.0305
96. Sulaiman, S., Yamato, S., Kanaya, E., Kim, J. J., Koga, Y., Takano, K., & Kanaya, S. (2012). Isolation of a novel cutinase homolog with polyethylene terephthalate-degrading activity from leaf-branch compost by using a metagenomic approach. Applied and Environmental Microbiology, 78(5), 1556–1562. https://doi.org/10.1128/AEM.06725-11
97. Suresh, V., Shams, R., Dash, K. K., Shaikh, A. M., & Béla, K. (2025). Comprehensive review on enzymatic polymer degradation: A sustainable solution for plastics. Journal of Agriculture and Food Research, 20, 101788. https://doi.org/10.1016/j.jafr.2025.101788
98. Ratajczak, A., Geißdörfer, W., & Hillen, W. (1998). Alkane Hydroxylase from Acinetobacter sp. Strain ADP1 Is Encoded by alkM and Belongs to a New Family of Bacterial Integral-Membrane Hydrocarbon Hydroxylases. Applied and Environmental Microbiology, 64(4), 1175–1179. https://doi.org/0099-2240/98/$04.0010
99. Romano, D., Bonomi, F., de Mattos, M. C., Fonseca, T. de S., de Oliveira, M. da C. F., & Molinari, F. (2015). Esterases as stereoselective biocatalysts. Biotechnology Advances, 33(5), 547–565. https://doi.org/10.1016/j.biotechadv.2015.01.006
100. Ru, J., Huo, Y., & Yang, Y. (n.d.). Microbial Degradation and Valorization of Plastic Wastes. Department of Biology, School of Life Science, Beijing Institute of Technology, Beijing, China; Key Laboratory of Molecular Medicine and Biotherapy.
101. Tang, K. H. D., Lock, S. S. M., Yap, P.-S., Cheah, K. W., Chan, Y. H., Yiin, C. L., Ku, A. Z. E., Loy, A. C. M., Chin, B. L. F., & Chai, Y. H. (2022). Immobilized enzyme/microorganism complexes for degradation of microplastics: A review of recent advances, feasibility and future prospects. Science of The Total Environment, 832, 154868. https://doi.org/10.1016/j.scitotenv.2022.154868
102. Temporiti, M. E. E., Nicola, L., Nielsen, E., & Tosi, S. (2022). Fungal Enzymes Involved in Plastics Biodegradation. Microorganisms, 10(6), 1180. https://doi.org/10.3390/microorganisms10061180
103. Thermo Fisher Scientific. (2023). GeneJET PCR Purification Kit user guide (MAN0012662). https://assets.thermofisher.com/TFSAssets/LSG/manuals/MAN0012662_GeneJET_PCR_Purification_UG.pdf [Accessed 20 March,2025]
104. Tischler, D., Gröning, J. A. D., Kaschabek, S. R., & Schlömann, M. (2012). One-component styrene monooxygenases: An evolutionary view on a rare class of flavoproteins. Applied Biochemistry and Biotechnology, 167, 931-944. https://doi.org/10.1007/s12010-012-9624-4
105. Tischler, D., Schwabe, R., Siegel, L., Joffroy, K., Kaschabek, S. R., Scholtissek, A., & Heine, T. (2018). VpStyA1/VpStyA2B of Variovorax paradoxus EPS: An Aryl Alkyl Sulfoxidase Rather

than a Styrene Epoxidizing Monooxygenase. Molecules, 23(4), 809. https://doi.org/10.3390/molecules23040809
106. Tournier, V., Topham, C.M., Gilles, A. et al. An engineered PET depolymerase to break down and recycle plastic bottles. Nature 580, 216–219 (2020). https://doi.org/10.1038/s41586-020-2149-4)
107. Ufarté, L., Laville, E., Duquesne, S., Morgavi, D., Robe, P., & Fernandez, B. (2017). Discovery of carbamate degrading enzymes by functional metagenomics. PLOS ONE, 12(12), e0189201. https://doi.org/10.1371/journal.pone.0189201
108. Veluru, S., & Seeram, R. (2024). Biotechnological approaches: Degradation and valorization of waste plastic to promote the circular economy. Circular Economy, 3(1), 100077. https://doi.org/10.1016/j.cec.2024.100077
109. Vierstraete, A. R., & Braeckman, B. P. (2022). Amplicon_sorter: A tool for reference-free amplicon sorting based on sequence similarity and for building consensus sequences. Ecology and evolution, 12(3), e8603. https://doi.org/10.1002/ece3.8603
110. Wang, C., Zhao, J., & Xing, B. (2021). Environmental source, fate, and toxicity of microplastics. Journal of Hazardous Materials, 407, 124357. https://doi.org/10.1016/j.jhazmat.2020.124357.
111. Webb, J. S., Van der Mei, H. C., Nixon, M., Eastwood, I. M., Greenhalgh, M., Read, S. J., et al. (1999). Plasticizers increase adhesion of the deteriogenic fungus Aureobasidium pullulans to polyvinyl chloride. Appl. Environ. Microbiol. 65, 3575–3581. doi: 10.1128/aem.65.8.3575-3581.1999
112. Wei, R.; Zimmermann, W. Microbial enzymes for the recycling of recalcitrant petroleum-based plastics: How far are we? Microb. Biotechnol. 2017, 10, 1308–1322.
113. Wintzingerode, F. V., Göbel, U. B., & Stackebrandt, E. (1997). Determination of microbial diversity in environmental samples: Pitfalls of PCR-based rRNA analysis. FEMS Microbiology Reviews, 21(3), 213–229. https://doi.org/10.1111/j.1574-6976.1997.tb00351.x
114. Wojnowska-Baryła, I., Bernat, K., & Zaborowska, M. (2022). Plastic Waste Degradation in Landfill Conditions: The Problem with Microplastics, and Their Direct and Indirect Environmental Effects. International journal of environmental research and public health, 19(20), 13223. https://doi.org/10.3390/ijerph192013223
115. Xin, K., Lu, J., Zeng, Q., Zhang, T., Liu, J., Zhou, J., Dong, W., & Jiang, M. (2024). Depolymerization of the polyester–polyurethane by amidase GatA250 and enhancing the production of 4,4′-methylenedianiline with cutinase LCC. Biotechnology Journal, 19, e2300723. https://doi.org/10.1002/biot.202300723
116. Wyss Institute. Plastic Degradation Company, Breaking, Emerges from Stealth with Naturally-Derived Solution to Degrade Multiple Plastics with $10.5M in Seed Funding. (2024). https://wyss.harvard.edu/news/plastic-degradation-company-breaking-emerges-from-stealth-with-naturally-derived-solution-to-degrade-multiple-plastics-with-10-5m-in-seed-funding/ [Accession 3 March, 2025]
117. Xu, J., Cui, Z., Nie, K., Cao, H., Jiang, M., Xu, H., et al. (2019). A quantum mechanism study of the cc bond cleavage to predict the bio-catalytic polyethylene degradation. Front. Microbiol. 10:489.
118. Yan, Z., Liu, Y., Zhang, T., Zhang, F., Ren, H., & Zhang, Y. (2022). Analysis of microplastics in human feces reveals a correlation between fecal microplastics and inflammatory bowel disease status. Environmental Science & Technology, 56(1), 414-421. doi:10.1021/acs.est.1c03924.
119. Yoshida, S., Hiraga, K., Takehana, T., Taniguchi, I., Yamaji, H., Maeda, Y., ... & Oda, K. (2016). A bacterium that degrades and assimilates poly(ethylene terephthalate). Science, 351(6278), 1196-1199.

120. Yuan, Z., Nag, R., & Cummins, E. (2022). Human health concerns regarding microplastics in the aquatic environment – From marine to food systems. Science of The Total Environment, 823, 153730. https://doi.org/10.1016/j.scitotenv.2022.153730
121. Zampolli, J., Mangiagalli, M., Vezzini, D., Lasagni, M., Ami, D., Natalello, A., Arrigoni, F., Bertini, L., Lotti, M., & Di Gennaro, P. (2023). Oxidative degradation of polyethylene by two novel laccase-like multicopper oxidases from Rhodococcus opacus R7. Environmental Technology & Innovation, 32, 103273. https://doi.org/10.1016/j.eti.2023.103273
122. Zepeda, B., & Verdonk, J. C. (2022). RNA extraction from plant tissue with homemade acid guanidinium thiocyanate phenol chloroform (AGPC). Current Protocols, 2, e351. doi: 10.1002/cpz1.351
123. Zhang, G. S., & Liu, Y. F. (2018). The distribution of microplastics in soil aggregate fractions in southwestern China. Science of The Total Environment, 642, 12-20. https://doi.org/10.1016/j.scitotenv.2018.06.193
124. Zhang, Y., Pedersen, J. N., Eser, B. E., & Guo, Z. (2022). Biodegradation of polyethylene and polystyrene: From microbial deterioration to enzyme discovery. Biotechnology Advances, 107991. https://doi.org/10.1016/j.biotechadv.2022.107991.
125. Zhao, J., Guo, Z., Ma, X., Liang, G., and Wang, J. (2004). Novel surface modification of high-density polyethylene films by using enzymatic catalysis. J. Appl. Polym. Sci. 91, 3673–3678. doi: 10.1002/app.13619
126. Zrimec, J., Kokina, M., Jonasson, S., Zorrilla, F., & Zelezniak, A. (2021). Plastic-degrading potential across the global microbiome correlates with recent pollution trends. mBio, 12(6), e02155-21. https://doi.org/10.1128/mBio.02155-21
127. Zymo Research. (n.d.). ZymoBIOMICS™ DNA Miniprep Kit (D4300). Accessed May 15, 2025, from https://zymoresearch.eu/products/zymobiomics-dna-miniprep-kit

APPENDICES

Appendix A. Scheme of enzymatic degradation of PET

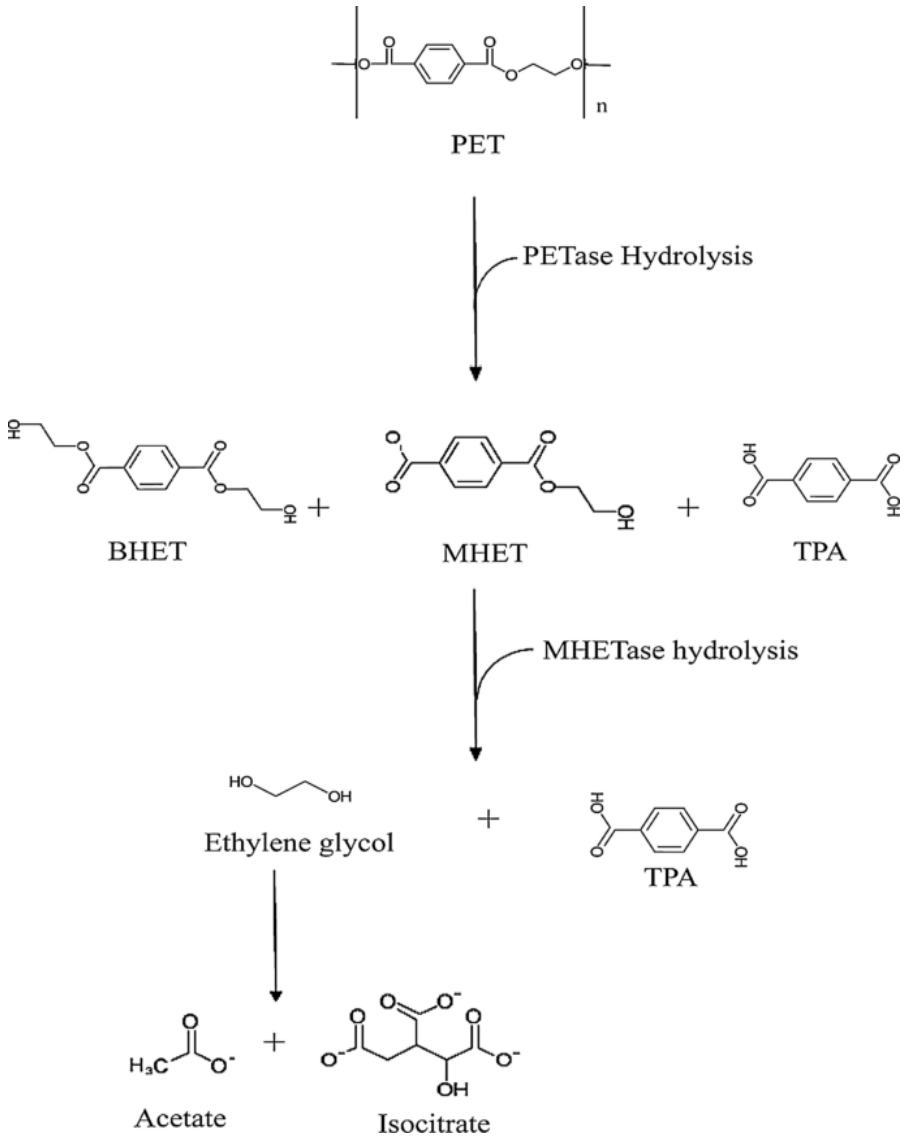

Fig A1. Enzymatic degradation mechanism of polyethylene terephthalate. TPA: terephthalic acid, BHET: bis(2-hydroxyethyl)-terephthalic acid, MHET: mono(2-hydroxyethyl) terephthalic acid

Appendix B. Enzymes associated with polyurethane (PUR) biodegradation

Table B1. Enzymes associated with polyurethane (PUR) biodegradation

Enzyme	**Available description**	**Reference**
LC cutinase, *Thermobifida fusca* cutinase Cut2, *Thermomonospora curvata* Tcur1278 and Tcur0390 polyester hydrolases	Emulsify polyester PUR	Schmidt et al., 2017
Efficient amidase E4143	Hydrolyses the urethane bond of a low molar mass molecule	Magnin et al., 2019b
PudA	Esterase, emulsify polyester PUR	Akutsu et al., 1998
Pseudomonas chloroaphis, lipase Polyurethanases PueA, PueB	Catalyse the hydrolysis of the ester and amide bonds, resulting formation of polyol and a carboxylic acid or amine and a carboxylic acid respectively	Stern et al., 2000
Esterase E3576	Hydrolyse a waterborne polyester polyurethane dispersion	Magnin et al., 2019b
Polyurethanase PulA	Serine-hydrolase	Ruiz & Howard, 1999
Lysinibacillus fusiformis strain SC02 urethanase	Hydrolyses ester and urethane bonds	Jia et al, 2020
PurH	Hydrolyses ester and urethane bonds	Zhang et al., 2025
Rhodococcus equi 55kDa enzyme urethanese	Urethane hydrolase, hydrolyses both aliphatic urethane compound as well as aromatic ones	Akutsu-Shigeno et al. 2006
Rhodococcus erythropolis CCM2595, MP50 urethanase	Annotated as Asp-tRNAAsn/Glu-tRNAGln amidotransferase A subunit and related amidases	Kang, et al 2021;
Sporosarcina ureae P17a urethanase	Annotated as glutamyl-tRNA amidotransferase; amidase	Kang, et al 2021;
Comamonas (Delftia) acidovorans TB-35, PudA	Amidase	Shigeno-Akutsu et al ,1999
Halopseudomonas formosensis, *Hfor*_PE-H	Hydrolase, cutinase-like polyester hydrolase, acts upon both ester bonds and urethane bonds	de Witt, et al 2023
Klebsiella oxytoca 1686	Amidase	Kang, et al 2021;
Agrobacterium tumefaciens d3, AmdA	Enantioselective amidase, belongs to the amidase signature (AS) family; hydrolyses short-chain aliphatic amides as well as aromatic amides	Kang, et al 2021;
Burkholderia phytofirmans DSM17436	Amidase, annotated as urate catabolism protein	Kang, et al 2021;
Microbacterium hydrocarbonoxydans	Gamma-lactamase, active against C-N bond	Wang et al, 2012
GatA250 (no organism, metagenome derived DNA)	Amidase, acts only upon urethane bond	Xin et al., 2024
UMG-SP-1, UMG-SP-2, UMG-SP-3	Isolated from soil contained PUR wastes, Urethanases catalysing the cleavage of urethane bonds	Branson et al., 2023
Metagenome-derived, CE_Ubrb	Isolated from bovine rumen metagenome, activity was testred on Imprail, active against carbamates Carboxyl-ester hydrolase belonging to the lipolytic family IV	Ufarté et al., 2017

Appendix C. Satellite maps of aquatic sample collection sites

a)

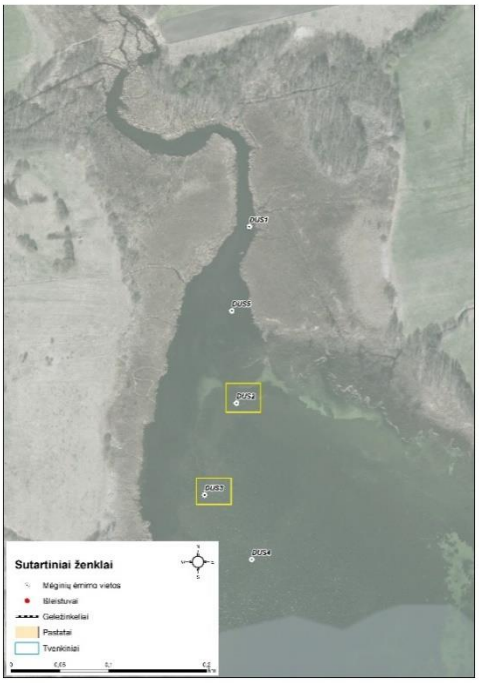

b)

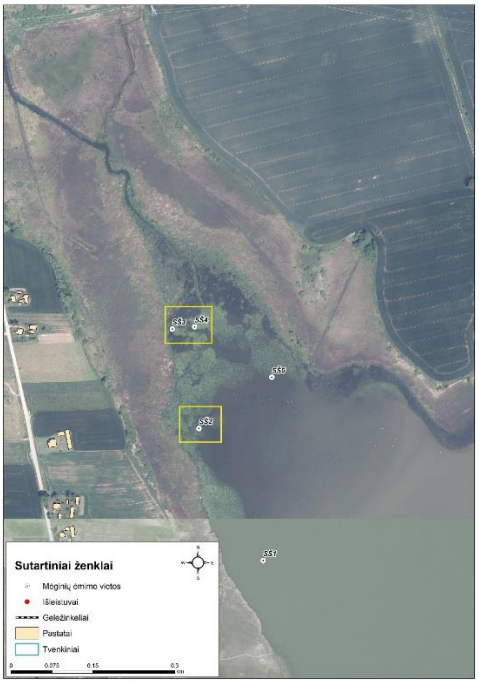

Fig. C1 Sattelite maps with marked sample collection spots a) Dusia lake (b) Simnas fishery reservoir

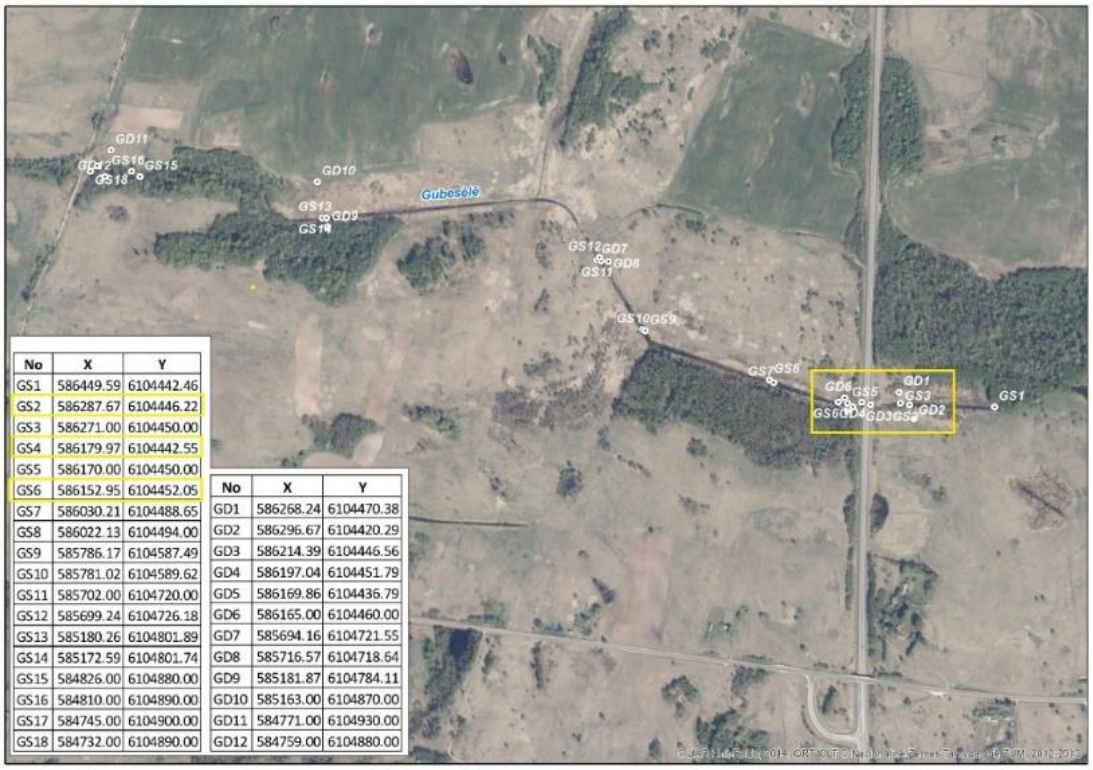

No	X	Y
GS1	586449.59	6104442.46
GS2	586287.67	6104446.22
GS3	586271.00	6104450.00
GS4	586179.97	6104442.55
GS5	586170.00	6104450.00
GS6	586152.95	6104452.05
GS7	586030.21	6104488.65
GS8	586022.13	6104494.00
GS9	585786.17	6104587.49
GS10	585781.02	6104589.62
GS11	585702.00	6104720.00
GS12	585699.24	6104726.18
GS13	585180.26	6104801.89
GS14	585172.59	6104801.74
GS15	584826.00	6104880.00
GS16	584810.00	6104890.00
GS17	584745.00	6104900.00
GS18	584732.00	6104890.00

No	X	Y
GD1	586268.24	6104470.38
GD2	586296.67	6104420.29
GD3	586214.39	6104446.56
GD4	586197.04	6104451.79
GD5	586169.86	6104436.79
GD6	586165.00	6104460.00
GD7	585694.16	6104721.55
GD8	585716.57	6104718.64
GD9	585181.87	6104784.11
GD10	585163.00	6104870.00
GD11	584771.00	6104930.00
GD12	584759.00	6104880.00

Fig. C2 Sattelite map with marked samples collection spots near the Gubesėlė River

Appendix D. Sets of primers used in work with PCR conditions

Table D1 Primers used in analysis and PCR condition

Name of primer	Primers sequences (5' → 3')	PCR conditions	Gene/enzyme	Source
Cut4_F	ATCGAGGACCTCGACTCG	Initial denaturation: 5 min 94 °C; 35 cycles: 45 s 94 °C; 45 s 60 °C; 30 s 72 °C; final elongation: 5 min 72°C.	*Fusarium solani* cutinase	Alexandrakis et al., 1998
Cut4_R	GCAGCAACGATCAAGCTA			
Cut2_F	GGAATTCGGATCCAATGGCTGTGATGACCCCCCG	Initial denaturation: 5 min 94 °C; 35 cycles: 45 s 94 °C; 30 s 55 °C; 30 s 72 °C; final elongation: 8 min 72°C	*Thermobifida fusca* cutinase Cut2	Hedge et al., 2013
Cut2_R	GAAGCTTCTCGAGGAACGGGCAGGTGGAGC			
Tfh_F	GGGAAGATCTTGGCCAACCCCTACGAGC	Initial denaturation: 5 min 94 °C; 35 cycles: 30 s 94 °C; 30 s 57 °C; 60 s 72 °C; final elongation: 8 min 72°C.	*Thermobifida fusca* hydroxylase	Dresler et al, 2006
Tfh_R	GACTGCCGGCCTAGAACGGGCAGGTGGAGC			
PHL7_F	ATGGCGAACCCGTACGAGCGCGGGCC	Initial denaturation: 5 min 94 °C; 35 cycles: 45 s 94 °C; 35 s 63 °C; 60 s 72 °C; final elongation: 8 min 72°C.	Compost metagenome, hydrolase gene, clone 7	this study
PHL7_R	TCAGAACGGGCAGGTGGAGCGGTACTC			
LCC_F	GCGTCGCCATGGATTCCAACCCGTACCAG	Initial denaturation: 5 min 94 °C; 35 cycles: 45 s 94 °C; 45 s 62 °C; 60 s 72 °C; final elongation: 10 min 72°C.	Leaf Branch Compost Cutinase	Sulaiman et al., 2012
LCC_R	CAGGATCCACTACTGGCAGTGGCG			
Lf_Ure_F	ATGACAACTGATTTACATTTAAAATCTG	Initial denaturation: 5 min 94 °C; 35 cycles: 60 s 94 °C; 60 s 54 °C; 90 s 72 °C; final elongation: 10 min 72°C.	Urethanase /glutamyl–tRNA amidotransferase	Jia et al., 2021
Lf_Ure_R	TTAGATATTAGCAAAAATATTTGGTTTTC			
TS2S	TCAACTACACGCGACGTCACTGAAGCT	Initial denaturation: 5 min 94 °C; 40 cycles: 30 s 94 °C; 30 s 58 °C; 30 s 72 °C; final elongation: 8 min 72°C	*alkB, alkM* (alkane hydroxylases)	Olivera et al., 2009
Deg1RE	CCGTAAGTGCTTCACGTACTAGTAAGTT			
AlkB484F	GGKCAYTTCTWCRTYGARCA	Initial denaturation: 5 min 94 °C; 40 cycles: 30 s 94 °C; 30 s 59 °C; 30 s 72 °C; final elongation: 8 min 72°C.	*alkB* (alkane hydroxylase)	Olivera et al., 2009
AlkB824R	CCGTAGTGYTCRABRTARTT			
MonF	TCAAYACMGSNCAYGARCT	Initial denaturation: 5 min 94 °C; 40 cycles: 30 s 94 °C; 30 s 58 °C; 30 s 72 °C; final elongation: 5 min 72°C	*alkB,* (alkane hydroxylases)	Olivera et al., 2009
MonR	CCGTARTGYTCNAYRTARTT			
Alk1-F	TCGAGCACATCCGCGGCCACCA	Initial denaturation: 5 min 94 °C; 35 cycles: 1 min 94 °C; 30 s 58 °C; 45 s 72 °C; final elongation: min 72°C	*alkB, alkB1* (alkane hydroxylases)	Kohno et al., 2002
Alk1-R	CCGTAGTGCTCGACGTAGTT			
LCMO2_F	ATGATCGAACAGTTCCCGACCGCCG	Initial denaturation: 5 min 94 °C; 38 cycles: 45 s 94 °C; 45 s 57 °C; 100 s 72 °C; final elongation: 8 min 72°C	*Rhodococcus opacus* R7 laccase-like multicopper oxidase LCMO2	Sonnendecker et al., 2021
LCMO2_R	TTATTCGGTGTAGGACAGGGTGGTCAT			
VpSty_F	CTAATCAGCATCATCTGT	Initial denaturation: 5 min 94 °C; 35 cycles: 40 s 94 °C; 45 s 58 °C; 40 s 72 °C; final elongation: 7 min 72°C.	*Variovorax paradoxus* styrene monooxygenase styA2B	this study
VpSty_R	TAATACCCACTGTGAAAG			
Sty F01	CGSRGSTGGGSNCRNTGG	Initial denaturation: 5 min 94 °C; 35 cycles: 45 s 94 °C; 30 s 65 °C; 30 s 72 °C; final elongation: 5 min 72°C	Styrene monooxygenase StyA2B	Tischler et al., 2012
Sty R02	SAGSGGSGGRTCSAKSGA			
PueA_F	CGGGATCCGCCCGGGCCACTACCTGGGTC	Initial denaturation: 5 min 94 °C; 35 cycles: 60 s 94 °C; 35 s 68 °C; 60 s 72 °C; final elongation: 7 min 72°C.	*Pseudomonas chlororaphis* PueA polyurethanase	Langlois & Howard, 2002
PueA_R	GCGTCGACTTAGCCGCTGTCGCG GAACGTATC			

Table D1 *(continued)*

Name of primer	Primers sequences (5' → 3')	PCR conditions	Gene/enzyme	Source
Ce_Ubr_F	ATGAGCATTCGCGTCATACCG AACAATCC	Initial denaturation: 5 min 94 °C; 40 cycles: 45 s 94 °C; 35 s 53 °C; 60 s 72 °C; final elongation: 8 min 72°C.	Carboxyl-ester hydrolase CE_Ubrb	this study
Ce_Ubr_R	TCAATCATTTTCGAATCCCTC CGTATTTCT			
IsPETase_F	GCGCCCATGGCGCGCGGTCCG AATCCGACAGCCG	Initial denaturation: 5 min 94 °C; 35 cycles: 45 s 94 °C; 45 s 66 °C; 60 s 72 °C; final elongation: 7 min 72°C.	*Ideonella sakaiensis* PETase	Joo et al., 2018
Is PETase_R	GCGCCTCGAGGCTGCAATTCG CTGTACGAAAATC			
IsMHETase_F	GCGCCCATGGCGTGTGCTGGC GGTGGGTCCACGC	Initial denaturation: 5 min 94 °C; 35 cycles: 45 s 94 °C; 120 s 72 °C; final elongation: 10 min 72°C.	*Ideonella sakaiensis* MHETase	Joo et al., 2018
IsMHETase_R	GCGCCTCGAGGGGAGGAGC CGCGCAGGCGAAGTT			

Degenerate nucleotide code (IUPAC): V means A or C or G in this position; N=A/C/G/T; D=A/T/G; B= T/C/G; H=A/T/C; W=A/T; S=C/G; K=T/G; M=A/C; Y=C/T; R= A/G.

Appendix E. Amplicon sequencing

Library preparation and sequencing (after extraction from the gel approach)

DNA sequencing was performed on the Oxford Nanopore platform. For the DNA library preparation, Native Barcoding Kit 96 V14 (SQK-NBD114.96) was used. The procedure was done with MinION™ portable DNA/RNA sequencer (Flow Cell (R10.4.1)).

Obtained reads were basecalled using Dorado (version 0.9.0) with the dna_r10.4.1_e8.2_400bps_sup@v5.0.0 model. Read length histogram (200 bins) was drawn using Matplotlib, and reads were split by length using Seqkit (version 2.6.0) to represent the expected read lengths. Each read file was then analysed using amplicon_ sorter, tool designed for analysis of short Oxford Nanopore reads with default parameters (Vierstraete & Braeckman, 2022).

Library preparation Sequencing of PCR product mixtures

Following cleaning, DNA library was prepared with the Rapid sequencing DNA V14 - barcoding kit (Oxford Nanopore Technologies). The prepared libraries were sequenced using Flongle flow cell on MinION™ sequencer, Oxfrod Nanopore Technologies). Following sequencing, primary bioinformatical analysis was done, resulting in fasta files containing the sequences of PCR products.

Appendix F. Nucleotide alignments between amplification product after PCR for phl7 gene and best search hit

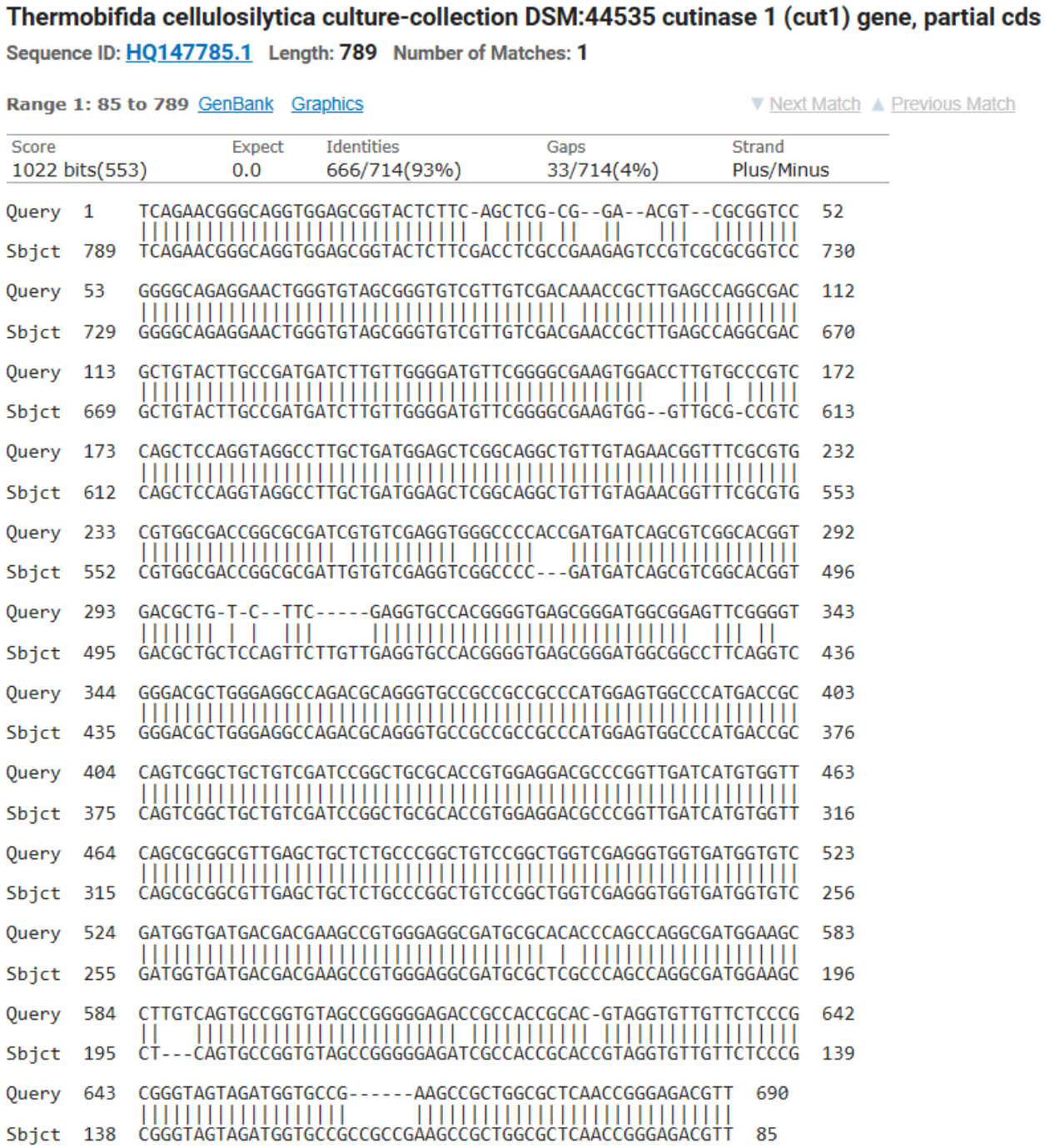

Fig F1 Nucleotide alignments between 691 bp product of amplification with phl7F/R pair of primers (sample P4) (subject) and best search hit according to e-value (object)

Appendix G. Nucleotide alignment of Thermobifida fusca cut1 gene with phl7 gene

Score	Expect	Identities	Gaps	Strand
194 bits(214)	2e-53	532/799(67%)	41/799(5%)	Plus/Plus

```
Query  2147  GCCAACCCCTACGAGCGCGGCCCCAACCCGACCGACGCCCTGC-TCGAAGCCAGCAGCGG  2205
             || ||||| |||||||| || ||  |||| ||||| |  || | | || ||   | ||||
Sbjct  4     GCGAACCCGTACGAGCGGGGGCCTGACCCCACCGA-GAGCTCCATTGAGGCTGTCCGCGG  62

Query  2206  CCCCTTCTCCGTCAGCGAGGAGAACGTCTCCCGGTTGAGCGCCAGCGGCTTCGGCGGCGG  2265
              |||||| | |||  | ||   |  |||  |||| |    ||    || || || |||||
Sbjct  63    GCCCTTCGCTGTCGCCCAGACCACGGTCAGCCGGCTCCAGGCTGATGGGTTTGGTGGCGG  122

Query  2266  CACCATCTACTACCCGCGGGAGAACAAC------ACCTACGGTGCGGTGGCGATCTCCCC  2319
              |||||| |||||||||   || |  | |       |||| |||||| ||||| ||   |||
Sbjct  123   CACCATTTACTACCCGACCGACACGAGCCAGGGGACCTTCGGTGCTGTGGCTATTAGCCC  182

Query  2320  CGGCTACACCGGCACTGAGGCTTCCATCGCCTGGCTGGGCGAGCGCATCGCCTCCCACGG  2379
              ||||| ||||| |    |||    ||| || ||||| ||    |||||||| || || ||
Sbjct  183   CGGCTTCACCGCCGGCCAGGAGAGCATTGCGTGGCTCGGTCCTCGCATCGCGTCGCAGGG  242

Query  2380  CTTCGTCGTCATCACCATCGACACCATCACCACCCTCGACCAGCCGGACA-GC-CGGGCA  2437
              ||| |||||||| ||||| || ||||||||   ||| |||||||| |||  || |||||
Sbjct  243   CTTTGTCGTCATTACCATTGATACCATCACGCGCCTGGACCAGCCTGACTCGCGCGGGCG  302

Query  2438  GAGCAGCTCAACGCCGCGCTGAACCACATGATCAACCGGGCGTCCTCCACGGTGCGCAGC  2497
                 |||||  | || |||||| | ||| ||  ||  ||  |  | ||    || || | |
Sbjct  303   C--CAGCTGCAGGCGGCGCTGGATCACCTGCGCA--CGAACAGCGTC----GTCCGGAAC  354

Query  2498  CGGATCGACAGCAGCCGACTGGCGGTCATGGGCCACTCCATGGGCGGCGGCGGCACCCTG  2557
              || |||||    | |||  ||||||| ||||| ||   |||||| || || ||  | |||
Sbjct  355   CGCATCGATCCTAACCGGATGGCGGTGATGGGGCATAGCATGGGTGGGGGTGGTGCGCTG  414

Query  2558  CGTCTGGCCTCCCAGCGTCCCGAC-CTGAAGGCCGCCATCCCGCTCACCCCGTGGCACCT  2616
               |    || | ||| |  | || | ||| |||| ||||||||||||       ||||||
Sbjct  415   AGCGCCGC-TGCCAACAACACGTCGCTGGAGGCGGCCATCCCGCTCCAGGGTTGGCACAC  473

Query  2617  CAACAAGAACTGGAGCAGCGTC---ACCGTGCCGACGCTGATCATCGGGGCCGACCTCGA  2673
              |  ||||||||||     ||||   |||   ||||||||| |  | || ||  | || ||
Sbjct  474   CCGCAAGAACTGGTCGTCCGTCCGGACC---CCGACGCTGGTGGTGGGTGCTCAGCTGGA  530

Query  2674  CACAATCGCGCCGGTCGCCACGCACGCGAAACCGTTCTACAACAGCCTGCCGAGCTCC-A  2732
               || ||||| |||||| |  | ||| || |  | |||||||||   |||||   |||  |
Sbjct  531   TACCATCGCCCCGGTCTCGTCCCACTCGGAGGCCTTCTACAACTCGCTGCC---CTCGGA  587

Query  2733  TCAGCA--AGGCCTACCTGGAGCTGGACGGCGCAACCCACTTCGCCCCGAACATCCCCAA  2790
              || | |  |||| ||| ||||||||   |||||  | ||  | | |   |||| |||  |
Sbjct  588   TCTGGATAAGGCTTACATGGAGCTGCGGGGCGCTTCGCATCTGGTCAGCAACACCCCGGA  647

Query  2791  CAAGATCATCGGCAAGTACAGCGTCGCCTGGCTCAAGCGGTTCGTCGACAACGACACCCG  2850
              ||  | || || |||||||||| | || ||||| |||||||| || ||| | |||  |||
Sbjct  648   CACCACCACCGCCAAGTACAGCATTGCTTGGCTGAAGCGGTTTGTGGACGATGACCTCCG  707

Query  2851  CTACACCCAGTTCCTCTGCCCCGGACCGCGCGACGGACTCTTCGGCGAGGTCGAAGAGTA  2910
               |||   |||||||||| ||||| ||       | |||  ||  ||||  ||   |||||
Sbjct  708   GTACGAGCAGTTCCTCTG-CCCGGCCC------CCGACGATTTTGCGATTTC--CGAGTA  758

Query  2911  CCGCTCCACCTGCCCGTTC  2929
              |||||| |||||||| |||
Sbjct  759   CCGCTCGACCTGCCCTTTC  777
```

Fig G1. Nucleotide alignment of *Thermobifida fusca cut1* gene with *phl7* gene

Appendix H. Results of blastx search of amplicons of expected size after PCR with primers TS2S/Deg1RE

Table H1. Results of blastx homology search of amplicons of expected size after PCR with primers TS2S/Deg1RE for alkane haydroxylase genes

Sample	Seq. len.	Ident. (%)	Align. Len. (aa)	E-value	Bit score	Protein ID	Annotation
	557	98.37	184	5.08E-129	378	WP_052054245.1	alkane 1-monooxygenase [Corynebacterium freneyi]
	557	97.28	184	6.51E-128	375	SQB94629.1	Alkane 1-monooxygenase 1 [Clostridium paraputrificum]
P1_1	557	97.28	184	6.53E-128	375	KKO82090.1	alkane 1-monooxygenase [Corynebacterium xerosis]
	558	80.22	182	1.40E-106	322	WP_066585432.1	alkane 1-monooxygenase [Corynebacterium provencense]
2	558	81.86	182	5.32E-106	320	WP_071057518.1	alkane 1-monooxygenase [Corynebacterium jeikeium]
	558	89.78	186	7.66E-110	328	OGA83339.1	alkane 1-monooxygenase [Burkholderiales bacterium
	558	89.78	186	8.55E-110	328	MBA4111126.1	alkane 1-monooxygenase [Leptothrix sp. (in: Bacteria)]
3	558	89.24	186	1.15E-108	326	WP_058088019.1	alkane 1-monooxygenase [Aquabacterium parvum]
P2_1	558	91.43	105	8.68E-82	210	OGA83339.1	alkane 1-monooxygenase [Burkholderiales bacterium]
	555	97.06	102	6.25E-96	211	WP_052054245.1	alkane 1-monooxygenase [Corynebacterium freneyi]
	555	95.10	102	4.33E-95	207	SQB94629.1	Alkane 1-monooxygenase 1 [Clostridium paraputrificum]
2	555	95.10	102	5.24E-95	207	WP_060925339.1	alkane 1-monooxygenase [Corynebacterium xerosis]
	557	98.37	184	3.43e-129	378	WP_052054245.1	alkane 1-monooxygenase [Corynebacterium freneyi]
	557	97.28	184	6.25e-128	375	KKO82090.1	alkane 1-monooxygenase [Corynebacterium xerosis]
3	557	97.28	184	6.87e-128	375	SQB94629.1	Alkane 1-monooxygenase 1 [Clostridium paraputrificum]
4	558	98.91	183	5.37e-127	372	TXH94376.1	alkane 1-monooxygenase [Pseudomonas sp.]
_5	558	99.46	173	8.23e-128	378	WP_182643528.1	alkane 1-monooxygenase [Dietzia sp. E1]
P3_1	558	80.87	183	6.64E-106	319	MSV86104.1	alkane 1-monooxygenase [Actinobacteria bacterium]
	557	89.67	184	2.42E-108	325	MBA4111126.1	alkane 1-monooxygenase [Leptothrix sp. (in: Bacteria)]
2	557	89.67	184	2.45E-108	325	OGA83339.1	alkane 1-monooxygenase [Burkholderiales bacterium]
3	557	98.37	184	3.43E-129	378	WP_052054245.1	alkane 1-monooxygenase [Corynebacterium freneyi]
4	558	98.91	183	5.37E-127	372	TXH94376.1	alkane 1-monooxygenase [Pseudomonas sp.]

5	558	99.46	184	8.23E-128	378	WP_182643528.1	fatty acid desaturase [Dietzia sp. E1]

Table H1 *(continued)*

Sample	Seq. len.	Ident. (%)	Align. Len. (aa)	E-value	Bit score	Protein ID	Annotation
P4_1	556	100.00	182	5.45E-130	381	WP_014008680.1	alkane 1-monooxygenase [Corynebacterium variabile]
2	556	100.00	182	2.55E-118	351	WP_066585432.1	alkane 1-monooxygenase [Corynebacterium provencense]
3	556	100.00	164	1.62E-105	317	HCT13643.1	alkane 1-monooxygenase [Corynebacterium nuruki]
4	556	94.41	179	9.32E-123	363	WP_141328173.1	alkane 1-monooxygenase [Corynebacterium variabile]
	555	91.06	179	5.24E-112	335	WP_038545347.1	alkane 1-monooxygenase [Corynebacterium glyciniphilum
P5_1	558	99.46	180	7.51E-131	384	HAJ52165.1	alkane 1-monooxygenase [Corynebacterium variabile]
2	555	100.00	180	7.63E-120	353	HCT13643.1	alkane 1-monooxygenase [Corynebacterium nuruki]
3	556	96.72	180	9.09E-126	369	WP_052054245.1	alkane 1-monooxygenase [Corynebacterium freneyi]
C2B_1	558	95.68	185	3.43E-125	368	TMK57753.1	alkane 1-monooxygenase [Actinobacteria bacterium]
	558	90.16	183	5.15E-117	339	ABB96083.1	putative alkane monooxygenase, partial [uncultured bacterium]
2	558	93.01	186	1.18E-120	357	WP_056403194.1	alkane 1-monooxygenase [Aeromicrobium sp. Root236]
	558	92.7	178	2.00E+00	346	AEY77878.1	alkane-1-monooxygenase, partial [Stenotrophomonas sp. MS192a]
3	558	85.23	176	2.46E-105	317	OJU85240.1	alkane 1-monooxygenase, partial [Solirubrobacterales bacterium 70-9]
4	559	86.81	182	1.04E-102	311	MBA3300326.1	alkane 1-monooxygenase [Thermoleophilaceae bacterium]
5	558	77.6	183	4.90E-105	317	WP_090193511.1	alkane 1-monooxygenase [Pseudomonas pohangensis
6	568	91.26	183	8.35E-124	357	AEY77890.1	alkane-1-monooxygenase, partial [Pedobacter sp. MS245e]
	568	90.71	183	2.59E-123	355	AEY77872.1	alkane-1-monooxygenase, partial [Agrobacterium sp. MS189b]
C3T_1	557	84.44	180	3.35E-109	327	TMQ04550.1	alkane 1-monooxygenase [Deltaproteobacteria bacterium]
	557	84.44	180	3.35E-109	327	TMQ04550.1	alkane 1-monooxygenase [Deltaproteobacteria bacterium]
2	557	95.06	182	4.12E-117	339	AEY77879.1	alkane-1-monooxygenase, partial [Stenotrophomonas sp. MS192a]
	557	93.96	182	3.07E-115	335	AEY77908.1	alkane-1-monooxygenase, partial [Acetobacteraceae bacterium MS302e]
3	557	87.43	183	2.38E-107	315	AID55457.1	alkane monooxygenase, partial [uncultured bacterium]
KR1B	566	98.4	187	5.71E-131	385	WP_036492677.1	fatty acid desaturase [Nocardioides sp. CF8]

Table H1 *(continued)*

Sample	Seq. len.	Ident. (%)	Align. Len. (aa)	E-value	Bit score	Protein ID	Annotation
KR2B	567	97.88	189	8.51E-132	388	AAK31348.1	alkane 1-monooxygenase [Nocardioides sp. CF8]
KR3B_1	557	89.07	183	3.75E-115	334	ACZ64755.1	alkane rubredoxin-dependent monooxygenase, partial [uncultured bacterium]
	556	92.82	183	1.36E-122	353	AID55576.1	alkane monooxygenase, partial [uncultured bacterium]
	556	92.78	180	7.59E-122	351	AEY77879.1	alkane-1-monooxygenase, partial [Stenotrophomonas sp. MS192a]
	558	90.63	64	6.69E-67	127	TMK57753.1	alkane 1-monooxygenase [Actinobacteria bacterium]
2	558	92.06	63	2.99E-65	127	MBA3864872.1	alkane 1-monooxygenase [Solirubrobacterales bacterium]
KZ2_1	557	86.26	182	9.12E-96	293	WP_012937191.1	alkane 1-monooxygenase [Conexibacter woesei]
	561	89.31	187	1.52E-119	357	WP_056710941.1	alkane 1-monooxygenase [Nocardioides sp. Root614
2	561	89.31	187	1.11E-118	355	WP_038675890.1	alkane 1-monooxygenase [Pimelobacter simplex
	556	94.44	36	8.88E-63	73.9	MBA2524067.1	fatty acid desaturase [Solirubrobacterales bacterium]
3	554	82.35	17	1.68E-13	33.5	TMK57753.1	alkane 1-monooxygenase [Actinobacteria bacterium]
4	567	84.13	189	2.72E-110	330	WP_084215945.1	alkane 1-monooxygenase [Pseudonocardia spinosispora]
	567	80.95	189	5.22E-106	317	RYY46357.1	alkane 1-monooxygenase, partial [Actinomycetales bacterium]
	567	80.95	189	2.29E-105	318	WP_055969037.1	alkane 1-monooxygenase [Aeromicrobium sp. Leaf245]
KZ3_1	567	96.72	182	5.39E-129	369	AID23747.1	alkane monooxygenase, partial [uncultured bacterium]
	567	94.05	185	1.04E-127	366	AEY77895.1	alkane-1-monooxygenase, partial [Pedobacter sp. MS245e]
	567	87.3	189	1.32E-119	354	NUR09898.1	alkane 1-monooxygenase [Nocardioidaceae bacterium]
2	566	91.98	187	5.21E-113	340	WP_165239550.1	alkane 1-monooxygenase [Nocardioides anomalus]
3	566	93.55	62	5.35E-61	120	WP_082503265.1	fatty acid desaturase [Nocardioides sp. Leaf307]
4	559	97.75	178	1.86E-127	365	AID55582.1	alkane monooxygenase, partial [uncultured bacterium]
KZ4T_1	560	87.1	178	3.15E-73	176	WP_038118604.1	alkane 1-monooxygenase [Variovorax sp. URHB0020]
	560	84.38	96	4.93E-73	171	HBH38890.1	alkane 1-monooxygenase [Curvibacter sp.]
2	565	98.91	183	7.34E-129	380	WP_036492677.1	fatty acid desaturase [Nocardioides sp. CF8]
3	556	92.31	65	4.20E-62	128	MBA3327915.1	alkane 1-monooxygenase [Solirubrobacterales bacterium]

Table H1 *(continued)*

Sample	Seq. len.	Ident. (%)	Align. Len. (aa)	E-value	Bit score	Protein ID	Annotation
KZ4T_3	556	98.46	65	1.04E-60	135	WP_012937191.1	alkane 1-monooxygenase [Conexibacter woesei]
	556	90.77	65	1.51E-60	128	TML97537.1	alkane 1-monooxygenase [Actinobacteria bacterium]
4	558	85.71	182	6.42E-106	311	AEY77879.1	alkane-1-monooxygenase, partial [Stenotrophomonas sp. MS192a]
5	559	87.64	178	1.94E-114	333	AEY77906.1	alkane-1-monooxygenase, partial [Acetobacteraceae bacterium MS302e]
6	567	95.24	189	3.52E-129	381	WP_036492677.1	fatty acid desaturase [Nocardioides sp. CF8]
KZ5B	558	75.54	184	7.72E-85	266	KAB7754083.1	alkane 1-monooxygenase [Mycolicibacterium mucogenicum DSM 44124]
	559	96.26	107	1.03E-95	219	AID55582.1	alkane monooxygenase, partial [uncultured bacterium]

Appendix I. Results of blastx search of amplicons of expected size after PCR with AlkB484F/ AlkB824R set of primers for alkane hydroxylase genes

Table I 1. Results of blastx search of amplicons of expected size after PCR with AlkB484F/ AlkB824R set of primers for alkane hydroxylase genes

Sample	Seq. len.	Ident. (%)	Align. Len. (aa)	E-value	Bit score	Protein ID	Annotation
P1_1	342	99.11	113	6.57E-74	233	WP_110844388.1	alkane 1-monooxygenase [Mycolicibacterium thermoresistibile]
	340	97.24	109	1.86E-68	220	WP_052054245.1	alkane 1-monooxygenase [Corynebacterium freneyi]
	340	95.41	109	3.94E-67	217	WP_060925339.1	alkane 1-monooxygenase [Corynebacterium xerosis]
2	340	95.41	109	4.89E-67	217	SQB94629.1	Alkane 1-monooxygenase 1 [Clostridium paraputrificum]
	342	92.04	113	2.78E-68	223	WP_182632929.1	alkane 1-monooxygenase [Dietzia aerolata]
	342	90.27	113	3.98E-66	217	WP_131885604.1	alkane 1-monooxygenase [Dietzia cinnamea]
	342	89.38	113	8.99E-66	216	WP_108846117.1	alkane 1-monooxygenase [Dietzia lutea]
3	342	97.34	113	7.46E-72	229	WP_005625831.1	alkane 1-monooxygenase [Mycolicibacterium hassiacum]]
	340	100	108	1.54E-68	221	WP_043660285.1	alkane 1-monooxygenase [Thermocrispum municipale]
4	340	95.37	108	3.66E-65	209	PZM91380.1	alkane 1-monooxygenase [Thermocrispum agreste]
	342	98.23	113	1.06E-73	234	WP_005625831.1	alkane 1-monooxygenase [Mycolicibacterium hassiacum]
P2_1	342	83.19	113	3.97E-67	207	ABB13509.1	AlkB, partial [Mycolicibacterium smegmatis MC2 155]
2	342	98.23	113	1.02E-73	234	VCT88828.1	Alkane 1-monooxygenase [Mycolicibacterium hassiacum DSM 44199]
P3_1	340	99.08	109	9.31e-71	227	VCT88828.1	alkane 1-monooxygenase [Mycolicibacterium hassiacum]
2	341	99.12	113	6.57e-74	233	WP_110844388.1	alkane 1-monooxygenase [Mycolicibacterium thermoresistibile]
3	340	99.08	109	1.14e-69	223	WP_003927986.1	alkane 1-monooxygenase [Mycolicibacterium thermoresistibile]
4	342	92.04	113	2.78e-68	223	WP_182632929.1	fatty acid desaturase [Dietzia aerolata]
	345	91.23	114	1.82e-70	218	API65146.1	alkane 1-monooxygenase, partial [Rhodococcus gordoniae]
	345	91.30	115	4.05e-68	219	WP_193902584.1	fatty acid desaturase [Rhodococcus pyridinivorans]
5	345	91.30	115	4.37e-68	219	WP_071935702.1	alkane 1-monooxygenase [Rhodococcus sp. 2G]
6	342	97.35	114	5.88e-72	229	WP_052054245.1	alkane 1-monooxygenase [Corynebacterium freneyi]

Table I 1 *(continued)*

Sam-ple	Seq. len.	Ident. (%)	Align. Len. (aa)	E-value	Bit score	Protein ID	Annotation
	342	95.58	113	1.38e-70	226	KKO82090.1	alkane 1-monooxygenase [Corynebacterium xerosis]
P3_6	342	95.58	113	1.47e-70	226	SQB94629.1	Alkane 1-monooxygenase 1 [Clostridium paraputrificum]
	340	98.2	111	1.20E-61	202	HCT13643.1	alkane 1-monooxygenase [Corynebacterium nuruki]
P4_1	340	92.79	111	2.70E-58	195	HAJ52165.1	alkane 1-monooxygenase [Corynebacterium variabile]
	341	88.45	113	4.50E-62	196	ACJ22761.1	alkane hydroxylase, partial [Corynebacterium variabile]
2	341	99.16	113	5.31E-62	204	WP_066585432.1	alkane 1-monooxygenase [Corynebacterium provencense]
	342	99.16	113	1.16E-73	234	AMO60461.1	Alkane 1-monooxygenase [Mycolicibacterium phlei]
3	342	91.15	113	6.16E-71	217	ABB13509.1	AlkB, partial [Mycolicibacterium smegmatis MC2 155]
	342	98.23	113	1.06E-73	234	WP_005625831.1	alkane 1-monooxygenase [Mycolicibacterium hassiacum]
4	342	83.19	113	3.97E-67	207	ABB13509.1	AlkB, partial [Mycolicibacterium smegmatis MC2 155]

Appendix J. Results of blastx search of amplicons of obtained with primers MonF / MonR for alkane hydroxylases genes

Table J1. Results of blastx search of amplicons of expected size after PCR with primers MonF / MonR for alkane hydroxylases genes

Sam-ple	Seq. len.	Ident (%)	Align. Len. (aa)	E-value	Bit score	Protein ID	Annotation
P1_1	424	97.86	140	6.33 E-93	284	WP_052054245.1	alkane 1-monooxygenase [Corynebacterium freneyi]
	424	97.14	140	4.51 E-92	285	WP_105943622.1	fatty acid desaturase [Gordonia iterans]
2	424	92.14	140	1.03 E-88	274	WP_009679531.1	alkane 1-monooxygenase [Gordonia neofelifaecis]
3	425	98.58	141	8.34 E-95	288	WP_110844388.1	alkane 1-monooxygenase [Mycolicibacterium thermoresistibile]
P2_1	425	96.45	141	2.55 E-92	283	WP_052054245.1	alkane 1-monooxygenase [Corynebacterium freneyi]
2	425	95.04	141	4.46 E-91	280	WP_060925339.1	alkane 1-monooxygenase [Corynebacterium xerosis]
3	425	95.04	141	7.31 E-91	280	SQB94629.1	alkane 1-monooxygenase [Corynebacterium freneyi]
P3_1	424	97.86	141	6.33e-93	284	WP_052054245.1	alkane 1-monooxygenase [Corynebacterium freneyi]
	424	96.43	141	9.66e-92	281	KKO82090.1	alkane 1-monooxygenase [Corynebacterium xerosis]
	424	96.43	141	9.79e-92	281	SQB94629.1	Alkane 1-monooxygenase 1 [Clostridium paraputrificum]
2	424	98.57	141	2.21e-94	288	VCT88828.1	Alkane 1-monooxygenase [Mycolicibacterium hassiacum DSM 44199]
3	425	100.0	142	4.57e-84	263	WP_105193194.1	alkane 1-monooxygenase [Amnimonas aquatica]
P4_1	424	97.86	140	6.33 E-93	284	WP_052054245.1	alkane 1-monooxygenase [Corynebacterium freneyi]
	424	96.43	140	9.66 E-92	281	KKO82090.1	alkane 1-monooxygenase [Corynebacterium xerosis]
	424	96.43	140	9.79 E-92	281	SQB94629.1	Alkane 1-monooxygenase 1 [Clostridium paraputrificum]
2	424	91.43	139	1.24 E-83	251	ACJ22761.1	alkane hydroxylase, partial [Corynebacterium variabile]
	424	97.84	139	8.39 E-81	254	WP_066585432.1	alkane 1-monooxygenase [Corynebacterium provencense]
3	423	98.52	139	4.69 E-89	275	WP_073884045.1	alkane 1-monooxygenase [Corynebacterium variabile]
4	423	98.29	117	1.74 E-76	234	ABB92358.1	putative alkane monooxygenase, partial [bacterium alkW27]
	423	96.58	117	3.24 E-75	231	CDI44588.1	alkane monooxygenase, partial [Pseudomonas lini]
	423	96.58	117	3.80 E-75	229	AAV41375.1	alkane monooxygenase, partial [Pseudomonas stutzeri]
P4_4	423	96.55	116	7.22 E-75	229	AEY77858.1	alkane-1-monooxygenase, partial [Chitinophagaceae bacterium MS98c]

Table J1 *(continued)*

Sample	Seq. len.	Ident (%)	Align. Len. (aa)	E-value	Bit score	Protein ID	Annotation
	423	98.29	117	5.48 E-74	236	WP_124412454.1	alkane 1-monooxygenase [Pseudomonas synxantha]
P4600	613	96.58	117	1.03 E-68	229	SCQ72189.1	ABC transporter related protein [Propionibacterium freudenreichii]
	424	97.86	140	6.33 E-93	284	WP_052054245.1	alkane 1-monooxygenase [Corynebacterium freneyi]
	424	96.43	140	9.66 E-92	281	KKO82090.1	alkane 1-monooxygenase [Corynebacterium xerosis]
P5_1	424	96.43	140	9.79 E-92	281	SQB94629.1	Alkane 1-monooxygenase 1 [Clostridium paraputrificum]
	424	99.29	140	1.62 E-95	283	ABB92358.1	alkane monooxygenase, partial [Pseudomonas brassicacearum]
	424	97.86	140	2.37 E-94	280	CDI44588.1	alkane monooxygenase, partial [Pseudomonas lini]
	424	97.14	140	4.07 E-94	278	AAV41375.1	alkane monooxygenase, partial [Pseudomonas stutzeri]
2	424	97.12	139	5.53 E-93	275	AEY77858.1	alkane-1-monooxygenase, partial [Chitinophagaceae bacterium MS98c]
3	424	99.29	140	5.06 E-93	285	WP_017846506.1	alkane 1-monooxygenase [Pseudomonas veronii]
4	424	91.43	140	8.91 E-88	269	WP_068116790.1	fatty acid desaturase, partial [Nocardioides massiliensis]
C1T_1	425	97.14	140	1.93 E-95	283	ACZ64781.1	alkane rubredoxin-dependent monooxygenase, partial [uncultured bacterium]
2	425	84.4	141	9.89 E-70	224	HBH38890.1	alkane 1-monooxygenase [Curvibacter sp.]
3	426	87.36	87	8.25 E-54	137	WP_184527912.1	fatty acid desaturase [unclassified Variovorax]
4	425	58.87	141	2.18 E-53	182	WP_073857305.1	alkane 1-monooxygenase [Mycolicibacterium diernhoferi]
	425	58.16	141	1.35 E-52	181	WP_087028293.1	alkane 1-monooxygenase [Mycolicibacterium aurum]
C2T_1	424	75	140	7.28 E-74	228	AID23785.1	alkane monooxygenase, partial [uncultured bacterium]
	424	72.86	140	4.96 E-73	226	AHA51154.1	alkane-1-monooxygenase, partial [Rhodococcus aetherivorans]
2	429	76.81	138	1.20 E-62	207	WP_174986635.1	fatty acid desaturase [Burkholderia lata]
	425	92.91	141	2.11 E-92	275	AEY77892.1	alkane-1-monooxygenase, partial [Pedobacter sp. MS245e]
3	426	75.91	137	1.99 E-70	224	OHC29796.1	fatty acid desaturase, partial [Pseudomonadales bacterium RIFCSPLOWO2_12_59_9]
	426	78.26	138	2.01 E-70	226	KEF32438.1	Alkane-1 monooxygenase [Marinobacter nitratireducens]
4	424	92.31	117	2.73 E-64	204	AEY77908.1	alkane-1-monooxygenase, partial [Acetobacteraceae bacterium MS302e]

Table J1 *(continued)*

Sample	Seq. len.	Ident (%)	Align. Len. (aa)	E-value	Bit score	Protein ID	Annotation
C2T_4	424	92.31	117	7.89 E-64	202	AEY77879.1	alkane-1-monooxygenase, partial [Stenotrophomonas sp. MS192a]
	424	93.16	117	1.03 E-63	202	AEY77874.1	alkane-1-monooxygenase, partial [Agrobacterium sp. MS189b]
5	425	58.87	141	8.10 E-54	184	WP_087028293.1	alkane 1-monooxygenase [Mycolicibacterium aurum]
	425	58.87	141	1.16 E-53	183	WP_073857305.1	alkane 1-monooxygenase [Mycolicibacterium diernhoferi]
6	425	87.86	140	9.56 E-87	275	AIY15653.2	Alkane-1 monooxygenase [Pimelobacter simplex]
	425	88.65	141	7.75 E-86	269	WP_056710941.1	fatty acid desaturase [unclassified Nocardioides]
7	426	82.96	88	6.23 E-61	157	WP_102142883.1	alkane 1-monooxygenase [Mycobacterium sp. QGD 101]
8	427	83.33	84	5.75 E-45	153	ACJ22759.1	alkane hydroxylase, partial [Pseudomonas oleovorans]
	427	82.96	88	1.09 E-44	160	RLT95103.1	alkane 1-monooxygenase [Ketobacter sp.]
9	425	100	95	4.44 E-62	69.7	AEY77908.1	alkane-1-monooxygenase, partial [Acetobacteraceae bacterium]
	425	100	95	1.43 E-61	69.7	AEY77874.1	alkane-1-monooxygenase, partial [Agrobacterium sp. MS189b]
C3T_1	424	85.51	138	1.91 E-84	255	AEY77905.1	alkane-1-monooxygenase, partial [Rhodopseudomonas sp. MS279c]
2	424	92.14	140	1.75 E-90	270	AEY77892.1	alkane-1-monooxygenase, partial [Pedobacter sp. MS245e]
3	424	97.14	140	7.90 E-92	284	WP_191193851.1	fatty acid desaturase [Nocardioides cavernae]
4	424	96.33	109	5.75 E-69	216	AEY77879.1	alkane-1-monooxygenase, partial [Stenotrophomonas sp. MS192a]
	424	95.41	109	8.54 E-69	215	AEY77908.1	alkane-1-monooxygenase, partial [Acetobacteraceae bacterium]
	424	95.41	109	2.88 E-68	214	AEY77874.1	alkane-1-monooxygenase, partial [Agrobacterium sp. MS189b]
	424	92.86	140	4.48 E-78	239	AEY77904.1	alkane-1-monooxygenase, partial [Rhodopseudomonas sp. MS279c]
5	425	92.91	141	4.39 E-91	271	AEY77883.1	alkane-1-monooxygenase, partial [Bradyrhizobiaceae bacterium]
6	425	95.75	141	1.90 E-90	280	WP_027861711.1	fatty acid desaturase [Marmoricola sp. URHB0036]
7	423	78.57	140	3.35 E-71	228	WP_191842995.1	fatty acid desaturase [Catellatospora chokoriensis]
	423	75	140	1.28 E-70	226	WP_189334879.1	fatty acid desaturase [Actinoplanes ianthinogenes]
	423	77.86	140	3.19 E-70	225	WP_120315559.1	alkane 1-monooxygenase [Catellatospora citrea]
8	424	92.25	125	1.41 E-83	252	AGQ21063.1	AlkB, partial [uncultured soil bacterium]
	424	79.29	140	4.97 E-76	233	AEY77868.1	alkane-1-monooxygenase, partial [Gordonia sp. MS121b]

Table J1 *(continued)*

Sample	Seq. len.	Ident (%)	Align. Len. (aa)	E-value	Bit score	Protein ID	Annotation
C3_9	424	87.14	140	5.20E-86	273	AIY15653.2	Alkane-1 monooxygenase [Pimelobacter simplex]
10	425	97.16	141	4.90E-83	251	AEY77904.1	alkane-1-monooxygenase, partial [Rhodopseudomonas sp. MS279c]
KR1T_1	420	89.52	124	8.69E-75	230	ACZ64759.1	alkane rubredoxin-dependent monooxygenase, partial [uncultured bacterium]
2	416	90.65	139	5.22E-81	256	WP_135267320.1	fatty acid desaturase [Nocardioides seonyuensis]
3	418	79.76	84	1.08E-42	147	GGO94232.1	hypothetical protein GCM10011584_34780 [Nocardioides phosphati]
4	425	90.71	140	6.05E-83	261	WP_027861711.1	fatty acid desaturase [Marmoricola sp. URHB0036]
5	428	68.79	141	4.15E-63	199	ACJ22759.1	alkane hydroxylase, partial [Pseudomonas oleovorans]
6	429	94.69	113	2.05E-71	222	ACZ64780.1	alkane rubredoxin-dependent monooxygenase, partial [uncultured bacterium]
KR2B_1	423	68.61	137	2.30E-55	181	AEY77904.1	alkane-1-monooxygenase, partial [Rhodopseudomonas sp. MS279c]
	422	78.17	142	1.58E-62	199	ACZ64771.1	alkane rubredoxin-dependent monooxygenase, partial [uncultured bacterium]
2	426	95.16	62	5.76E-54	127	WP_135267320.1	fatty acid desaturase [Nocardioides seonyuensis]
	426	95.16	62	6.51E-54	127	WP_108343222.1	alkane 1-monooxygenase [Nocardioides currus]
KR3B_1	423	90.58	138	1.09E-88	265	AEY77908.1	alkane-1-monooxygenase, partial [Acetobacteraceae bacterium]
	423	90.58	138	3.20E-88	264	AEY77879.1	alkane-1-monooxygenase, partial [Stenotrophomonas sp. MS192a]
2	423	90.58	138	3.69E-88	264	AEY77874.1	alkane-1-monooxygenase, partial [Agrobacterium sp. MS189b]
	847	86.99	146	2.31E-78	245	AEY77879.1	alkane-1-monooxygenase, partial [Stenotrophomonas sp. MS192a]
KR5	424	93.62	140	4.11E-75	231	AID55574.1	alkane monooxygenase, partial [uncultured bacterium]
KZ1_1	436	99.31	144	3.32E-98	298	WP_013829920.1	transmembrane alkane 1-monooxygenase AlkB [Mycolicibacter sinensis]
2	424	95.75	141	3.52E-94	280	ABB92366.1	putative alkane monooxygenase, partial [bacterium alkW69]
	424	97.87	141	2.01E-92	283	WP_017846506.1	alkane 1-monooxygenase [Pseudomonas veronii]
KZ3	425	97.86	140	1.07E-95	283	ACZ64771.1	alkane rubredoxin-dependent monooxygenase, partial [uncultured bacterium]
	425	95.75	141	6.98E-91	281	WP_172257420.1	fatty acid desaturase [Nocardioides sp. zg-1230]
	423	97.3	37	3.79E-50	83.6	WP_180934973.1	fatty acid desaturase [Nocardioides ungokensis]
2	425	93.57	140	5.46E-92	274	ACJ22748.1	putative alkane monooxygenase, partial [uncultured bacterium]

Appendix K. Results of blastx homology search for amplicons obtained with primers designed for *styA2B* gene of *Variovorax pardoxus*

Table K1 Results of blastx search of amplicons of expected size after PCR for *Variovorax pardoxus styA2B*

Sample	Seq. len.	Ident. (%)	Align. Len. (aa)	E-value	Bit score	Protein ID	Annotation
	211	85.71	70	3.12E-38	141	HBJ99908.1	alanine-phosphoribitol ligase [Delftia acidovorans]
P2'_1	211	85.71	70	5.95E-38	140	WP_143772804.1	FAD-binding oxidoreductase [Skermania sp. ID1734]
	210	83.08	65	1.01E-30	120	WP_088953870.1	alanine-phosphoribitol ligase [Variovorax sp. HW608]
	210	81.54	65	3.79E-30	115	EWS62618.1	Styrene monooxygenase StyA [Hydrogenophaga sp. T4]
	210	83.08	65	5.61E-30	119	WP_175131763.1	Styrene monooxygenase StyA [Achromobacter pulmonis]
_2	210	81.54	65	7.28E-30	119	WP_198484541.1	FAD-binding oxidoreductase [Achromobacter deleyi]
	227	92.86	70	6.90E-40	145	PKO58172.1	alanine-phosphoribitol ligase, partial [Betaproteobacteria bacterium]
	227	88.57	70	7.71E-37	137	WP_015435485.1	putative styrene monooxygenase [Azoarcus sp. KH32C]
	227	87.14	70	4.09E-36	135	WP_159693667.1	FAD-binding oxidoreductase [Azoarcus halotolerans]
3	227	85.71	70	9.12E-36	135	WP_065340412.1	putative styrene monooxygenase [Azoarcus olearius]
	228	92.54	67	8.97E-37	136	HHX82080.1	FAD-binding oxidoreductase [Pseudomonadaceae bacterium]
4	228	92.54	67	5.25E-36	137	NLC62364.1	FAD-binding oxidoreductase [Gammaproteobacteria bacterium]
C2T_1	211	90	70	3.01E-38	140	WP_068644024.1	alanine-phosphoribitol ligase [Variovorax soli]
	211	91.43	70	1.55E-38	144	WP_126025012.1	flavin reductase [Variovorax guangxiensis]
2	211	90	70	1.76E-38	141	WP_126471522.1	FAD-binding oxidoreductase [Variovorax gossypii]
3	211	89.29	56	2.59E-28	114	WP_153282742.1	FAD-binding oxidoreductase [Variovorax paradoxus]
4	211	90	70	2.81E-37	138	WP_047786609.1	styrene monooxygenase StyA [Variovorax paradoxus]
5	211	94.29	70	4.28E-40	145	WP_129413203.1	FAD-binding oxidoreductase [Mesorhizobium sp. Pch-S]
	211	95.71	70	4.07E-40	145	RZL81384.1	FAD-binding oxidoreductase [Rhodococcus sp.]
6	211	94.29	70	3.51E-39	143	WP_065490891.1	styrene monooxygenase [Rhodococcus opacus]
7	211	85.71	70	4.60E-38	142	CAA2109773.1	Styrene monooxygenase StyA [Variovorax paradoxus]
8	212	94.03	67	3.35E-35	135	WP_125967142.1	flavin reductase [Variovorax beijingensis]

Table K1 *(continued)*

Sample	Seq. len.	Ident. (%)	Align. Len. (aa)	E-value	Bit score	Protein ID	Annotation
	211	90	70	2.81E-40	138	REM31795.1	flavin reductase, partial [Mycobacterium tuberculosis]
	211	92.86	70	2.52E-38	141	WP_093176809.1	alanine-phosphoribitol ligase [Variovorax sp. YR266]
C2B_1	211	94.29	70	6.99E-38	142	WP_125967142.1	flavin reductase [Variovorax beijingensis]
2	209	92.75	69	7.20E-38	139	WP_129413203.1	FAD-binding oxidoreductase [Mesorhizobium sp. Pch-S]
3	211	92.86	70	1.12E-38	142	WP_192691479.1	hypothetical protein [Mesorhizobium sp. OAS926]
5	211	90	70	3.01E-38	140	WP_068644024.1	alanine-phosphoribitol ligase [Variovorax soli]
C3T_1	210	87.14	70	1.86E-37	141	WP_081269018.1	flavin reductase [Variovorax paradoxus]
2	210	92.31	65	6.54E-35	134	WP_126025012.1	flavin reductase [Variovorax guangxiensis]
3	210	90	70	7.57E-38	139	WP_126471522.1	FAD-binding oxidoreductase [Variovorax gossypii]
4	211	95.71	70	2.66E-40	146	WP_159924265.1	FAD-binding oxidoreductase [Rhodococcus sp. WAY2]
5	211	94.29	70	6.22E-40	145	WP_061043975.1	alanine-phosphoribitol ligase [Rhodococcus sp. ACPA1]
C3B_1	209	92.31	65	3.51E-35	132	WP_093209758.1	alanine-phosphoribitol ligase [Variovorax sp. YR750]
	209	92.31	65	3.82E-35	132	WP_126471522.1	FAD-binding oxidoreductase [Variovorax gossypii]
2	211	85.71	70	8.38E-37	137	WP_106722753.1	alanine-phosphoribitol ligase [Mesorhizobium soli]
3	211	85.71	70	8.35E-37	137	WP_063327106.1	alanine-phosphoribitol ligase [Delftia sp. GW456-R20]
	211	81.43	70	2.34E-35	133	WP_153233596.1	FAD-binding oxidoreductase [Glaciimonas soli]
C4_1	211	82.86	70	3.16E-34	130	WP_064477858.1	FAD-binding oxidoreductase [Ralstonia solanacearum]
2	211	91.43	70	1.55E-38	144	WP_126025012.1	flavin reductase [Variovorax guangxiensis]
	211	90	70	3.01E-38	140	WP_068644024.1	alanine-phosphoribitol ligase [Variovorax soli]
	211	90	70	7.57E-38	139	WP_126471522.1	FAD-binding oxidoreductase [Variovorax gossypii]
3	211	82.86	70	7.92E-38	139	WP_137154977.1	FAD-binding oxidoreductase [Rhizobium sp. FKL33]
4	211	87.14	70	2.97E-36	135	WP_129413203.1	alanine-phosphoribitol ligase [Mesorhizobium sp. Pch-S]
KR2B_1	211	81.43	70	1.22E-34	131	WP_153233596.1	FAD-binding oxidoreductase [Glaciimonas soli]
2	209	75	24	6.49E-24	41.2	WP_153282742.1	FAD-binding oxidoreductase [Variovorax paradoxus]
3	210	92.86	70	1.88E-38	141	WP_129413203.1	FAD-binding oxidoreductase [Mesorhizobium sp. Pch-S]